On the Use of Drive-by Measurement for Indirect Bridge Monitoring

Abdollah Malekjafarian

This thesis is submitted to University College Dublin in fulfilment of the requirements for the degree of Doctor of Philosophy

May 2016

School of Civil Engineering
University College Dublin

Head of school:
Dr. Aoife Ahern

Supervisor:
Prof. Eugene OBrien

Contents

List of figures

The velocity differences obtained from Eq. B-4 are shown in Figure B- 6. As a result, a bridge response at the moving coordinate is obtained which can show the most important characteristics of the bridge dynamics. The frequency spectrum of the obtained bridge

List of tables

Abstract

Indirect bridge monitoring methods, using the responses measured from vehicles passing over bridges, are under development for about a decade. A major advantage of these methods is that they use sensors mounted on the vehicle – no sensors or data acquisition system needs to be installed on the bridge. Most of the proposed methods are based on the identification of dynamic characteristics of the bridge from responses measured on the vehicle, such as natural frequency, mode shapes and damping. In addition, some of the methods seek to directly detect bridge damage based on the interaction between the vehicle and the bridge. A critical review of indirect methods for bridge monitoring is presented and discussion and recommendations on the challenges to be overcome for successful implementation in practice are provided.

A novel Short Time Frequency Domain Decomposition (STFDD) method is proposed to estimate bridge mode shapes from the dynamic response of the vehicle. In Frequency Domain Decomposition (FDD), several segments are defined on the bridge and the measurement is performed using two instrumented axles. Here, the FDD method is employed in a multi-stage procedure applied to the bridge segments in sequence. A rescaling process is used to construct the global mode shape vector. Numerical case studies are investigated using Finite Element (FE) models of vehicle bridge interaction (VBI) to validate the effectiveness and performance of the proposed method. In other indirect bridge identification methods, the road profile may excite the vehicle, making it difficult to detect the bridge modes. This is addressed using two concepts: applying external excitation to the bridge and subtracting signals in the axles of successive trailers towed by the vehicle. The results obtained from the numerical investigation demonstrate that the proposed method can estimate the bridge mode shapes with acceptable accuracy. The sensitivity of the method to added white noise is also investigated.

A novel algorithm for bridge damage detection based on the mode shapes estimated from a passing vehicle is also presented. The bridge response at the moving coordinate is measured from an instrumented vehicle with laser vibrometers and accelerometers. A modified version of the Short Time Frequency Domain Decomposition (STFDD) method is applied to the measured responses. The bridge mode shapes are estimated with high resolution as is

appropriate for damage detection. A damage index based on mode shape squares (MOSS) is used to detect the presence and location of the damage. A numerical case study of a half-car model passing over a bridge is described which validates the performance of the proposed approach. Several damage scenarios are considered including different locations and severities. It is shown that the presence and location of the damage can be detected with acceptable accuracy when the vehicle is moving very slowly. In addition, the performance of the method using higher vehicle speeds is investigated and shows that the approach works well for speeds up to 8 m/s. The sensitivity of the algorithm to measurement noise is also studied by adding several levels of noise to the responses measured on the vehicle.

It is shown theoretically that such a response includes three main components; vehicle frequency, bridge natural frequency and a vehicle speed pseudo-frequency component. The Empirical Mode Decomposition (EMD) method is used to decompose the signal into its main components. A damage detection method is proposed using the Intrinsic Mode Functions (IMFs) corresponding to the vehicle speed component of the response measured on a passing vehicle. Numerical case studies using Finite Element modelling of Vehicle Bridge Interaction are used to show the performance of the proposed method. It is demonstrated that it can successfully localise the damage location in the absence of road profile. A difference in the acceleration signals of healthy and corresponding damaged structures is used to identify the damage location in the presence of road profile.

A truck-trailer system is assumed, equipped with an external excitation at a frequency close to one of the bridge natural frequencies. The excitation makes the bridge response dominant at its natural frequency. The acceleration responses are measured on two following axles of the vehicle. It is shown that the amplitude of the signal includes the bridge mode shape data. The energy of the responses measured on two following axles is obtained using the Hilbert Huang Transform. It is shown that the bridge mode shape can be constructed with high resolution using a rescaling process. The presence of road roughness introduces additional contributions to the response measured on the vehicle, in addition to the bridge response. The concept of subtraction of the responses measured from two identical axles is used to remove the effect of road roughness.

Declaration

I hereby certify that the submitted work is my own work, was completed while registered as a candidate for the degree stated on the title page, and I have not obtained a degree elsewhere on the basis of the research presented in this work.

The author confirms that the library may lend or copy this thesis, upon request, for academic purposes.

Abdollah Malekjafarian

Acknowledgment

First of all, I would like to express my sincere gratitude to my supervisor Prof. Eugene OBrien for the continuous support of my PhD study and related research, for his patience, motivation and immense knowledge. His guidance helped me in all the time of research and writing of this thesis. I truly could not have imagined having a better advisor and mentor for my PhD study. I also would like to thank Dr. Arturo Gonzalez for his advice during my DSP meetings and Dr. Patrick McGetrick for his support and comments in writing the review paper.

I wishes to express my gratitude for the financial support received from Transport Infrastructure Ireland (TII), the Irish Research Council's *PhD in Sustainable Development* Graduate Research Education Programme and Science Foundation Ireland towards this investigation under the US-Ireland Partnership Scheme.

I would like to thank the staff in Newstead for their advice and encouragement. In particular, I would like to thank Andrew, who was always good for a chat and so incredibly approachable and helpful.

In my daily work I have been blessed with a friendly and cheerful group of fellow students. Omar, thanks for all the funs that you provided for me, keep training, I am sure you will get six pack soon. Daniel, thanks for all the football you organised for us, you are the best organiser in the world. Alex and Alexandra for all good times that we spent together. Paul, thanks for being always up for buying lunch. To Enrique, Longwei and all other postgraduate students in Newstead for the good times when we were together, particularly at lunch time.

A special thanks to my parents, Mohammad and Zahra. Words cannot express how grateful I am to you for all of the sacrifices that you have made for me. Your prayer for me was what sustained me thus far. Thanks also to my parents-in-law Mohammad and Nahid for their continuous support and care. Thanks also to my brothers Rohollah and Saeed for their support and encouragements. This work would have not been possible without these people.

Finally, a special thanks to my lovely wife Fatemeh. She has faith in me and my intellect even when I felt like digging a hole and crawling into one because I didn't have faith in myself. These past several years have not been an easy ride, both academically and personally. I truly thank Fatemeh for sticking by my side, even when I was irritable and depressed. We both learned a lot about life and strengthened our commitment and determination to each other and to live life to the fullest. Thank you again for your love and support, for your patient and understanding, for making me smile and for always being there for me when I needed you.

Chapter 1: Introduction

Chapter 1: Introduction

1.1. Background

There is an increasing demand for improved condition monitoring of transport infrastructure all over the world. Bridges are key components of transportation infrastructure and require such monitoring. Rehabilitating and extending the lives of these structures raise important maintenance and safety issues. Traditionally, bridge maintenance has relied on visual inspection methods, which are highly variable, lack resolution and can only detect damage when it is visible. Therefore, structurally deficient bridges may be left undiscovered. A number of bridge collapses have occurred due to a lack of structural capacity information. Chupanit and Phromsorn (2012) have suggested that visual inspection alone may not be adequate for bridge health monitoring.

Structural Health Monitoring (SHM) methods rely on the automatic detection of anomalous structural behaviour. SHM approaches using the dynamic response of structures is becoming an increasingly popular part of infrastructure maintenance and management systems. One of the most popular SHM approaches is the use of structural vibration data for non-destructive damage assessment. The underlying principle is that if damage occurs in a structure, it leads to changes in its physical properties, e.g. a loss of stiffness, and consequently causes measurable changes in its dynamic properties.

In most vibration-based bridge health monitoring techniques, large numbers of sensors are installed on the structure to monitor the dynamic properties (Carden and Fanning, 2004). In these approaches which are referred to here as *direct* methods, sensors are installed directly on the bridge. The common practice is to mount the vibration sensors at different positions on the bridge and connect them to a data acquisition system. However, the on-site instrumentations are costly, time-consuming, and even dangerous, depending on the location and type of bridge. Moreover, for the case where the ongoing traffic cannot be restricted for the purpose of installation, the task of equipment mounting may be even more difficult. At present, the implementation of Structural Health Monitoring is not widespread for short and medium span bridges, which are the greatest proportion of bridges in service.

The idea of an *indirect* approach, in which the dynamic properties of bridge structures are extracted from the dynamic responses measured in a passing vehicle, is proposed by Yang

et al. (2004). Such an approach is low cost at the network level and is aimed at reducing the need for any direct installation of equipment on the bridge itself. It involves a vehicle instrumented with sensors through which dynamic properties of the bridge such as natural frequencies are extracted. Through interaction between the bridge and vehicle, the moving vehicle can be considered as both exciter and receiver. The measured vehicle response needs to include relatively high levels of bridge dynamic response in this vehicle-bridge interaction (VBI). The feasibility of this method in practice was experimentally confirmed by Lin and Yang (2005) by passing an instrumented vehicle over a highway bridge in Taiwan. In the case that only bridge frequency is required, the indirect approaches show many advantages compared to direct methods in terms of equipment needed, specialist personnel on site, economy, simplicity, efficiency and mobility.

In recent years, several researchers have developed methods to identify the bridge frequency from the acceleration signal in a passing vehicle and to improve the accuracy of the results. In addition, some authors obtain the damping ratio of the bridge using indirect approaches, but very few have obtained mode shapes of the bridge indirectly. Estimation of bridge mode shape is very important in a dynamic investigation of a bridge. For instance, there are discontinuities at the damaged points in the mode shapes of a damaged bridge, including slope discontinuities at cracks (Zhu and Law, 2006, Pandey et al., 1991). Furthermore, the bridge mode shape can be used as an important tool in model updating of a bridge (Arora et al., 2009).

1.2. Research objectives and outline

The main purpose of this study is to develop an indirect approach for monitoring of short to medium span bridges using the response measured on a passing vehicle. Identification of bridge mode shapes using indirect measurements is investigated in Chapters 3, 4 and 6. A mode shapes-based bridge damage detection approach is studied in Chapter 4. In addition, the application of Empirical Mode Decomposition (EMD) for bridge damage detection using indirect measurement is discussed in Chapter 5. A summary of the thesis chapters is shown in Figure 1-1, which highlights the links between the different chapters and the key contributions of this work.

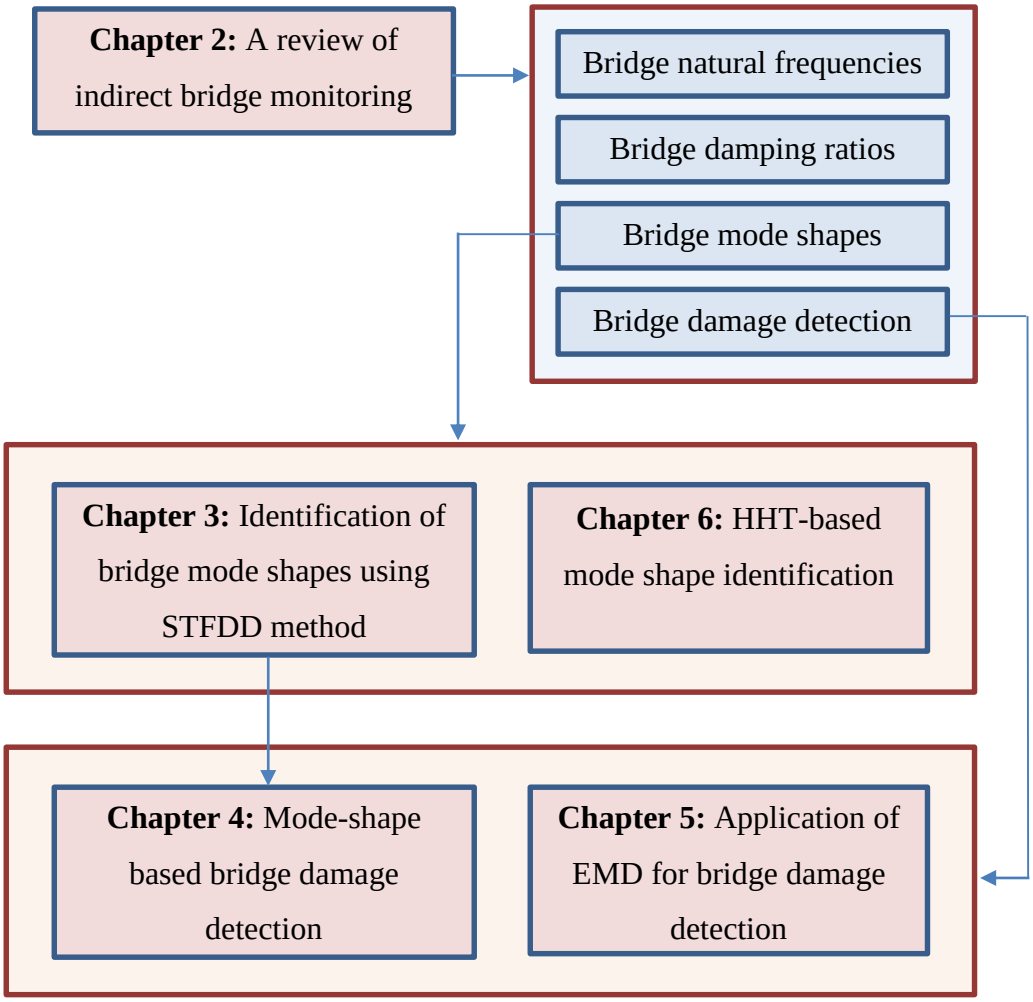

Figure 1-1 Flow chart showing the outline of the thesis.

Chapter 2 presents a critical review of indirect methods for bridge monitoring and provides discussion and recommendations on the challenges to be overcome for a successful implementation in practice. It is shown that most of the proposed methods are based on the identification of dynamic characteristics of the bridge from the responses measured on the vehicle, such as natural frequency, mode shapes and damping. In addition, some of the methods seek to directly detect bridge damage based on the interaction between the vehicle and the bridge.

Chapter 3 proposes a novel Short Time Frequency Domain Decomposition (STFDD) approach using multi-stage measurements to obtain bridge mode shape indirectly from the accelerations in two connected passing axles. The proposed method is based on Frequency Domain Decomposition (FDD), which is an output-only modal testing method. It involves

two main parts. In the first part, several segments are defined in the bridge and a multi-stage measurement procedure is done based on the defined segments. The FDD method is applied to the time history acceleration responses from the two following axles in each stage. As a result, small local sections of the mode shapes are estimated in each stage in the first part of the method. In the second part, a correction procedure is performed to construct the global mode shape vectors of the bridge from the estimated local mode shape parts. This study is among the earliest studies proposed for indirect identification of bridge mode shapes.

In Chapter 4, a novel algorithm is proposed for indirect damage detection of a bridge based on the mode shapes obtained using the STFDD method (proposed in Chapter 3). A new measurement procedure inspired by Oshima et al. (2014) is proposed to overcome the effect of road profile. The STFDD method is also slightly modified to provide enough resolution in the mode shape estimated and to provide more accurate local information about the damage. It is shown that the method can detect the occurrence and location of the damage with acceptable accuracy.

In Chapter 5, the theoretical response of a vehicle passing over a bridge is presented. It is shown by Yang et al. (2004) that the response measured on a passing vehicle contains three main components; vehicle frequency, bridge natural frequency and the pseudo frequency associated with vehicle speed. The first one relates to the vehicle dynamic response and the last two correspond to the bridge dynamic response. Generally, those components corresponding to bridge dynamics reflect the bridge condition. The pseudo-frequency component of the response is separated and used here for damage detection. EMD is applied to the axle response to decompose it into different components using a sifting process. It is shown that the damage location can be detected using the IMFs corresponding to the pseudo-frequency. However, the method is sensitive to any change in the pavement profile in successive runs of the vehicle.

Chapter 6 presents a novel algorithm for the identification of bridge mode shapes using the response measured on a passing vehicle. A truck-trailer system, which is equipped with an external excitation at a frequency close to one of the bridge natural frequencies, is assumed. The excitation makes the bridge response dominant at its natural frequency. The acceleration responses are measured on two following axles of the vehicle. It is shown that the amplitude of the signal includes the bridge mode shape data. The energy of the responses measured on two following axles is obtained using the Hilbert Huang Transform. It is shown that a high

resolution bridge mode shape can be constructed using a rescaling process. The presence of road roughness introduces additional contributions to the response measured on the vehicle, in addition to the bridge response. The concept of subtraction of the responses measured from two identical axles is used to remove the effect of road roughness.

1.3. Thesis structure

The thesis includes five journal/draft journal papers, one in each of the Chapters 2-6. The current status of each paper (submitted or published) is highlighted in Table 1-1 and at the start of each chapter, along with a clarification of the author's contribution. It is the policy of the research group, generally, to rotate the first authorship of the publication.

The appendices comprises one additional journal paper (Appendix A), for which the author contributed to the numerical processing of the measured strain data using MATLAB and some more evaluations. Appendix B evaluates the application of laser measurement to the drive-by inspection of bridges. Appendix C presents further investigation on the STFDD method.

Table 1-1 Journal publications.

Chapter	Title	State
2	A review of indirect bridge monitoring using passing vehicles	Published in *Shock and Vibration*
3	Identification of bridge mode shapes using Short Time Frequency Domain Decomposition of the responses measured in a passing vehicle	Published in *Engineering Structures*
4	A mode shape-based damage detection approach using laser measurement from a vehicle crossing a simply-supported bridge	Published in *Structural Control and Health Monitoring*
5	Application of Empirical Mode Decomposition to the Drive-by Bridge Damage Detection	Submitted to *European Journal of Mechanics-A/Solids*
6	Application of Hilbert-Haung Transform to Drive-by Identification of Bridge Mode Shapes	Submitted to *Journal of Sound and Vibration*

Chapter 2: A review of indirect bridge monitoring using passing vehicles

Authors:

Abdollah Malekjafarian

Patrick McGetrick

Eugene J. OBrien

Paper status:

Published in *Shock and Vibration*, Volume 2015, Article ID 286139, DOI: 10.1155/2015/286139.

Not to the reader:

This work is substantially the work of the author under the supervision of Prof. Eugene OBrien. Dr. McGetrick provided some paragraphs, comments and corrections to this chapter.

Chapter 2: A review of indirect bridge monitoring using passing vehicles

2.1. Introduction

There is an increasing demand for improved condition monitoring of transport infrastructure all over the world. Bridges are key components of transportation infrastructure and require such monitoring. There are 66,405 structurally deficient bridges in the United States (more than 11 percent of all bridges) and most of them are more than 65 years old (Davis and Goldberg, 2013). In Europe, the majority of bridges were built in the post-war period from 1945 to 1965 (Znidaric et al., 2011). The loading conditions of these bridges have changed in recent decades due to increased freight volumes and vehicle sizes. In addition, most of these bridges are subject to gradual deterioration over time and many are now structurally deficient. Rehabilitating and extending the lives of these structures raises important maintenance and safety issues.

Traditionally, bridge maintenance has relied on visual inspection methods which are highly variable, lack resolution and can only detect damage when it is visible. Therefore, structurally deficient bridges may be left undiscovered. A number of bridge collapses have occurred due to a lack of structural capacity information and Chupanit and Phromsorn (2012) have suggested that visual inspection alone may not be adequate for bridge health monitoring. In countries like Japan, which is prone to natural disasters, it is recommended that monitoring of engineering infrastructure such as bridges should be conducted continuously (Fujino and Siringoringo, 2011), particularly after each disaster. Bridge management systems (BMS's) with integrated bridge inspections have been developed in various countries (Akgul, 2012). It follows that an increase in bridge inspections to address existing structurally deficient bridges has considerable cost and practical implications for road owners and managers.

Structural Health Monitoring (SHM) methods rely on the automatic detection of anomalous structural behaviour. SHM using the dynamic response of structures is becoming an increasingly popular part of infrastructure maintenance and management systems. Some authors distinguish four levels for categorising SHM methods, most falling within the first three levels (Rytter, 1993, Carden and Fanning, 2004):

- Establish that damage is present
- Establish the location
- Quantify the severity
- Predict the remaining service life.

One of the most popular SHM approaches is the use of structural vibration data for non-destructive damage assessment. The underlying principle is that if damage occurs in a structure, it leads to changes in its physical properties, e.g. a loss of stiffness, and consequently causes measurable changes in its dynamic properties. Based on which dynamic properties or damage features are considered, such damage identification methods can generally be categorised in the following four groups (Fan and Qiao, 2011):

- Natural frequency-based methods;
- Mode shape-based methods;
- Curvature/strain mode shape-based methods;
- Other methods based on modal parameters.

All of these methods can be applied to a bridge as many of them assume beam and plate type structures. In most vibration-based bridge health monitoring techniques, large numbers of sensors are installed on the structure to monitor the dynamic properties (Carden and Fanning, 2004). For example, many sensors have been mounted in a case study in Southern California for bridge health monitoring over an eight year period, which included the occurrence of three earthquakes (Gomez et al., 2011). These approaches, in which sensors are installed directly on the bridge, are referred to here as direct methods and the on-site instrumentations may be costly, time-consuming, and even dangerous, depending on the location and type of bridge. The common practice is to mount the vibration sensors at different positions on the bridge and connect them to a data acquisition system. For the case where the ongoing traffic cannot be restricted for the purpose of installation, the task of equipment mounting may be risky. In addition, the implementation of SHM is not widespread for short and medium span bridges, which form the greatest proportion of bridges in service.

The idea of an *indirect* approach, in which the dynamic properties of bridge structures are extracted from the dynamic response of a passing vehicle, was proposed by Yang et al. (2004), (Yang and Lin, 2005). Such an approach is low cost and is aimed at reducing the

need for any direct installation of equipment on the bridge itself. It involves a vehicle instrumented with sensors through which dynamic properties of the bridge such as natural frequencies are extracted. Through interaction between the bridge and vehicle, the moving vehicle can be considered as both exciter and receiver. The measured vehicle response needs to include relatively high levels of bridge dynamic response in this vehicle-bridge interaction (VBI). The feasibility of this method in practice was experimentally confirmed by Lin and Yang (2005) by passing an instrumented vehicle over a highway bridge in Taiwan. In the case that only bridge frequency is required, the indirect approach shows many advantages in comparison with direct methods in terms of equipment needed, specialist personnel on site, economy, simplicity, efficiency and mobility.

Over the past decade, many researchers have presented new methods based on indirect bridge monitoring. Although the idea only considered the fundamental frequency of the bridge at first, it was later extended to the estimation of bridge damping and mode shapes, primarily targeting level 1 SHM. In addition, some other damage detection techniques have been proposed based on the dynamic response measured on the vehicle. This review is intended to introduce and summarise these approaches and provide recommendations for future development. It also aims to guide researchers and practitioners in choosing and implementing the available bridge damage identification algorithms and signal processing methods using the dynamic response of a moving vehicle.

2.2. Theoretical background for indirect bridge monitoring

The concept of an indirect approach utilising an instrumented vehicle, sometimes also referred to as 'drive-by bridge health monitoring', is illustrated by Figure 2-1. The vehicle is fitted with sensors, most commonly accelerometers and most commonly on its axles. Therefore, the vehicle passing over the bridge is effectively used as a 'moving sensor'. Figure 2-2 shows an example of a simplified VBI model used for a theoretical study of such an approach, a so-called quarter-car model. This simple model can be used to briefly explain the theoretical background supporting the concept. In Figure 2, the parameters m_s and m_u refer to the sprung and unsprung masses, representing the vehicle body and tyre assemblies respectively. K_s and K_t are the suspension and tyre stiffnesses respectively while C_s corresponds to the suspension damping. y_s and y_u are the time dependent vertical displacements of the sprung and unsprung masses respectively. The vehicle is assumed to travel at constant velocity c here.

As a vehicle crosses a bridge, both the vehicle and bridge vibrate and there is dynamic interaction between them. Therefore, the vehicle response is influenced by the bridge response. From the principle underlying SHM, it follows that if the bridge is damaged, e.g. due to bridge bashing or concrete cracking, the stiffness, damping and/or mass of the bridge change due to this damage and its vibration characteristics will also change. Eq. (2-1) and Eq. (2-2) give the equations of motion for the sprung and unsprung masses:

$$m_s\ddot{y}_s + C_s(\dot{y}_s - \dot{y}_u) + K_s(y_s - y_u) = 0 \tag{2-1}$$

$$m_u\ddot{y}_u - C_s(\dot{y}_s - \dot{y}_u) - K_s(y_s - y_u) + K_t(y_u - y_b - r) = 0 \tag{2-2}$$

where r and y_b are the road profile and bridge displacement, respectively. It can be seen from these equations that change due to damage can be detected in the vehicle response via the presence of the term y_b, the bridge displacement under the wheel of the vehicle. Therefore it is theoretically feasible to detect damage by using acceleration measurements in the vehicle alone – without using sensors on the bridge or the need to stop the vehicle. There is an added advantage of an indirect approach in that the moving sensor passes over all cross-sections of the bridge, unlike sensors at fixed positions. This can provide greater spatial information compared to direct SHM (Khorram et al., 2012, Kong et al., 2015).

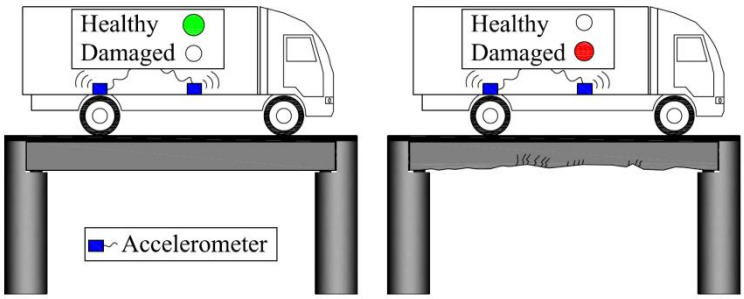

Figure 2-1 Indirect bridge health monitoring concept.

The theoretical study of the indirect monitoring concept can be extended to a range of VBI models of varying complexity incorporating, for example, vehicle pitching and rolling motions, inertial and centrifugal forces. A variety of models which allow for simplification of the problem have been used in the papers reviewed here. A comprehensive survey of the most commonly used VBI models is given by González (2010).

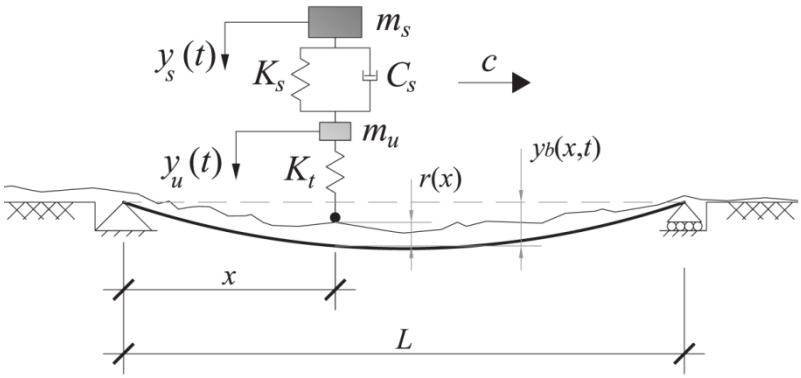

Figure 2-2 Quarter-car vehicle-bridge interaction model.

2.3. Indirect bridge monitoring

2.3.1. Indirect bridge frequency monitoring

The feasibility of extracting bridge frequencies from the dynamic response of a passing vehicle was first established by Yang et al. (2004). They use a theoretical closed-form solution of vehicle-bridge interaction – the vehicle is modelled as a sprung mass while the bridge is represented by a simply-supported beam, considering its first mode of vibration only. Vehicle acceleration measurements are processed using a Fast Fourier Transform (FFT) in order to obtain the bridge frequency. Through the analytical study, it is shown that the vehicle response is dominated by four specific frequencies; the vehicle frequency, driving frequency of the moving vehicle ($2\pi v/L$ in Figure 2-3 (a)) and two shifted frequencies of the bridge ($\omega_b \pm \pi v/L$ in Figure 2-3 (a)). In addition, it is shown that the extraction of bridge frequencies from the vehicle response is not restricted by any of the assumptions adopted in the analytical study. It is highlighted that frequency matching between the vehicle and bridge can be beneficial, a conclusion also reached in some subsequent studies (González, 2010, González et al., 2010b). The authors note that if the bridge and vehicle frequencies are close, vehicle resonance conditions can be achieved by adjusting the vehicle speed. As greater peak visibility is desirable, such conditions can be favourable for increasing the vehicle response magnitude and improving bridge frequency extraction. However, the speeds required to induce some resonance conditions may be unrealistic in practice unless the vehicle's dynamic characteristics can be altered. Nevertheless, it is noted that in general, higher speeds of up to 25 m/s (90 km/h) provide

higher visibility of the bridge frequency, as they induce higher amplitude responses in the bridge. This is an important initial finding as it suggests that it is feasible and possibly advantageous to implement the approach at highway speeds. Yang et al. (2004) find that increased bridge damping reduces visibility, but they do not study this effect in detail. This relationship between damping and peak magnitude has been investigated further for indirect SHM methods by a number of authors (McGetrick et al., 2009, González et al., 2012b, Keenahan et al., 2014, Keenahan et al., 2012). Further investigations are carried out by Yang and Lin (2005) to confirm the feasibility of the bridge frequency extraction idea.

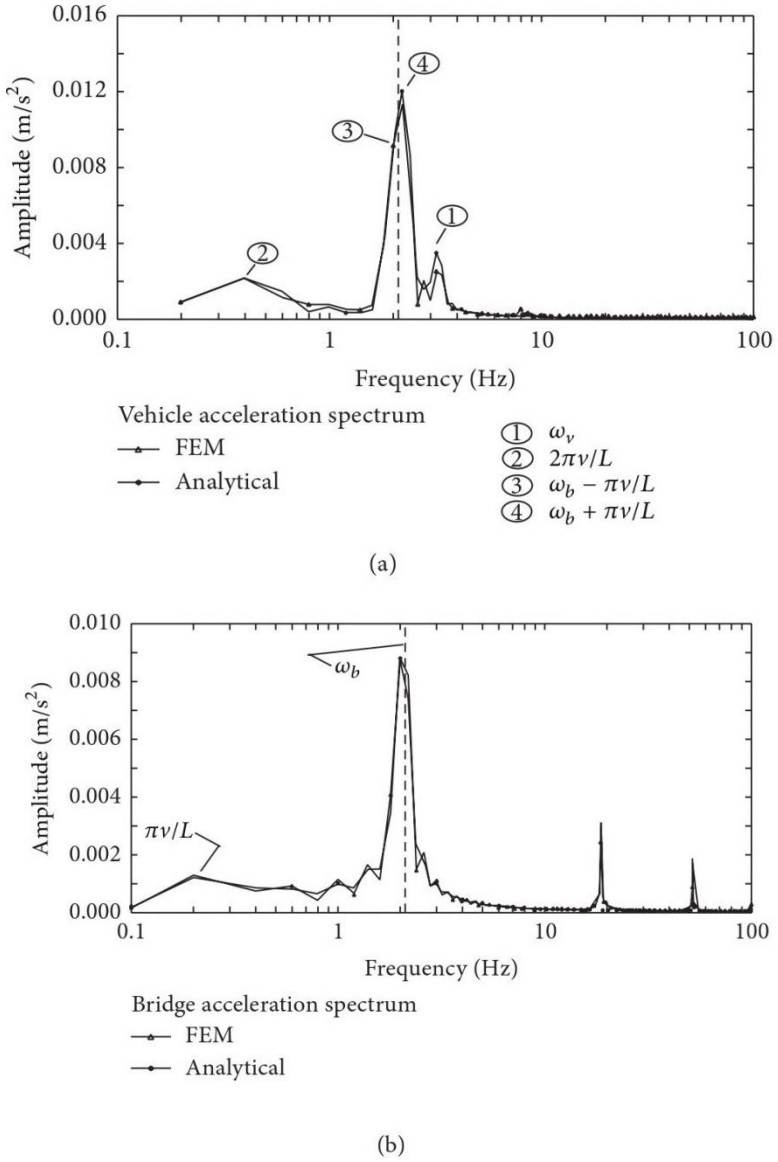

Figure 2-3 Vertical acceleration spectrum of (a) vehicle and (b) bridge midpoint. (Speed, v, is 10 m/s, ω_b is bridge natural frequency and ω_v is vehicle frequency) (Yang et al., 2004).

Following publication of the concept (Yang et al., 2004), many researchers have carried out studies extending the theoretical work and targeting experimental validations. The feasibility of extracting the bridge's fundamental frequency from the response of a passing vehicle is confirmed experimentally by Lin and Yang (2005). The authors employ a tractor-trailer system in a field test on a 30 m span prestressed concrete bridge in Taiwan. The tractor acts as the bridge exciter, while the trailer acts as the receiver of bridge vibration via accelerometers. In particular, they note that lower vehicle speeds (less than 40 km/h, or 11.1 m/s) provide the best results due to higher spectral resolution and a lesser influence of road surface profile on the trailer response. At higher speeds, high frequency components relating to the trailer structure and road profile become more dominant in the trailer response. This observation is in contrast to the original finding (Yang et al., 2004) that higher speeds can provide better visibility. However, the influences of the road profile and to a lesser extent, the trailer system, are not considered by Yang et al. (2004) which would account for this difference. These are also factors in the failure to extract higher bridge frequencies than the 1st from the trailer response. The authors recommend carrying out three tests at different speeds before confirming extraction of the bridge frequency. It is suggested that the existence of ongoing traffic is beneficial for the identification of bridge frequency from the vehicle. In particular, a heavy truck of weight 21.05 tons is used as ongoing traffic and is found to increase the bridge response, hence increasing the amplitude of the trailer response and improving frequency peak visibility.

Identifying the importance of the bridge excitation level, Oshima et al. (2008) also suggest using a heavy vehicle, one which incorporates an excitation machine, in addition to the scanning vehicle, in order to yield a constant vibration on the bridge. In a field experiment, it is shown that using such an excitation machine and repeating the test several times, can be beneficial for the extraction of low-order bridge frequencies. Oshima et al. (2009) also use independent component analysis (ICA) in a numerical study for the estimation the eigenfrequencies of a bridge from the vehicle response. The VBI system model is formed by combining state space and autoregressive (AR) models and a road profile is included in simulations. It is concluded that the approach estimates the road profile well but does not estimate the bridge response very well due to its dependence on the order of the assumed AR model. It is noted that several AR models should be evaluated to determine the best order while estimation was only possible at 20 km/h and 40 km/h.

Having confirmed the feasibility of the idea, Yang and Chang (2009a) study the effect of several key parameters, related to vehicle speed and acceleration amplitude ratios, on the dynamic response of a vehicle passing over a bridge in order to enable a more successful extraction of the bridge frequencies from the test vehicle. The authors note that the magnitudes of shifted bridge frequency peaks in the vehicle response relative to that of the vehicle frequency peak, are important for successful bridge frequency extraction. It is suggested that the most important variable is the initial vehicle/bridge acceleration amplitude ratio; the smaller this ratio, the higher the probability of successful bridge frequency extraction will be. The results of the investigation suggest that for speed, the primary consideration will be the practical amount of time needed for data collection on the bridge.

As the indirect approach proposed by Yang et al. (2004) only considers the first bridge mode, Yang and Chang (2009b) adopt the empirical mode decomposition (EMD) technique for pre-processing of vehicle measurements in order to make the bridge frequencies of higher modes more visible. The authors show that using the proposed method, the first few frequencies of the bridge are extracted in a numerical study and the second natural frequency is detected in a full scale experimental case study. As recommended by Lin and Yang (2005), at least three crossings of the bridge are completed in order to confirm successful frequency extraction. In contrast to the original study, it is suggested that it is preferable to adjust the frequencies of the test vehicle to avoid their coincidence with the bridge frequencies. In practice, this suggests using a specific monitoring vehicle for which all dynamic properties are known and/or designed.

Kim et al. (2011) and Toshinami et al. (2010) present the results of scaled laboratory experiments aiming to verify the feasibility of a drive-by inspection approach incorporating frequency detection. The experimental setup consists of a two-axle moving vehicle crossing a simply supported steel beam adopted as the bridge. A scaled road surface profile is incorporated via two tracks on the bridge. The authors show that the bridge frequency is extracted from the vehicle response, although the spectra of vehicle accelerations are dominated by the vehicle frequency. Three scaled vehicle speeds are investigated: 0.46 m/s, 0.93 m/s and 1.63 m/s, which correspond to speeds in reality of 10 km/h, 20 km/h and 40 km/h, respectively. Higher vehicle speeds provide larger magnitude frequency peaks in the spectra of the vehicle response; however, this also corresponds to lower spectral resolution. This suggests that speed should potentially be selected in order to provide a balance between

resolution and peak magnitude, although a practical alternative may be to carry out multiple runs at different speeds (Lin and Yang, 2005, Yang and Chang, 2009b).

Siringoringo and Fujin (2012) study a similar approach for the estimation of the bridge fundamental frequency. Theoretical simulations and a full-scale field experiment are carried out to support their approach, which is aimed at periodic bridge inspections using accelerations of a light commercial vehicle (Fujino et al., 2005). In theoretical simulations and a parametric study, it is shown that bridge frequency can be extracted from the vehicle response. In a field experiment, it is found that vehicle velocities below 30 km/h provide the best accuracy, for which a maximum estimation error of 11.4% is obtained. Similarly to a previous study (Lin and Yang, 2005), it is recommended to carry out modal testing of the inspection vehicle before bridge testing. In addition, it is noted that the dynamic response of the vehicle is dominated by its own bouncing and pitching motions at the bridge entrance/exit; this is due to the bridge expansion joints. Therefore, this part of the vehicle response should not be considered when seeking to estimate bridge frequency. Due to the short amount of time a monitoring vehicle will be on the bridge, losing any portion of the signal can be significant in terms of accuracy, particularly for short span bridges. Therefore, the effect of expansion joints on the vehicle response is an important issue to be overcome. The road profile can also have a similar effect on the vehicle response to that observed by Siringoringo and Fujin (2012) (i.e., the vehicle frequencies will usually appear as dominant peaks in the spectrum of the vehicle response and this makes it difficult to detect the bridge frequency peak). Yang et al. (2013a) address this issue by applying some filtering techniques to remove the vehicle frequency from the spectrum. They suggest that if the vehicle natural frequencies are available, it is possible to filter them out from the spectrum and enhance the visibility of the bridge frequency.

One of the most recent attempts at extraction of bridge frequency from a passing vehicle is based on optimization. Li et al. (2014) develop a new theoretical method based on the Generalized Pattern Search Algorithm (GPSA) which is a typical search method in optimization. The method is applied to the responses of a simplified vehicle-bridge interaction system consisting of a sprung mass vehicle and simply supported beam model. The algorithm is fast and an advantage of this approach is that it can identify other parameters besides the bridge's 1st natural frequency, e.g., the bridge stiffness, and thus may have potential to be developed for damage detection purposes. It is shown that the bridge frequency and stiffness can be identified with reasonable accuracy. The authors show that

the proposed method can still estimate the frequency accurately in the presence of noise. Although the method shows good robustness for different noise levels (with a maximum identification error of 3.3% for a signal to noise ratio of 5), the authors acknowledge that a road profile is not considered in the study, which can be one of the most significant factors in real applications.

In a theoretical investigation, Malekjafarian and OBrien (2014a) utilise a well-known output-only modal analysis method called Frequency Domain Decomposition (FDD), which is based on singular value decomposition (SVD) of the power spectral density (PSD) of the measured response, to process the acceleration response from a passing vehicle. In simulations, vehicles are represented by sprung masses in a simplified VBI model. The FDD method is applied to acceleration signals measured on two following quarter-cars. The effectiveness of the FDD method for the case of close bridge and vehicle frequencies is investigated in the presence of a road profile and for a low vehicle speed of 2 m/s. The authors show that the FDD method can identify both bridge and vehicle frequencies in this case and may be a useful alternative to classical Fast Fourier Transform (FFT) analysis, which does not reveal the frequencies clearly for the simulated scenarios.

In the original work by Yang et al. (2004), the vehicle acceleration spectrum for the simplified model was dominated by four frequencies; vehicle, driving and two shifted bridge frequencies respectively. However, in reality, variations in frequencies of the bridge and/or vehicle may occur due to the interaction between them during a vehicle crossing. Based on this, Yang et al. (2013c) study the variation of the instantaneous frequencies of bridges under moving vehicles. A theoretical framework is presented for the problem, considering the variation in frequencies for both the bridge and the moving vehicle. It is shown that, if a moving vehicle is to be used as a tool for measuring the bridge frequencies or for detecting bridge damage, the frequency variation caused by the moving vehicle should be taken into account, particularly for the case where the vehicle mass is not negligible compared with the bridge mass or when the resonance condition is approached.

Similar to variations observed by Yang et al. (2013c), Chang et al. (2014) find that the bridge frequency within a VBI system is different from that observed for the bridge system vibrating alone. In numerical simulations, a laboratory experiment and a field experiment, they investigate the variation of bridge frequencies due to interaction with a vehicle, focusing on bridge measurements and those of a vehicle parked on the bridge. The authors

derive an analytical formula to represent this variation, based on the frequency and mass ratios between the vehicle and the bridge. It is highlighted as an important consideration for VBI systems and has implications for indirect approaches as this variation, if not accounted for, may mask changes due to damage. Despite this, the authors' results indicate that the bridge frequency identified from the VBI system can also be extracted from the vehicle response.

Thus far, vehicle-based indirect approaches have been discussed. Recently, Yang et al. (2013b) introduce an alternative hand-drawn test 'cart' (trailer) in an experimental study aiming to measure bridge frequencies in a human-controlled, efficient, and mobile way. The authors highlight that the dynamic characteristics of the test cart are crucial for the successful extraction of the frequencies of the bridge. It is mentioned that the natural frequency of the cart is the key parameter that determines the transmission of energy from the bridge to the cart. It is also recommended that the cart frequency be selected so as to be greater than the fundamental frequency of the bridge for better visibility of the bridge frequencies in the cart response. In this study, the most suitable type of wheel is selected by conducting dynamic tests on three types of wheel; namely an inflatable wheel, a solid rubber wheel and a PU wheel respectively. The PU wheel consists of a metal wheel surrounded by a thin layer of polyurethane (PU). It is highlighted that the PU wheel is the most suitable for reliable frequency extraction as it has no frequencies in the bridge frequency range of interest and it maintains better contact with the road. Heavier carts provide better bridge peak visibility as they are less sensitive to the road surface roughness, while larger ongoing traffic flows are found to be beneficial for this alternative indirect approach also. The study illustrates the feasibility of accurate extraction of bridge frequencies using a well-designed cart and, based on these results, further development of the cart is recommended. While the qualitative conclusions are based on a hand-drawn cart; they are also likely to be relevant for vehicle-based indirect approaches operating at higher speeds.

Overall, it can be concluded that, although the feasibility of extracting the bridge frequency from the response of a passing vehicle, i.e. indirect bridge frequency monitoring, is now well established through theoretical and experimental investigations, there are a number of outstanding challenges that must be overcome before the approach becomes an effective and reliable system. The primary challenges that must be addressed are (1) the influence of the road profile on the vehicle response, which reduces the visibility of bridge frequency peaks and (2) the variation of the bridge frequency under a moving vehicle (Yang et al., 2013c,

Chang et al., 2014) during VBI. As this variation may mask any frequency change caused by damage, it is a significant challenge for bridge damage detection using indirect monitoring of the natural frequency.

Based on the literature presented, favourable conditions have been identified for successful bridge frequency extraction in practice as follows:

- Speeds below 40 km/h generally provide better results due to improved spectral resolution and reduced influence of road profile on the vehicle response.
- Multiple bridge crossings (at least 3) should be carried out at different vehicle speeds.
- Bridge excitation can be increased to improve bridge frequency peak visibility in the vehicle acceleration spectra. This can be done using a heavy vehicle, with or without an excitation machine, or by testing the bridge in the presence of other (ongoing) traffic. Increasing the vehicle speed will also have this effect but is not always recommended due to the consequent reduction in spectral resolution.
- Initial vehicle/bridge acceleration amplitude ratio should be small.
- Dynamic properties of the test vehicle or trailer should be obtained or calibrated *a priori*.

2.3.2. Indirect identification of bridge damping

Damping is another dynamic property which has been found to be damage sensitive (Curadelli et al., 2008, Modena et al., 1999). A small number of studies have been carried out in recent years for the estimation of bridge damping using an instrumented vehicle.

McGetrick et al. (2009) investigate the problem of identification of bridge natural frequency and damping ratio using a moving instrumented vehicle. The authors show that in the spectra of vehicle accelerations, the magnitude of PSD at both bridge and vehicle frequency peaks decreases with increased bridge damping (Figure 2-4). This suggests that even if a bridge frequency peak is not found, changes in bridge damping levels can be detected by analysing vehicle frequency peaks. It is suggested that changes in the magnitude of the PSD can be used as an indicator of damage in the bridge. However, the authors also note that it is difficult to detect both frequency and damping changes in the presence of a rough road profile. The results are confirmed experimentally in scaled laboratory experiments for repeated bridge

crossings and three vehicle speeds (McGetrick et al., 2010, Kim et al., 2014). The authors detect changes of the bridge damping in the vehicle spectrum, demonstrating the potential of the method for SHM.

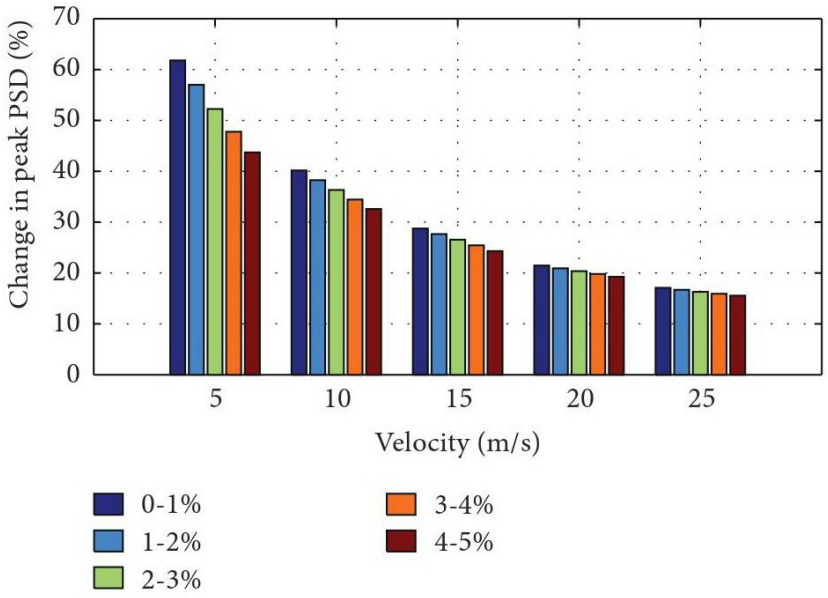

Figure 2-4 Peak vehicle PSD-bridge damping trends at bridge frequency peak for a 15 m span bridge for different velocities and a smooth road profile (McGetrick et al., 2009).

González et al. (2012b) propose a novel method for the identification of damping in a bridge using a moving instrumented vehicle, intended as a preliminary bridge condition screening method. The authors develop a six-step algorithm which uses the acceleration responses measured at the two axles of a half-car model. The bridge damping is identified with reasonable accuracy using an iterative procedure in theoretical simulations, with 88% of all simulations identifying the correct damping ratio within a 10% margin of error, and 40% of all simulations identifying the correct value within a 1% margin of error. In the parametric study, the method is found to be relatively insensitive to road profile, low levels of measurement noise and modelling errors. In particular, this method overcomes the effect of road profile highlighted in previous studies as the six-step algorithm actually estimates the road profile under each vehicle wheel; this is discussed in more detail in Section 3.4. Frequency matching between the vehicle and bridge is found to be beneficial when a pothole exists at the bridge entrance due to the resulting increase in bridge excitation. A stated advantage of this method is that it can also be extended to the estimation of the bridge

stiffness. This appears to be an important consideration, as damping can be difficult to quantify in practice (Williams and Salawu, 1997).

Although the indirect identification of bridge damping demonstrates some potential, it has certain limitations compared to approaches focusing on frequency and mode shapes etc. in terms of complexity related to the aforementioned quantification of damping. Therefore, the practical performance of indirect methods focusing on damping is a significant consideration and consequently, it may be beneficial to focus on alternative bridge dynamic properties, as presented in the other sections of this chapter. For example, the methodology presented by González et al. (2012b) for damping identification, can also be applied to the identification of bridge stiffness.

2.3.3. Indirect identification of bridge mode shapes

As mentioned, in recent years several researchers have developed methods to identify the bridge frequency from the acceleration signal in a passing vehicle while a limited number of authors obtain the damping ratio. A number of authors have also investigated the potential of an indirect approach to identify the mode shapes of a bridge. Estimation of bridge mode shapes is very important in a bridge dynamic investigation. This is because discontinuities occur in the mode shapes at points corresponding to the locations of damage in the bridge, including slope discontinuities at points of localised damage. Mode shape curvatures may be used to find these discontinuities (Zhu and Law, 2006, Pandey et al., 1991). Furthermore, bridge mode shapes can be used as an important tool in model updating of a bridge (Arora et al., 2009).

Zhang et al. (2012) model a moving vehicle passing over a bridge which is equipped with an accelerometer and shaker to control the applied force artificially, referred to as a ‘tapping vehicle’. They present a new damage index based on the point impedance measured from the vehicle, shown in Figure 2-5. A controlled force is applied to the bridge from the vehicle and the response of the vehicle to the load is measured and used for constructing the point impedance. It is shown that the amplitude of the spectrum obtained from the point impedance is approximately proportional to the square of the mode shape (MOSS, Figure 2-6) which can, in turn, be used for damage detection. Although the main purpose of the study is not estimation of bridge mode shapes, it is the first application known to the authors

of an indirect technique for identification of bridge mode shape-related properties. The authors highlight that the method can be extended to obtain the absolute value of the mode shapes. It should be noted however, that the levels of accuracy obtained with this method are for relatively low vehicle speeds – less than 5 m/s (18 km/h) – which has implications in practice.

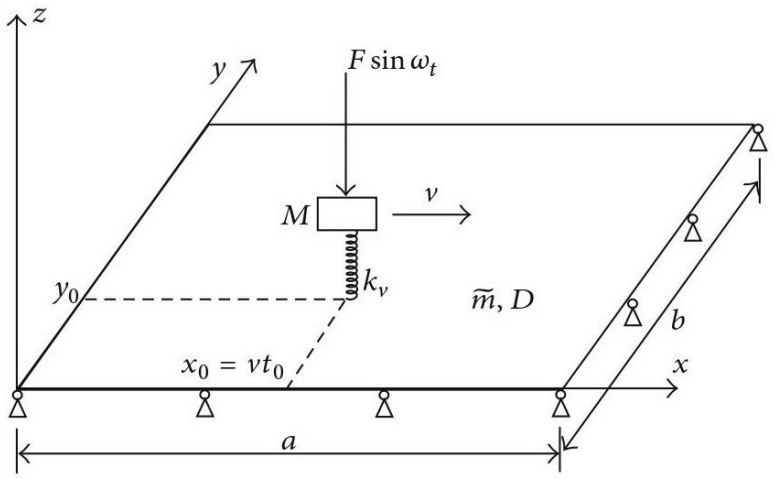

Figure 2-5 A passing tapping vehicle on a plate (Zhang et al., 2012).

Yang et al. (2014b) introduce a method for the indirect identification of bridge mode shapes based on a theoretical formulation. In the dynamic response of the test vehicle during its passage over the bridge, they show that the component response of the bridge frequency for a certain mode oscillates with a varying amplitude that is identical to the corresponding bridge mode shape. Therefore, once a bridge frequency is identified and its corresponding component response is separated from the vehicle response, the instantaneous amplitude history of the extracted component response can be regarded as being representative of the mode shape of the bridge. Hence, Yang et al. (2014b) propose a method based on the concept of instantaneous amplitudes obtained from the Hilbert transform of the band-pass filtered response of the vehicle. As the vehicle is effectively a moving sensor, the authors note that the indirect method can provide higher spatial resolution in mode shapes than corresponding direct approaches. Similar to Zhang et al. (2012), low vehicle speeds are tested, which are 2, 4 and 8 m/s (7.2, 14.4 and 28.8 km/h respectively). It is demonstrated that the method can detect mode shapes of lower modes accurately (Figure 2-7) while accuracy reduces for

higher vehicle speeds tested. Furthermore, additional random traffic on the bridge is found to have a negligible effect on extracted mode shape accuracy. However, the road surface profile causes a significant reduction in accuracy. The sensitivity of the method to measurement noise is not considered and the authors recommend experimental testing in order to confirm these findings.

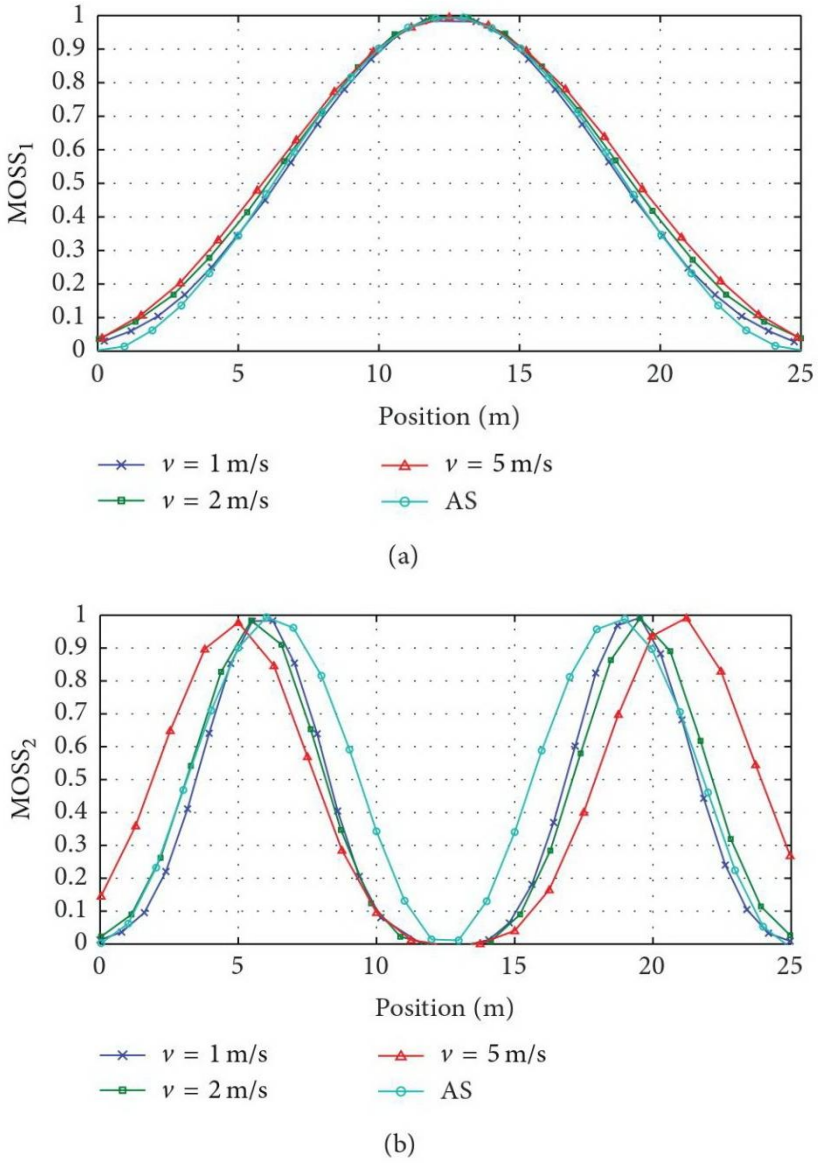

Figure 2-6 The extracted MOSS at different vehicle speeds compared with analytical solution: (a) mode 1 and (b) mode 2 (v is the velocity of the passing vehicle and AS is the analytical solution) (Zhang et al., 2012).

Oshima et al. (2014) investigate a theoretical bridge damage screening method which also involves the estimation of bridge mode shapes from the dynamic response of moving

vehicles. In this indirect approach, the estimated mode shapes, obtained in a four-step process via singular value decomposition, are used for damage detection. The authors note that mode shapes can be more sensitive to structural damage than frequencies and damping. The vehicle configuration consists of two heavy two-axle trucks (both of 10 t or 20 t mass), and at least four monitoring single-axle vehicles (0.1 t mass) at 1 m intervals; the trucks being used as bridge exciters. No additional excitation device other than the trucks is required – this is an advantage of the method over that of Zhang et al. (2012), which needs a tapping vehicle system to enhance bridge vibration. Accelerations of the monitoring vehicles and the relative displacement between the axle mass and the road surface are measured; it is proposed to obtain these measurements in practice using an accelerometer and a laser distance meter, respectively, fitted to the vehicle axles. Due to ill-conditioning of the inverse problem in this method, it is found that an increase in the number of vehicles can cause a decrease of estimation accuracy in simulations. However this may be counter-balanced by the increased nodes provided by additional vehicles for mode shape construction. Four monitoring vehicles are the focus as they are found to provide higher average Modal Assurance Criterion (MAC) values for the first 3 bridge modes than five or six vehicles. Damage scenarios include the fixing of one rotational support and a local bridge stiffness reduction of 40% at mid-span. In theoretical VBI simulations considering road profiles of varying roughness, damage is detected via the proposed mode shape estimation method by analysing average MAC values. Damage is detected for vehicle speeds varying from 5 m/s – 15 m/s (18 – 54 km/h), which are low compared to a highway speed range of 22.2 m/s – 27.8 m/s (80-100 km/h) but higher than speeds proposed for other indirect methods presented in this section, which could require temporary bridge and/or lane closures. However, when measurement noise greater than 1% is considered in simulations, it is found that the damage detection approach requires an impractical number of measurements. This is a drawback for the practical application of this indirect method and the authors acknowledge the necessity for further improvement of its robustness against noise.

Malekjafarian and OBrien (2014b) propose the use of Short Time Frequency Domain Decomposition (STFDD) for indirect identification of bridge mode shapes using responses measured from two following axles passing over a bridge. They apply the FDD method to the short time measured signals obtained at several defined stages and perform a rescaling procedure on local mode shape vectors to obtain the global mode shapes. The effect of road

profile in exciting the vehicle is a significant challenge for the method. It is shown in a case study that excitation of the bridge by external forces applied to all parts of the bridge (simulating other traffic) improves the situation. In the absence of other traffic, subtraction of signals in identical axles is shown to be a feasible alternative. If noise is sufficiently low and the vehicle speed is 2 m/s or less, mode shapes can be found with reasonable accuracy. In addition, it is found in this study that applying ongoing traffic can reduce the sensitivity of the method to noise.

Although the study by Zhang et al. (2012) can be considered as the first attempt at indirect identification of bridge mode shapes, the method is based on utilising an excitation machine via the vehicle and measuring the excitation force, which may be not an easy task to perform in a real case. However, a similar apparatus has been tested in a field experiment by Oshima et al. (2008). Recently, some interesting ideas (Yang et al., 2014b, Oshima et al., 2014, Malekjafarian and OBrien, 2014b) have been proposed which are based on only the response measured by a passing vehicle. The method proposed by Yang et al. (2014b) provides high resolution mode shapes with acceptable accuracy, particularly for the first mode shape (Figure 2-7). However, the performance of the method in the presence of measurement noise needs to be investigated. On the other hand, the methods proposed by Oshima et al. (2014) and Malekjafarian and OBrien (2014b) both provide the bridge mode shapes with low resolution. In addition, the former study (Zhu and Law, 2006) shows high sensitivity to measurement noise which is an inherent characteristic of a real measurement system. Malekjafarian and OBrien (2014b) suggest some ideas to minimise the effect of road profile which seems to be applicable in a noisy measurement. An important consideration here is vehicle speed; these approaches all focus on very low vehicle speeds which are likely to require bridge lane closures in practice, although the approach by Oshima et al. (2014) extends to a speed of 15 m/s (54 km/h).

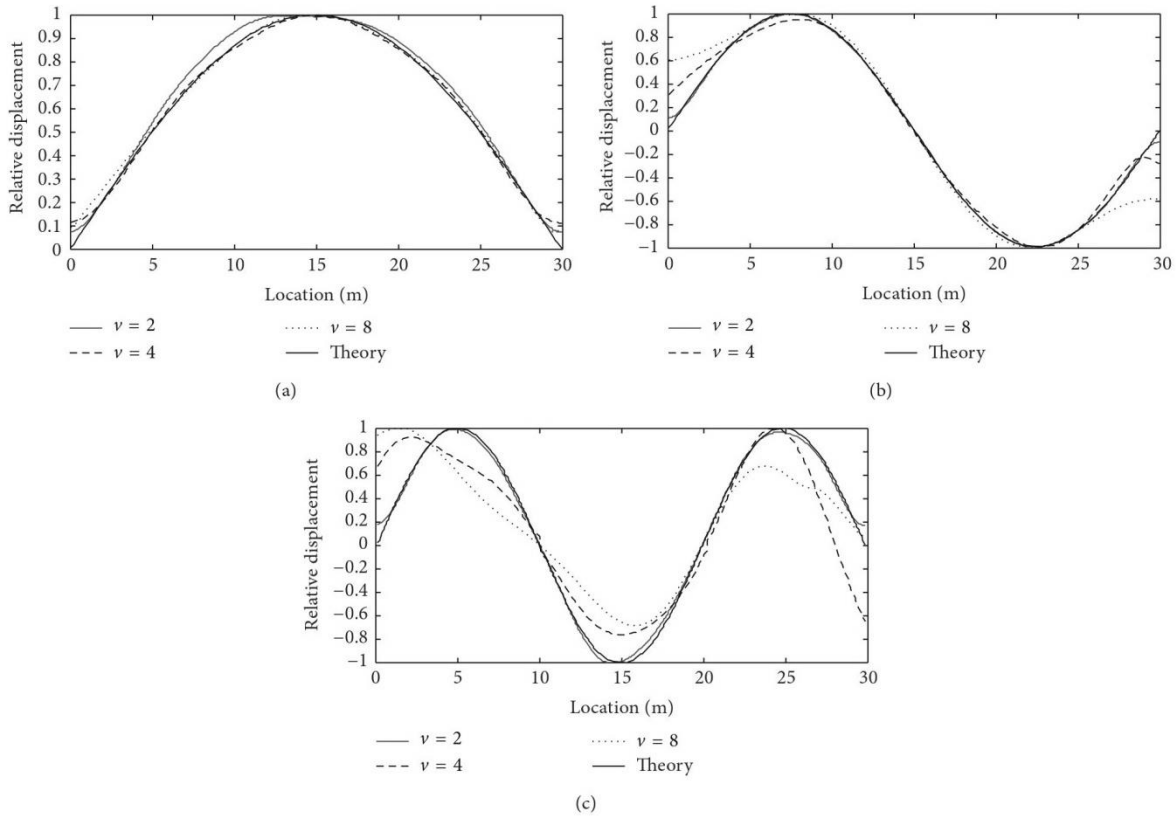

Figure 2-7 Mode shapes of the bridge obtained for different vehicle speeds (v, m/s) compared with theoretical result (theory): (a) 1st mode, (b) 2nd mode and (c)3rd mode (Yang et al., 2014b).

Overall, it seems that indirect bridge monitoring methods focused on the identification of bridge mode shapes have potential and possess many advantages in terms of damage detection and damage localization. However, these methods are currently limited by a lack of experimental case studies which may reveal practical challenges. Based on the existing investigations in the literature, it can be concluded that these methods need to be improved considerably and further validation is required to support successful implementation in practice, focusing on the following areas:

- Increased mode shape resolution
- Reduction in sensitivity to measurement noise
- Implementation at higher vehicle speeds
- Experimental case studies

2.3.4. Effect of road surface profile on vehicle-bridge interaction

As discussed above, the road profile on the bridge has been considered by authors to varying degrees; from ignoring it entirely to including a range of road profiles with varying roughness levels. Overall, it can be concluded that consideration of the road surface profile in indirect methods is a critical issue as it can excite vehicle-related frequencies to a much higher amplitude level than bridge-related ones, making it difficult to identify the bridge frequencies, damping ratios and mode shapes (Yang et al., 2012a, Yang et al., 2014a). It follows that any condition monitoring or damage detection methods which are based on these dynamic parameters are also significantly affected by the road surface profile unless some technique is applied to reduce its influence on the vehicle. Despite efforts to overcome the effect of road profile, it is still an important challenge for indirect methods that needs further investigation.

The first approach to resolving this issue is to use the excitation due to ongoing traffic to increase the relative influence of the bridge in the vehicle response (Yang et al., 2004, Yang and Chang, 2009a, Yang et al., 2013b, Malekjafarian and OBrien, 2014a, Malekjafarian and OBrien, 2014b). Unfortunately, this is not a good assumption for short-span bridges where the probability of multiple vehicles being present simultaneously on the bridge is small.

The indirect method developed by González et al. (2012b) shows potential for the removal of the road profile's influence. Instead of just considering the road profile as an extra input excitation to the VBI model, the algorithm identifies the damping ratio of the bridge by considering the differences in displacement under the wheels of the instrumented vehicle which effectively removes the influence of road profile. Other methods based on subtraction have also been investigated. Yang et al. (2012b) propose a new idea of using two connected vehicles to remove or reduce the effect of road profile from the vehicle spectrum. The authors introduce a residual spectrum by subtracting the acceleration spectra obtained from two connected axles passing over a bridge at the low speed of 2 m/s. It is demonstrated that the bridge frequency peaks are slightly improved, specifically for the case when two identical axles are used. In addition, too large of an axle spacing is not recommended, as the axles may lose their correlation.

Keenahan et al. (2014) propose another version of the subtraction idea. In this study, the accelerometers are mounted on the axles of a trailer that is being towed by a truck in a truck-

trailer system (Figure 2-8) moving at a speed of 20 m/s – much higher than that investigated by Yang et al. (2012b) – and the difference in the accelerations between the two axles is considered. It is demonstrated that the influence of road profile is removed in the FFT spectrum of the difference between accelerations, when two identical trailer axles are used. Although the authors provide an effective method to remove the effect of road profile, the accuracy of the method is highly dependent on the similarity of the axles, as was found by Yang et al. (2012b) for the lower speed. In addition, it seems that the method is sensitive to environmental noise so accurate accelerometers are required.

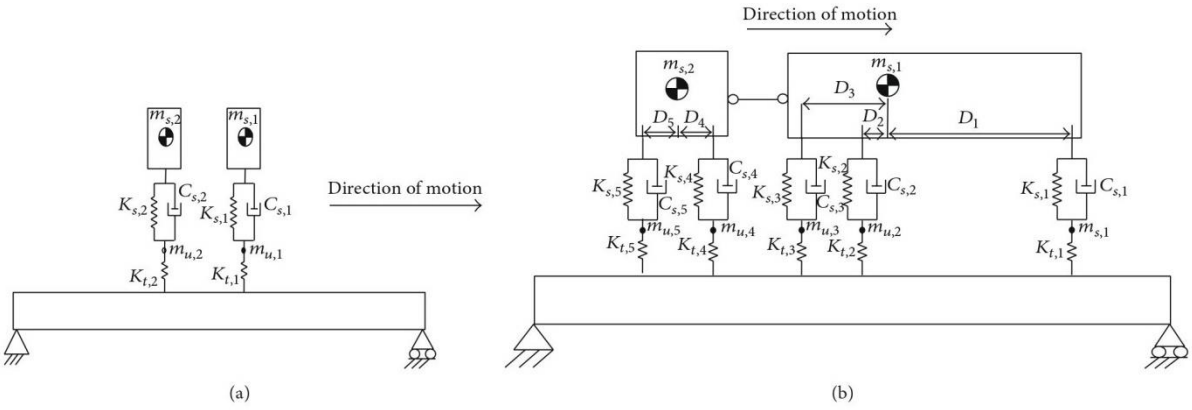

Figure 2-8 (a) Two identical quarter-cars, (b) Truck–trailer model (Keenahan et al., 2012).

Other indirect approaches have been developed which aim to measure road surface profile from the acceleration response of a moving vehicle (Fujino et al., 2005, González et al., 2008a) . The vehicle intelligent monitoring system (VIMS) presented by Fujino et al. (2005) targets highway pavements and bridge expansion joints and also utilises a GPS sensor mounted in the vehicle to identify the position where the acceleration response is recorded. The theory behind such algorithms and techniques incorporates optimisation, transfer and correlation functions which may provide a basis to further reduce the influence that road surface profile has on vehicle acceleration measurements.

2.4. Damage detection methods using indirect measurements

This section reviews indirect methods for the detection of bridge damage that do not explicitly require the identification of bridge dynamic properties. A range of miscellaneous ideas for damage detection are reviewed in section 2.4.1 including the use of Moving Force Identification (MFI), Operating Deflection Shape (ODS), displacement response, modal

strain energy, transmissibility and classification. Damage detection methods based on wavelet transforms are reviewed in section 2.4.2 and finally methods employing a traffic speed deflectometer (TSD) are introduced in section 2.4.3.

2.4.1. Miscellaneous methods

As one of the earliest efforts in indirect monitoring of bridges, Bu et al. (2006) propose a damage detection technique using an acceleration response sensitivity matrix that maps all the sensitivities as a function of vehicle position on the bridge. In a numerical investigation focusing on damage in terms of a reduction in bridge stiffness, a damage index is defined and updated in an iterative procedure. The numerical results obtained in this study show that the method is computationally stable and efficient for a quarter-car vehicle and can function in the presence of measurement noise and a road surface profile.

Kim and Kawatani (2009) investigate the feasibility of bridge drive-by inspection through a laboratory experiment, focusing on damage related to bridge stiffness, similar to Bu et al. (2006). It is shown that frequency changes caused by damage can be detected by the vehicle response. Furthermore, the authors integrate the indirect method with direct bridge measurements to find the location of the damage using a damage index called ESI which defines the change in the bending rigidity of the bridge at different locations. Kim et al. (2014) extend their method to include a combination of direct and indirect monitoring of short span bridges for structural diagnosis. In theoretical simulations and a scaled laboratory VBI experiment, three screening levels are presented which utilize vehicle and bridge responses both separately and together in order to identify bridge dynamic parameters and also to detect the severity and location of damage. Overall, each level is shown to be effective and for all screening levels, better identification results are found for lower vehicle speeds and for vehicles with bounce frequencies similar to the fundamental frequency of the bridge. The authors note that further study is required for accurate interpretation of damage patterns, damage sensitivity of the approaches and finally, for the simultaneous acquisition of accurate data from the moving vehicle and the bridge.

OBrien et al. (2014) apply Moving Force Identification, a method of finding the time history of forces applied to the bridge, and show that the calculated pattern of applied force is sensitive to bridge damage. The potential of the method to identify the global bending stiffness of the bridge is presented. Stiffness identification accuracy is found to be high for

a very good road profile and low levels of signal noise, although accuracy decreases with increasing signal noise and road roughness. It is suggested that increasing the bridge displacement under the vehicle would assist with this increase.

As discussed above, Zhang et al. (2012) propose a new damage index based on the point impedance measured from a tapping vehicle. It is shown that the method is very robust in the presence of noise. Although it shows very good accuracy, it is not based on the acceleration response of the vehicle only as the applied force is being controlled (by a shaker) and measured at the same time in order to construct the point impedance. Therefore, the practical application of such a moving shaker on a real bridge is an important issue to be addressed. The authors recently improved their method by using the Operating Deflection Shape Curvature (ODSC) extracted from the same device, for damage detection (Zhang et al., 2013). They use a pre-filtering process based on wavelet decomposition to obtain a smoother ODSC. Furthermore, a new damage detection algorithm called the Global Filtering Method (GFM) is proposed to eliminate the requirement of a baseline with the assumption that the intact structure is smooth and homogenous. The Gapped Smoothing Method (GSM) and GFM, based on the extracted ODSC's at relatively few frequencies near the first natural frequency of the structure, can detect local damage accurately and the latter exhibits better performance than the former in both numerical simulations and experiment.

Yin and Tang (2011) extend the application of the indirect method to a cable-stayed bridge. They seek to identify cable tension loss and deck damage using the displacement response of a moving vehicle crossing over the bridge. The vehicle is modelled as a sprung mass and the VBI is simulated by a finite-element method. The approach is based on Proper Orthogonal Decomposition (POD) of the difference between the displacement responses of a vehicle passing the damaged and the healthy bridges respectively; this difference being considered as a relative displacement response. The method appears to perform quite well but has some drawbacks. The authors do not consider any road profile in their investigation which has been shown to have a very important influence on the vehicle response in previous studies. In addition, the authors recommend the use of a more complex VBI model. Finally, they note that highly sensitive equipment, such as laser displacement sensors, would be required due to the small amplitude of the displacement response to a single vehicle on a large bridge.

Miyamoto and Yabe (2011), Miyamoto and Yabe (2012) develop a promising approach that could be termed crowd sourcing. They propose a bridge monitoring system based on vibration measurements on an in-service public bus. Safety, or damage indices are developed for short- and long-term monitoring, namely a structural anomaly parameter and a characteristic deflection, which are extracted from bus vibration measurements. In a field experiment, the effectiveness of using an accelerometer on the rear axle of the bus is compared with placing one at bridge mid-span and it is found that the approach is feasible as long as the same bus is used for all measurements. By taking a number of repeated measurements and averaging, the influence of noise is reduced. The characteristic deflection is estimated by using acceleration wave integrals obtained by the Fourier transform and is considered to be relatively insensitive to vibration characteristics of the bridge and vehicle and dynamics related to road profile. The authors suggest that when the characteristic deflection has exceeded a certain limit, it can be judged that the bridge is showing signs of deterioration. Yabe et al. (2013) extend the study of the monitoring system to include varying operating conditions such as weather, number of bus occupants, vehicle speed and oncoming traffic and illustrate its effectiveness.

Li and Au (2014) suggest a multi-stage damage detection method based on modal strain energy and the Genetic Algorithm (GA). The modal strain energy based method estimates the damage location by calculating a damage indicator from the frequencies of the vehicle response for both the intact and damaged states of the bridge. Frequencies are extracted using Empirical Mode Decomposition. At the second stage, the identification problem is transformed into a global optimization problem and is solved by GA techniques. The approach can successfully determine the location of damage in a two-span continuous bridge with one damaged element. As in other studies, it is found that the method is influenced by the road profile and measurement noise. The authors compare the proposed method with wavelet-based and frequency-based damage detection methods in (Li and Au, 2015) to show its ability in the presence of a road profile.

Kong et al. (2015) propose an indirect method for bridge damage detection utilising one or more vehicles passing over the bridge. The concept of transmissibility is applied to the dynamic response of moving vehicles in a coupled vehicle-bridge interaction system. Acceleration responses are measured on two vehicles as they pass over the bridge. However, these vehicles are required to stop at different locations on the bridge for measurement. The authors extract the natural frequencies and modal shape squares of the bridge for damage

detection using the transmissibility of these vehicle responses. Two different configurations are tested; firstly, one moving and one reference vehicle and secondly, two moving vehicles with constant spacing. It is found that vehicle transmissibility is sensitive to low-frequency bridge responses. The authors suggest that random traffic flows and vehicle speeds between 10 m/s and 20 m/s (36 km/h and 72 km/h) may provide more suitable conditions for damage detection in the real world application of this method, although it is quite sensitive to road profile.

Cerda et al. (2012) compare the results of an indirect bridge health monitoring technique with the direct approach in a laboratory scale model experiment in which bridge frequency changes are detected. In the experiment, a two-axle vehicle travels across a simply supported bridge consisting of an aluminium plate and angles. Changes to the bridge condition are made by adding localised mass at mid-span and bridge frequency changes are identified by averaging the short-time Fourier transform of acceleration measurements. Direct on-bridge measurements are found to be most stable in identifying frequency changes while the vehicle's front sprung mass measurement provided the best results for the indirect approach. The authors also note that lower vehicle speeds provide better results. Cerda et al. (2014) extend the experimental investigation of the indirect bridge health monitoring technique to include two further damage scenarios and a greater number of data samples while new frequency-based damage features are used to identify the severity and location of damage. The two damage scenarios involve rotational restraint of a support and an increase of damping at different locations using adjustable dampers. To classify the damage features, a support vector machine classifier is used. The authors note that overall, damage of greater severity is detected with higher classification accuracy and also, damage detection is not very sensitive to vehicle speed. However, it is also acknowledged that the technique requires training data. Lederman et al. (2014) expand on the work of Cerda et al. (2014) by performing a regression on a large dataset of damage locations and severities, using the same experimental model. The authors demonstrate that the new method can provide better resolution in terms of damage location and severity. Chen et al. (2014) suggest the application of the concept of classification to indirect bridge structural health monitoring. Generally, classification is a signal processing approach whose purpose is to design a map that relates each input with a predefined class label. Although the authors are aiming to improve the concept of classification, the proposed method has been applied well in indirect approaches.

Tsai et al. (2014) investigate a railway track inspection method but also study the possibility of detecting the response of the bridge in that of the inspection car. However, it is found that bridge responses and frequencies could not be easily identified by the inspection car without a sophisticated analysis while the duration of the vehicle crossing is also identified as being a drawback of such an approach. This highlights some practical considerations for real-world applications in highway and potential railway applications.

2.4.2. Wavelet transform

A number of damage detection approaches incorporating wavelet theory have been proposed. Nguyen and Tran (2010) apply a Symlet wavelet transform to the displacement response of a moving vehicle to identify the existence and location of cracks in a bridge. Theoretical simulations are carried out using a cracked finite element (FE) beam model and a 4 degree-of-freedom half-car vehicle model. A two-crack scenario is investigated for varying vehicle speed (2 m/s - 40 m/s), while crack depth is also varied as a percentage of the beam depth. Peaks at particular scales are observed in the wavelet transform of the vehicle displacement response when it passes over crack locations while crack depths of up to 10% are detected (cracks at A, B, C and D, Figure 2-9). It is found that deeper cracks are easier to detect while higher speeds provide poorer detection ability. The effect of white noise on crack detection is investigated and for 6% noise, a 50% crack depth is detected at 2 m/s. Overall, low speeds are recommended for accurate crack detection using this approach, which would have implications in practice, similar to a number of other indirect approaches presented in previous sections. Experimental testing is recommended by the authors who do not consider the road profile in their study.

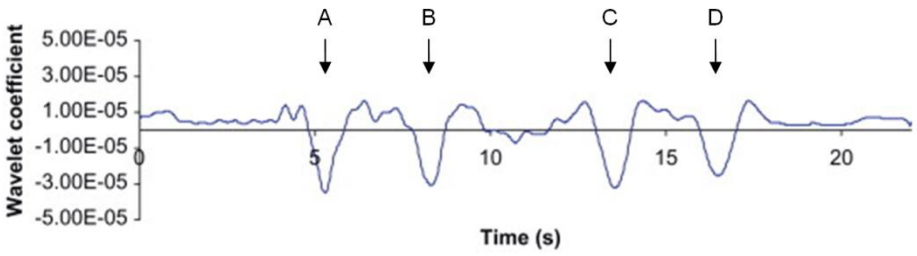

Figure 2-9 Wavelet transform of vehicle displacement when two cracks are considered at $L/3$ and $2L/3$ of the beam with 30% crack depth and speed of 2 m/s. (A; first axle passing $L/3$, B; second axle passing $L/3$, C; first axle passing $2L/3$, D; second axle passing $2L/3$). (Nguyen and Tran, 2010).

Khorram et al. (2012) also carry out a numerical investigation to compare the performance of two wavelet-based damage detection approaches. A very simple VBI model is used to compare two methods which utilise a Gaussian 4 wavelet transform: a "fixed sensor approach" and a "moving sensor approach", which are direct and indirect methods respectively. The continuous wavelet transform (CWT) coefficients of time varying beam and vehicle displacements respectively are used to identify cracks which are modelled as rotational springs connecting elements. The vehicle or 'moving' sensor is found to be more effective than the fixed sensor and small cracks with a depth of more than 10% of beam depth are detected. The authors develop a damage index which has an explicit expression and can identify crack depth as well as location. Although the proposed damage index shows good performance, the vehicle is idealised as a moving force and therefore does not consider the interaction between the vehicle and bridge or the effect of road profile.

McGetrick and Kim (2013), (McGetrick and Kim, 2014b)McGetrick and Kim (2014b) apply a CWT to the dynamic response of a vehicle passing over a bridge. It is shown that when the axle passes over a damaged section, any discontinuity in the signal affects the CWT coefficients, allowing damage to be identified and located. Based on these coefficients, a damage indicator (DI) is formulated which can distinguish between different damage levels, regardless of vehicle speed. Theoretical, experimental and field investigations are performed showing that the resulting DIs for the bridge and vehicle follow similar patterns. In simulations, vehicle speeds of 2, 5, 10, 15 and 20 m/s are tested. Lower vehicle speeds provide higher resolution allowing damage detection to be located more accurately. However, it is difficult to distinguish between different artificial damage scenarios in the field experiment for the test vehicle speed of 40 km/h (11.1 m/s). A pattern-adapted wavelet is formulated and found to be beneficial for damage localisation in theoretical and experimental investigations; however its formulation requires prior knowledge or accurate estimation of bridge damage discontinuities (McGetrick and Kim, 2014a). The vehicle's transverse position on the road is also highlighted as having a significant influence on the DI's sensitivity to damage level, which may have implications for such an approach in practice.

These findings suggest that there are several advantages supporting further investigation of the use of wavelets for indirect bridge damage detection. In indirect damage detection, the

vehicle is only on the bridge for a short length of time. This creates a challenge for conventional signal processing techniques (such as FFT), that are designed for infinite time series. Wavelets do not have this limitation which makes them particularly suited to this particular problem.

Wavelet methods have demonstrated the potential to detect, quantify and locate bridge damage, i.e. to achieve level 3 SHM. However, further investigation is recommended to improve damage detection accuracy at higher vehicle speeds. Currently, a drawback is the necessity to close bridge lanes due to low operational speeds of around 2 m/s (7.2 km/h) but there is a possibility that the advantages of a highly accurate wavelet-based method could offset this. In addition, unless the vehicle's transverse position on the bridge is well controlled, there is a need to overcome the high sensitivity to its variation.

2.4.3. Traffic speed deflectometer

The prototype Rolling Weight Deflectometer (RWD), presented first by Briggs et al. (2000) in the United States, was designed for the indirect measurement of road pavement stiffness. It is proposed as a replacement for the Falling Weight Deflectometer (FWD) which determines stiffness but which must stop at each test site for several minutes. More recently, the 'High-speed Deflectograph', later renamed the 'Traffic Speed Deflectometer' (TSD) has emerged, capable of performing stiffness surveys at speeds of up to 80 km/h, avoiding traffic disruption and expensive traffic management. The TSD is a collection of non-contact lasers mounted at equal spacing on a rigid beam, housed in the trailer of an articulated lorry. Laser vibrometers continuously and very accurately measure velocities (related to distances between sensors and the road surface). It is already a proven technology for flexible pavements and trials have been carried out in a number of countries (e.g., Flintsch et al. (2012)). For pavement applications, it only measures the 'trough' (local depression) under a heavy axle as an indicator of pavement stiffness.

In numerical vehicle-bridge interaction simulations, Keenahan and OBrien (2014) investigate the use of the TSD in a drive-by bridge damage detection context. A TSD model with three displacement sensors is proposed for bridge damage detection, which removes the bounce motion of the vehicle and the road profile influence. Different levels of damage are considered, and the approach also looks at changes in the transverse position of the

vehicle and the addition of noise. OBrien and Keenahan (2014) propose an alternative use of TSD vehicle data. They show that such a vehicle can accurately detect the 'apparent profile', i.e., the road profile that would be consistent with the velocity measurements if no bridge were present. They go on to show that this apparent profile is quite sensitive to bridge damage.

2.5. Conclusions and Recommendations

The authors' opinions on indirect methods of monitoring are summarised in Table 1. Historically, natural frequency is perhaps the most popular indicator of bridge damage and it can be found by indirect methods. However, it is generally accepted that the frequency changes caused by damage tend to be small and may be masked by the changes caused by environmental and operational conditions. Furthermore, frequency changes alone are not sufficient to uniquely define the location of structural damage (Fan and Qiao, 2011). Furthermore, most of the studies considered assume constant speed of the passing vehicles while in practice, it may not be easy to maintain this during the vehicle crossing. This factor becomes more significant when the signals of two axles are subtracted to minimise the influence of road profile. Therefore, speed variation should be investigated in future studies. The bridge damping coefficient can also be found from the response to a passing vehicle and most of the influence of road profile can be removed by subtracting the signals from successive trailer axles – provided those axles have identical properties. It is reasonable to assume that cracking in concrete structures would increase damping but it is less clear if such a link exists for steel structures. Furthermore, it is widely reported that damping is strongly influenced by environmental factors such as temperature which is likely to mask the effects of damage.

Mode shapes and modal curvature are generally considered to be good indicators of bridge damage, especially local damage that may cause a spatial discontinuity in the response. However, finding mode shapes indirectly remains a challenge. Recently, identification of bridge mode shapes from the vehicle response has attracted considerable interest. Zhang et al. (2012) model a tapping vehicle (with an oscillating mass on board) but, even at very slow speeds, only the first mode shape is found accurately and applying such a device in the case of a real bridge tends to be expensive. Other authors (Yang et al., 2014b, Oshima et al., 2014, Malekjafarian and OBrien, 2014b) do not require a tapping vehicle but the accuracy is generally poor unless there is a little measurement noise and the road surface is perfectly

smooth. However, indirect mode shape-based methods have good potential for further development in the future due to the strong influence of local damage on mode shape.

There have been several attempts to detect damage without finding the conventional dynamic properties of the bridge (e.g. Bu et al. (2006); Kim and Kawatani (2009); OBrien et al. (2014)). Many of these authors identify evidence of damage in wavelet transforms of the measured signal. Wavelets are a means of amplifying particular features, such as discontinuities in a signal and do not need long time series for good results. However, there are edge effects near the beginning and end of a bridge which can cause problems in these areas.

A particularly promising development is the concept of using vehicle-mounted laser vibrometers to obtain highly accurate measurements of the relative velocity (and hence displacement) between a moving vehicle and a bridge. OBrien and Keenahan (2014) have developed a damage indicator from such measurements that appears to be highly damage-sensitive. There is scope for a great deal of further development using such vehicles as the accuracy of the measurement should allow relatively minor damage to be detected.

A major obstacle to any form of rapid damage detection is temperature/environment which can have a significant effect on most damage indicators and whose influence is difficult to distinguish from real damage. It is shown in the literature that the natural frequency is highly influenced by temperature. In many cases the frequency shift due to damage in the structure is less than that corresponding to the temperature effect. This can be addressed by instrumenting vehicles that travel on the same route frequently as this allows environmental effects to be averaged out. The bridge mode shapes have been observed to be less sensitive to temperature change. It means they could be better criteria for damage detection.

In summary, the main challenges for indirect bridge monitoring methods are:

- The road profile.
- The limited VBI time.
- Environmental effects.

Good progress has been made in addressing the influence of the road profile with the concept of subtracting signals from identical axles, although this requires very high measurement accuracy. The speed of the vehicle means that it is only present on the bridge for a limited time. This results in an inevitable shortage of vehicle-bridge interaction measurement data.

Some studies require that speeds are very slow to address this problem but this is not ideal on busy roads where congestion may result. The final challenge in indirect monitoring is interference from environmental effects such as temperature. The most promising approach to tackle this issue is indirect monitoring using vehicles that repeatedly pass over the bridge. The potential of indirect methods is well illustrated in the literature, as discussed in this chapter. Therefore, overcoming these challenges would represent a big step towards successful implementation of indirect bridge monitoring methods in practice.

Table 2-1 Indirect bridge monitoring summary (SHM levels: 1 = Detect existence of damage, 2 = Detect damage location, 3 = Detect damage severity)

Method		SHM level	Advantages	Drawbacks
Modal parameter based methods	Natural frequency	1	Simple. Demonstrated in many experimental works. Acceptable vehicle speed.	Not always sensitive to damage. Low frequency resolution when vehicle speed is high.
	Damping	1	Sensitive to damage.	Complexity.
	Mode shape	1 and 2	Local information. Sensitive to damage.	Low vehicle speed. Sensitive to noise. No experimental confirmation.
Non-modal parameter based methods	Crowd sourcing	1	Field experiments. ongoing in service conditions.	Only feasible using same vehicle for all measurements. Damage sensitivity unconfirmed experimentally.
	Wavelet	1 ,2 and 3	Algorithms widely available.	Low vehicle speed. Relies on local anomalies in the signal. Results can be compromised by edge effects.
	TSD	1	Very high accuracy of measurements. High vehicle speed.	Expensive equipment. No experimental confirmation.
	Other	1, 2 and 3	Novel numerical algorithms for damage detection	Limited experimental confirmation.

Chapter 3: Identification of bridge mode shapes using Short Time Frequency Domain Decomposition of the responses measured in a passing vehicle

Authors:

Abdollah Malekjafarian

Eugene J. OBrien

Paper status:

Published in *Engineering Structures*, Volume 81, 15 December 2014, Pages 386–397

Not to the reader:

This work is entirely the work of the author under the supervision of Prof. Eugene OBrien.

Chapter 3: Identification of bridge mode shapes using Short Time Frequency Domain Decomposition of the responses measured in a passing vehicle

3.1. Introduction

There is a long history of the use of natural frequency as an indicator of structure and bridge health (Salawu, 1997, Kim and Stubbs, 2003). Damping ratios (Curadelli et al., 2008, Williams and Salawu, 1997) and mode shapes (Kim et al., 2003) have also been used as indicators of health and damage. The dynamic properties of bridges continue today to be a useful evaluation tool in non-destructive damage assessment. The principle is that damage in a bridge leads to some loss of stiffness and consequently to changes in its dynamic properties (Ewins, 2000, Carden and Fanning, 2004). In most vibration-based bridge health monitoring techniques, large numbers of sensors are installed on the structure to monitor the dynamic properties. Then, conventional modal testing methods (Ewins, 2000) or output-only modal methods (Zhang et al., 2005) can be used to process the measured signals. These approaches, in which sensors are installed directly on the bridge, are known as direct methods (Ren et al., 2005).

The idea of an indirect approach, in which the natural frequencies of bridge structures are extracted from sensors in a passing vehicle, was first proposed by Yang et al. (2004). In this approach, a vehicle is instrumented and dynamic properties of the bridge are extracted by processing the dynamic response of the moving vehicle to the bridge. Through interaction between bridge and vehicle, the moving vehicle can be considered as both exciter and receiver. The measured vehicle response needs to include high levels of bridge dynamic response. The feasibility of this method in practice was experimentally confirmed by Lin and Yang (2005) by passing an instrumented vehicle over a highway bridge in northern Taiwan. In the case that only bridge frequency is required, the indirect approach showed many advantages in comparison with direct methods in terms of: equipment needed, specialist personnel on site, economy, simplicity, efficiency and mobility.

Bu et al. (2006) also proposed a bridge condition assessment method based on the dynamic response of a passing vehicle. Yang and Chang (2009b) applied a pre-processing approach to the measured vehicle response using empirical mode decomposition (EMD) to enhance

the resolution of the approach. The effect of several key parameters on the dynamic response of the vehicle passing over the bridge was studied in (Yang and Chang, 2009a). It was demonstrated that, unsurprisingly, a larger bridge/vehicle acceleration amplitude ratio results in better accuracy in identifying the bridge frequencies.

McGetrick et al. (2009) demonstrated that with a road profile, better accuracy can be obtained at lower vehicle speed. At higher speeds, the road profile's influence on the vehicle vibration dominates the spectrum, hiding the bridge frequency. They showed that changes in bridge damping could be efficiently monitored using the proposed instrumented vehicle. Chang et al. (2010) showed that the existence of road surface roughness results in the appearance of vehicle frequencies which cannot be neglected in practice. The feasibility of using an instrumented vehicle to detect the natural frequency and changes in structural damping of a model bridge was investigated by Kim et al. (2011), McGetrick et al. (2010) through a scaled laboratory moving vehicle experiment . Yang et al. (2012b) used two connected vehicles to eliminate the blurring effect of road surface roughness when identifying bridge frequencies.

A novel method for the identification of the damping ratio of a bridge using acceleration measurements from a moving vehicle is proposed in González et al. (2012b). The appearance of vehicle frequencies in the sensor acceleration spectrum can be a problem, especially when they are close to the bridge first natural frequency (McGetrick et al., 2009). Yang et al. (2013a) propose some filtering techniques to remove vehicle frequency from the spectrum but these are not always effective. Several types of model test carts were designed and used to improve the experimental accuracy of identifying bridge frequencies from vehicle response in Yang et al. (2013b). Keenahan et al. (2014) propose a subtraction idea to remove the effect of road profile in the measured response of the vehicle. The obtained results were used to detect the damping changes in the bridge.

Zhang et al. (2012) propose a damage index that is based on the squares of the bridge mode shapes, extracted from the acceleration of a passing vehicle applying controlled dynamic forces. The method gives an estimate of the mode shapes. Zhang et al. (2013) extended this concept to find the operating deflection shape curvature of the bridges. An optimization method is proposed in Li et al. (2014) to identify bridge frequencies as well as bridge stiffness indirectly using a passing vehicle. Recently, vehicle-based measurement has been extended to construct the mode shapes of bridges theoretically (Yang et al., 2014b). The

instantaneous amplitude history of the bridge component response was obtained using a Hilbert transform of the response measured in the passing vehicle. Although the method worked well when a smooth road profile was used, the accuracy was less in the presence of road roughness. The sensitivity of the method to measurement noise was not considered.

In recent years, several researchers have developed methods to identify the bridge frequency from the acceleration signal in a passing vehicle (Yang et al., 2004, Yang and Lin, 2005, Yang et al., 2013a, Yang et al., 2013b) and to improve the accuracy of the results. In addition, some authors obtained the damping ratio of the bridge using indirect approaches (González et al., 2012b, Keenahan et al., 2014), but very few (Yang et al., 2014b) have obtained mode shapes of the bridge indirectly. Estimation of bridge mode shape is very important in a dynamic investigation of a bridge. For instance, there are discontinuities at the damage points in the mode shapes of a damaged bridge, including slope discontinuities at cracks (Zhu and Law, 2006, Pandey et al., 1991). Furthermore, the bridge mode shape can be used as an important tool in model updating of a bridge (Arora et al., 2009).

In this chapter a novel Short Time Frequency Domain Decomposition (STFDD), using multi-stage measurements, is proposed to obtain bridge mode shapes indirectly from accelerations in two connected passing axles. The proposed method is based on the Frequency Domain Decomposition (FDD) method that is an output-only modal testing method. This was first proposed by Brincker et al. (2000) to obtain modal parameters of a structure from direct measurements. The proposed method involves two main parts. In the first part, several segments are defined in the bridge and then a multi-stage measurement procedure is done based on the defined segments. The FDD method is applied to the time history acceleration responses from the two following axles in each stage. As a result, local mode shape elements are estimated in each stage in the first part of the method. In the second part, a correction procedure is performed to construct the global mode shape vectors of the bridge from the local estimated mode shape elements.

Numerical case studies are investigated using Finite Element (FE) models of vehicle bridge interaction (VBI) to validate the effectiveness and performance of the proposed method. As noted by many authors (McGetrick et al., 2009, Chang et al., 2010, Yang et al., 2012b) the presence of road roughness causes the dominance of vehicle frequencies. Therefore, in the present study, two concepts are tested to address this problem: (a) excitation of the bridge by traffic other than the test vehicle and (b) subtraction of signals measured on following

axles. The simulations confirm the capability of the proposed method to identify the mode shapes of a bridge using signals from passing vehicles. Only one accelerometer is assumed on each of the two axles so the proposed method is more efficient than traditional modal testing methods, which usually require the installation of several sensors on the structure. More numerical investigations are also provided in Appendix C.

3.2. Finite Element modelling of vehicle bridge interaction

In recent years, much research has been carried out on the modelling of vehicle bridge interaction (VBI) (Tan et al., 1998, Kim et al., 2005, Harris et al., 2007, Cantero et al., 2010). González (2010) carry out a comprehensive review of coupled and uncoupled VBI models in the literature. A Finite Element (FE) VBI model similar to that used by Keenahan et al. (2014) is used here for the numerical investigation of the proposed method. In this model, VBI is modelled as a coupled system in which the solution is calculated at each time step. The vehicle and bridge models and the iterative VBI procedure employed in this chapter are set out in the following sub-sections.

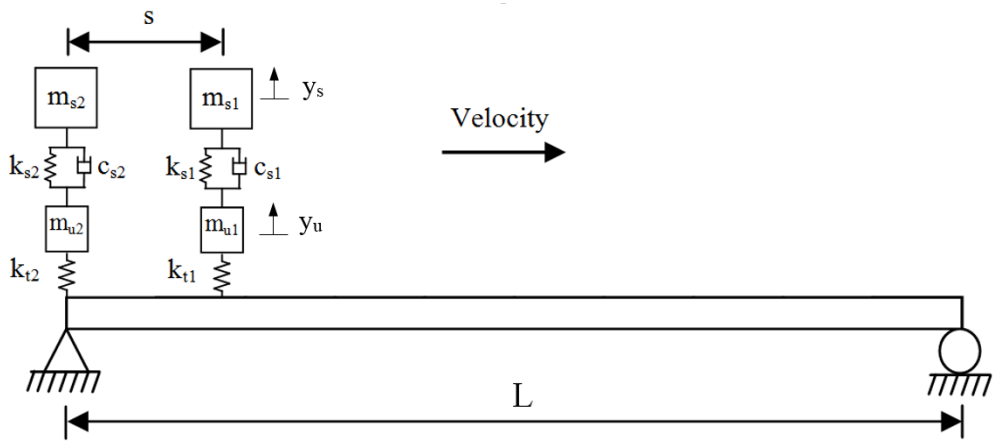

Figure 3-1 Two following quarter-cars travelling over a bridge.

3.2.1. Vehicle model

The two-quarter-car model shown in Figure 3-1 illustrates many of the important characteristics of VBI (Cebon, 1999). This is used here to represent a 2-axle vehicle and not connecting quarter-cars is a deliberate simplification. Each quarter-car has two independent degrees of freedom corresponding to the translational displacements of body bounce, y_s and

axle hop, y_u. The vehicle body and axle component masses are represented by m_s and m_u (sprung and unsprung). The axle mass connects to the road surface via a spring with linear stiffness k_t which represents the tyre. The equations of motion of the vehicle model are obtained by imposing equilibrium of all forces and moments acting on the masses and expressing them in terms of the degrees of freedom:

$$M_v\ddot{y}_v + C_v\dot{y}_v + K_v y_v = f_{int}, \;\; y_v = [y_s \; y_u]^T \tag{3-1}$$

where M_v, C_v and K_v are the respective mass, damping and stiffness matrices of the vehicle and $\ddot{y}_v$, $\dot{y}_v$ and y_v are the respective vectors of nodal acceleration, velocity and displacement. f_{int} is the time-varying dynamic interaction force vector applied to the vehicle degrees of freedom.

3.2.2. Bridge model

A simply supported beam of total span length *L* is modelled using the FE method to represent the bridge (Figure 3-1). The model consists of discretised beam elements with 4 degrees of freedom (2 per node) which have constant mass per unit length, *m*, modulus of elasticity *E* and second moment of area *J*.

The response of the beam model to a series of moving time-varying forces is given by the system of equations:

$$M_b\ddot{y}_b + C_b\dot{y}_b + K_b y_b = f_{int} \tag{3-2}$$

where M_b, C_b and K_b are global mass, damping and stiffness matrices of the beam model, respectively and $\ddot{y}_b$, $\dot{y}_b$ and y_b are the vectors of nodal bridge accelerations, velocities and displacements, respectively.

The damping ratio of the bridge, ξ, is considered to be 3%. Although complex damping mechanisms may be present in the structure, viscous damping is typically assumed for bridge structures and is deemed to be sufficient to reproduce the bridge response accurately. Therefore, Rayleigh damping is adopted here to model viscous damping and is given by:

$$C_b = \alpha M_b + \beta K_b \tag{3-3}$$

where α and β are constants. The damping ξ is assumed to be the same for all modes and α and β are obtained from $\alpha = 2\xi\omega_1\omega_2/(\omega_1 + \omega_2)$ and $\beta = 2\xi/(\omega_1 + \omega_2)$ where ω_1 and ω_2 are the first two natural frequencies of the bridge (Clough and Penzien, 1993).

3.2.3. Coupling of the VBI system

The dynamic interaction between the vehicle and the bridge is implemented in MATLAB. The vehicle and the bridge are coupled at the tyre contact points via the interaction force vector. Combining equations (3-1) and (3-2), the coupled equation of motion is formed as:

$$M_g\ddot{u} + C_g\dot{u} + K_g u = F \tag{3-4}$$

where M_g and C_g are the combined system mass and damping matrices, respectively, K_g is the coupled time-varying system stiffness matrix and F is the system force vector. The vector, $u = \{y_v, y_b\}^T$, is the displacement vector of the system. The equations for the coupled system are solved using the Wilson-Theta integration scheme (Tedesco et al., 1999). The optimal value of the parameter θ =1.420815 is used for unconditional stability in the integration scheme. The initial condition of the solution is considered to be zero displacement, velocity and acceleration in all simulations.

3.3. Theory of Short Time Frequency Domain Decomposition method

In this section, the theory of estimation of the bridge mode shapes from the vehicle response using the proposed new method is described. The method contains two fundamental elements; first, applying the FDD method to the measured response of two following vehicles in several stages and second, correction of the estimated local mode shapes in each stage using a rescaling procedure. In order to introduce the method, a short theoretical background of the FDD method is first presented.

3.3.1. Theoretical background to the FDD method

FDD is an output-only modal analysis method in the frequency domain, first proposed by Brincker et al. (2000). This approach uses the fact that, in a lightly damped structure, modes can be estimated from the spectral densities calculated under a white noise input. In order to obtain the natural frequencies and mode shapes, the power spectral density matrix of the response for each frequency is decomposed by applying Singular Value Decomposition (SVD) to the matrix (Brincker et al., 2001):

$$\hat{G}_{yy}(\omega_i) = [U]_i[\Sigma]_i[U]_i^H \tag{3-5}$$

where $[U]_i = [\{u\}_{i1}, \{u\}_{i2}, \dots, \{u\}_{im}]$ is the unitary matrix including the singular vectors $\{u\}_{ik}$ and $[\Sigma]_i$ is a diagonal matrix including singular values σ_{ik}. The superscript "H" indicates the complex conjugate of the matrix and j is equal to $\sqrt{-1}$. If singular values obtained from outputs of the structure are plotted in an SVD diagram, dominant peaks are natural frequencies of the structure and the corresponding singular vectors are mode shapes. More details of the FDD method are provided in the literature (Brincker et al., 2000, Brincker et al., 2001).

3.3.2. STFDD method

Many studies have been reported in the literature that use measured accelerations in a passing vehicle for identification of bridge fundamental frequency and damping ratio (Yang et al., 2004, Yang and Lin, 2005, Yang et al., 2013a, Yang et al., 2013b, Zhang et al., 2013, Keenahan et al., 2014). The measured signal from the vehicle consists of both the bridge response (indirectly) and the vehicle response. Therefore, the fundamental frequency of the bridge and the vehicle frequency are both observable in the fast Fourier transform (FFT) spectrum of the vehicle response. The STFDD method is based on this fact that, if the FDD method is applied to the measured signals from sensors installed on the two following axles in discrete short time periods, the system mode shape can be obtained from a multi-stage procedure. In this chapter, the system mode shape is taken as an approximation of the bridge mode shape.

The bridge is divided into a number of segments, each equal in length to the axle spacing. In this example, the axle spacing is, $s=L/5$ and the bridge is divided into five segments, as illustrated in Figure 3-2. Four periods (stages) of measurment (Figure 3-2) are defined using the five segments of the bridge. The initial locations of the quarter-cars in each stage are shown dotted and the final locations with solid lines. Two short signals are measured in each stage that are assembeled in a matrix:

$$\ddot{Y}_j = \begin{bmatrix} \ddot{y}_{j,j} \\ \ddot{y}_{j,j+1} \end{bmatrix} \quad \text{j=1:4} \tag{3-6}$$

where $\ddot{y}_{j,j+1}$ and $\ddot{y}_{j,j}$ are the short acceleration response vectors that are measured from axle 1 and axle 2, respectively where the first index indicates the stage number and the second indicates the segment number that the response corresponds to. Therefore $\ddot{Y}_j$ is the response matrix obtained from each stage. The outputs of the measurement procedure in this case are four matrices of data, each including two discrete signals.

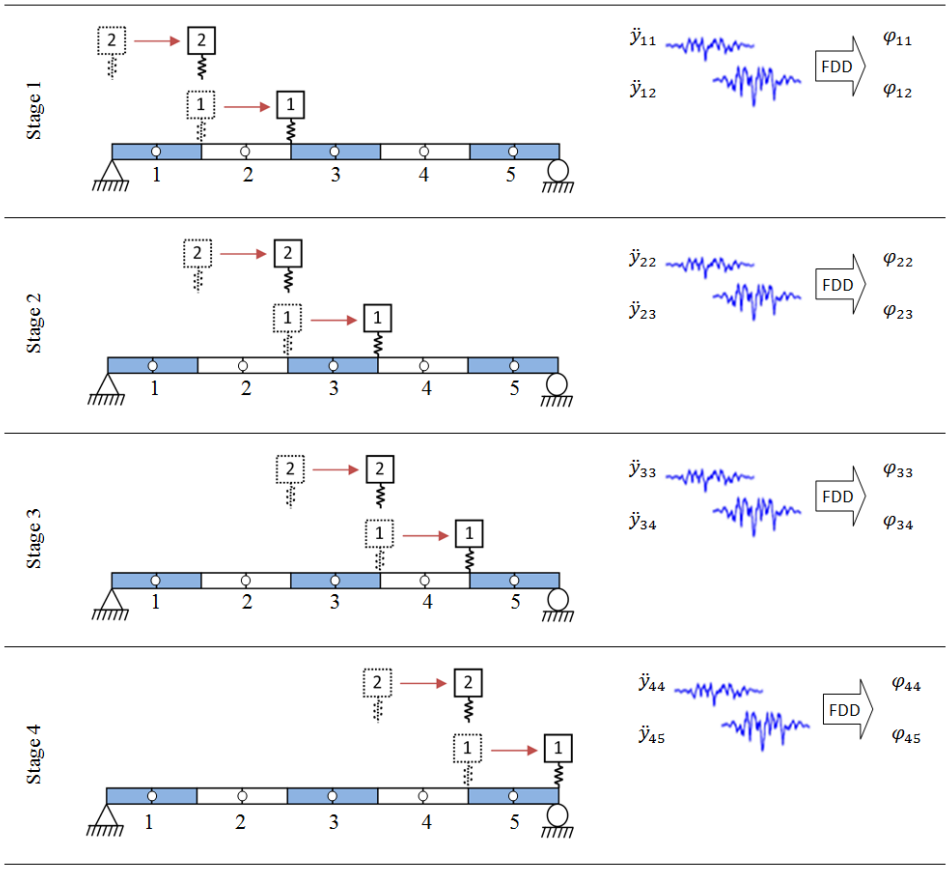

Figure 3-2 Measurement stages in a 5-segments example.

In order to estimate the mode shape vector for each stage, the FDD method is applied to the measured data $\ddot{Y}_j$ from each stage. Hence the singular value diagram can be plotted and the natural frequency and two-element vector describing the mode shape can be obtained for each stage as shown in the right hand side of Figure 3-2. In this example, four 2-element vectors of mode shape are obtained at four different locations which are called local mode shape vectors $\{\varphi_{j,j}, \varphi_{j,j+1}\}^T$. To estimate the global mode shape vector, a relationship between the local mode shape vectors from the different stages must be established. For this purpose, a progressive rescaling procedure is developed.

The basis of the proposed STFDD method is that the measured signal from each segment of the bridge represents the dynamic beahaviour of the bridge for that segment. The first and second elements of the global mode shape vector which are for the first and second segments respectively, are obtained from the first stage:

$$\Phi_1 = \varphi_{11} \tag{3-7}$$

$$\Phi_2 = \varphi_{12} \tag{3-8}$$

where Φ_1 and Φ_2 are the global mode shape elements corresponding to the mid-points of the first and the second segments of the bridge. As the signals from Stages 1 and 2 are not measured at the same time, φ_{23} must be rescaled to find the global mode shape of segment 3. The correction ratio is defined based on the local mode shape elements obtained for the common segment in Stages 1 and 2 which are φ_{22} and φ_{12} (or Φ_2). Therefore, the next element of the global mode shape vector Φ_3 is obtained using:

$$\Phi_3 = \varphi_{23} \frac{\Phi_2}{\varphi_{22}} \tag{3-9}$$

By applying a similar correction procedure, the other elements of the global mode shape vector are obtained, i.e.:

$$\Phi_{j+1} = \varphi_{j,j+1} \frac{\Phi_j}{\varphi_{j,j}} \qquad j=2:4 \tag{3-10}$$

where Φ_{j+1} is the global mode shape element corresponding to the $(j+1)^{th}$ segment which is obtained from the j^{th} stage. The location of the global mode shape elements obtained from the method for each segment is considered to be at the mid-point of that segment.

It should be noted that more mode shape data might be anticipated by considering more bridge segments. However, in increasing the number of segments, the quantities of the measured data for each segment are decreased which reduces the accuracy of the FDD identification process. Consequently, a compromise number of segments must be chosen for a successful identification prodecure.

Although the speed of the vehicle is assumed to be constant in this method, but it is not necessary to keep the speed constant during the implementation. The important thing is that the operator must know which part of the signal is measured in which segment; then it is possible to extract the local mode shapes from the signals, even with variable speed. However, for less complexity and a better result, it is recommended to keep the vehicle speed as constant as possible.

3.3.3. Example of two quarter-cars on a smooth profile

The STFDD method is tested via numerical simulation using the VBI model described in Section 3.2. The bridge is modelled using the FE method as a simply-supported beam with the properties given in Table 3-1. The first three natural frequencies of the bridge are given in Table 3-2 where it can be seen that the fundamental frequency is 5.65 Hz. The bridge is divided into ten equal segments as shown in Figure 3-3.

Table 3-1 Properties of the bridge.

Properties	Unit	Symbol	value
Length	m	*L*	15
Mass per unit	kg/m	*m*	28125
Modulus of elasticity	MPa	*E*	35000
Second moment of area	m4	*J*	0.5273

Table 3-2 First three natural frequencies of the bridge.

Mode No.	1	2	3
Natural frequency (Hz)	5.65	22.62	50.89

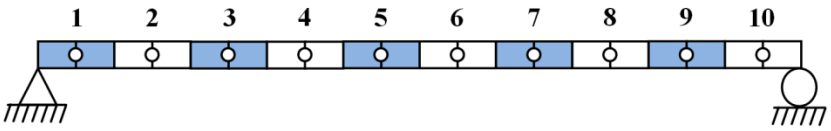

Figure 3-3 Bridge segments.

As before, the mid-point of each segment is considered to be the location of the global mode shape element obtained for that segment. Therefore, the mode shape vector obtained from the STFDD method will have ten elements corresponding to the ten points shown in the figure. As described in Section 3.2, two following quarter-cars are modelled passing over this bridge (see Figure 3-1) with the properties listed in Table 3-3. The body bounce frequency of both quarter-cars are the same and equal to 12.48 Hz. As explained in Section 3.2, nine stages are considered for the ten segments.

Table 3-3 Properties of the quarter-cars.

Properties	Unit	Symbol	Value
Body mass	kg	m_s	9300
Axle mass	kg	m_u	350
Suspension stiffness	N/m	k_s	4×10^5
Suspension damping	Ns/m	c_s	10×10^3
Tyre stiffness	N/m	k_t	1.75×10^6
Body bounce frequency	Hz	ω_b	0.94
Axle hop frequency	Hz	ω_a	12.48

The simulation is carried out using the VBI system outlined in Section 3.2 at the rather slow vehicle velocity of 2 m/s. The time histories of acceleration responses from the two

following axles are calculated using a time interval, dt = 0.001 s. The FDD method is applied to the nine short time responses of the following axles. The obtained SVD diagrams from the nine stages of the STFDD method are shown in Figure 3-4. As the road profile is smooth, vehicle frequencies are not strongly excited and two peaks are clear in all of the SVD diagrams corresponding to the first two natural frequencies of the bridge.

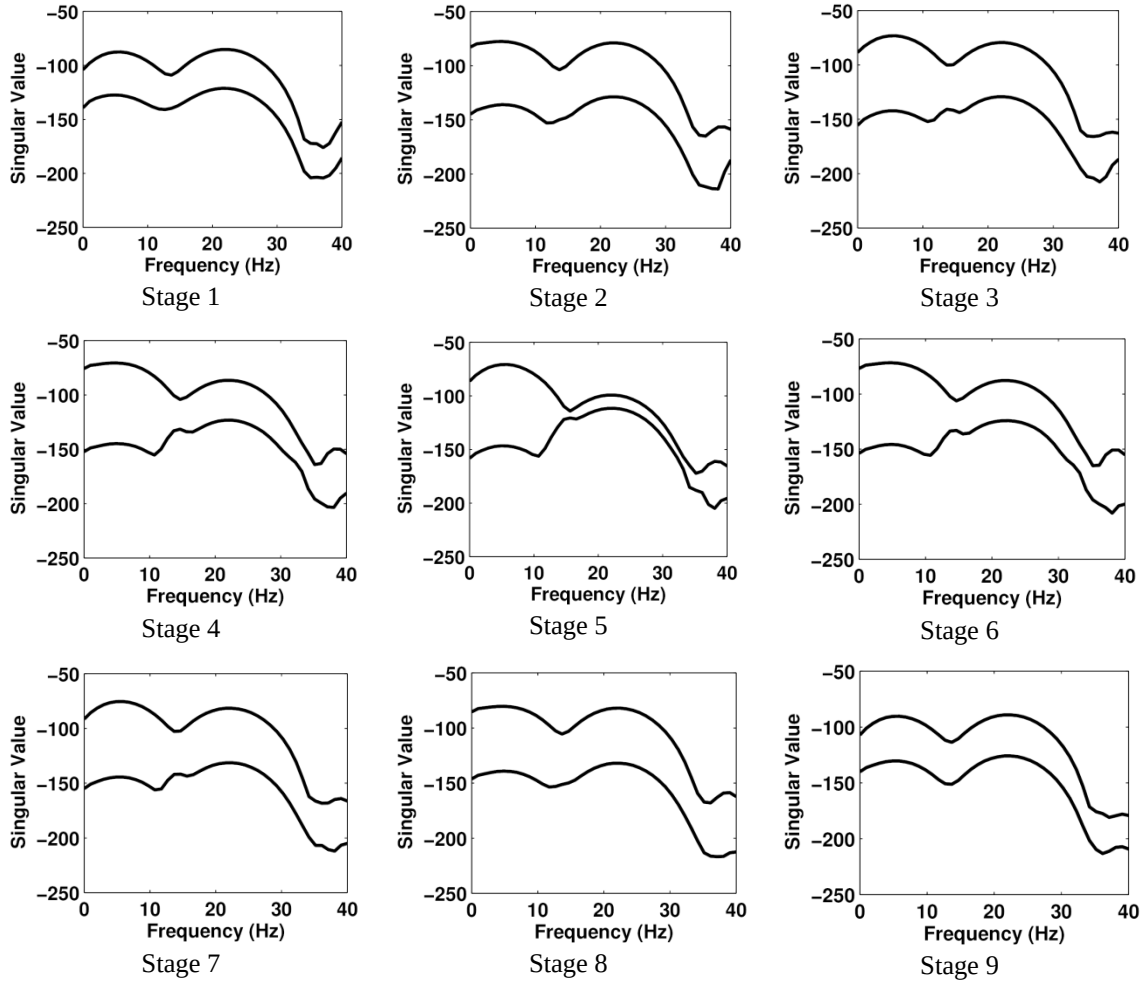

Figure 3-4 SVD diagrams obtained from nine stages.

As mentioned in Section 3.1, the singular vectors corresponding to these singular values obtained from the peaks of the SVD diagrams, define the local mode shape of each mode in each segment. By applying the rescaling process of the STFDD method to the local mode shapes obtained from the nine stages, the first two global mode shapes of the bridge are obtained and illustrated in Figure 3-5. The Modal Assurance Criterion (MAC), defined in Eq. 3-11, is used to compare the calculated mode shapes to the exact shapes obtained from the FE method:

$$\mathrm{MAC} = \frac{\left|\Phi_{\mathrm{STFDD}}{}^{\mathrm{t}}\Phi_{\mathrm{FE}}\right|^2}{\left|\Phi_{\mathrm{STFDD}}{}^{\mathrm{t}}\Phi_{\mathrm{STFDD}}\right|\left|\Phi_{\mathrm{FE}}{}^{\mathrm{t}}\Phi_{\mathrm{FE}}\right|} \tag{3-11}$$

where Φ_{STFDD} is the global mode shape obtained from the STFDD method and Φ_{FE} is the exact shape obtained from FE method and "t" defines transpose of the matrix. Excellent agreement is found in this case.

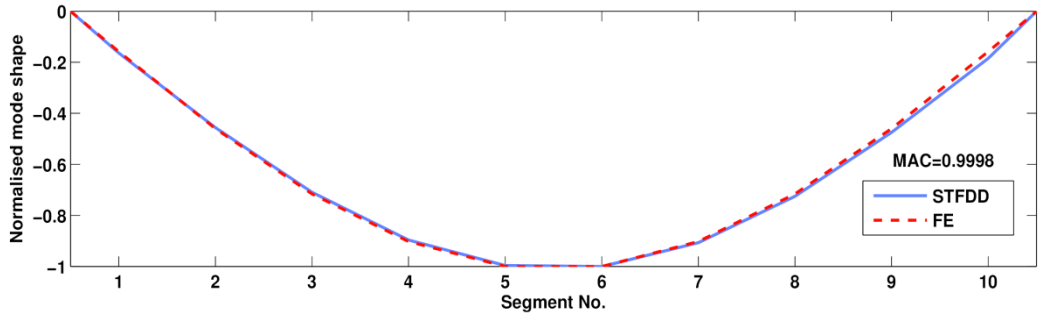

(a)

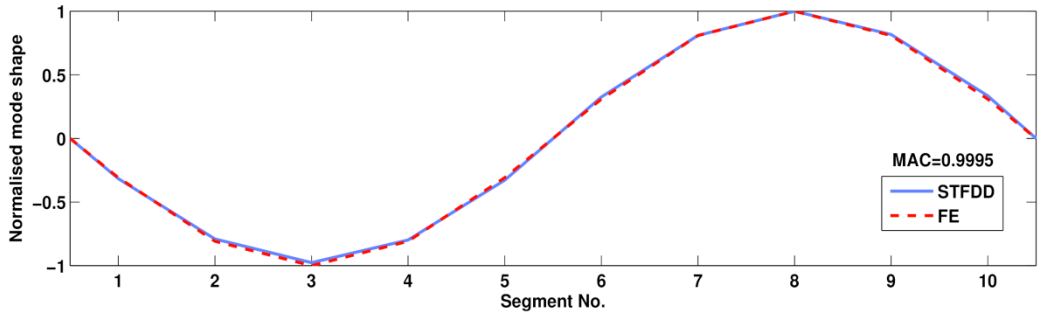

(b)

Figure 3-5 The first two mode shapes of the bridge. (a) First mode shape, (b) Second mode shape.

3.4. Effect of road profile

Previous studies have indicated that estimation of bridge frequency from the vehicle response is difficult in the presence of a road profile. In most cases, although the bridge frequency may be detectable in the spectrum of vehicle response, the vehicle frequencies are dominant.

Yang and Chang (2009a) addressed this challenge by investigating the effect of several key parameters on the dynamic response of the vehicle passing over the bridge and concluded that, with high vehicle/bridge acceleration amplitude ratios, the probability of successfully identifying the bridge frequency is less. In addition, it was demonstrated in (Yang et al., 2013a) that a larger volume of existing traffic tends to make the bridge frequency more visible. Generally, this solution seems to be practical, especially for longer spans where additional vehicles on the bridge are more likely. Bridge frequency is more visible in the measured response of the passing vehicle when ongoing traffic is modelled in the simulation. However, this is not a good assumption for short-span bridges where the probability of multiple vehicles being present simultaneously on the bridge is small.

Recently, Yang et al. (2012b) and Keenahan et al. (2014) proposed the idea of subtraction of the responses to improve the results in the presence of profile. Yang et al. (2012b) use two connected axles passing over the bridge. It is shown that subtracting the Fourier transform of the two responses gives a residual spectrum in which the bridge frequency is much more clear. However, the method is shown to have some limitations. Keenahan et al. (2014) propose the idea of subtracting the measured acceleration responses of two following axles travelling over a bridge. It is demonstrated that the effect of road profile is substantially removed from the residual acceleration response provided the two axles have the same properties.

Both methods of dealing with the road profile are used in this numerical investigation. In the proposed STFDD method, two axle responses are needed to estimate the mode shape values in each stage. Therefore, to implement the concept of subtraction, three following axles are necessary at each stage (see Figure 3-6). Four response difference matrices are obtained from the five stages:

$$\ddot{X}_j = \begin{bmatrix} \ddot{x}_{j,j-1} \\ \ddot{x}_{j,j} \end{bmatrix} = \begin{bmatrix} \ddot{y}_{j,j-1} - \ddot{y}_{j-1,j-1} \\ \ddot{y}_{j,j} - \ddot{y}_{j-1,j} \end{bmatrix} \quad \text{j=2:5} \tag{3-12}$$

where $\ddot{x}_{j,j-1}$ is the difference response obtained in stage *j* (first index) for segment *j-1* (second index). The same process of STFDD and the rescaling procedure explained in Section 3.2 is used to obtain the global mode shape vector from the response differences.

	Model	Measured response		
		Axle 3	Axle 2	Axle 1
Stage 1	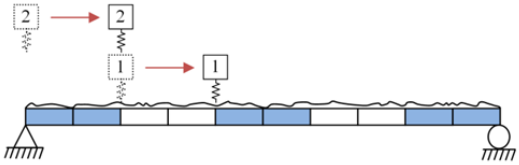	-	$\ddot{y}_{11}$	$\ddot{y}_{12}$
Stage 2	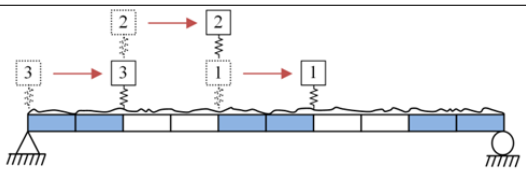	$\ddot{y}_{21}$	$\ddot{y}_{22}$	$\ddot{y}_{23}$
Stage 3	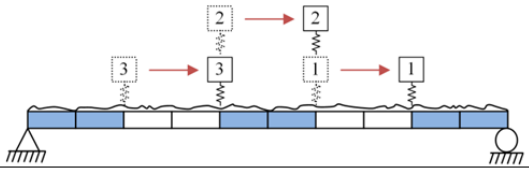	$\ddot{y}_{32}$	$\ddot{y}_{33}$	$\ddot{y}_{34}$
Stage 4	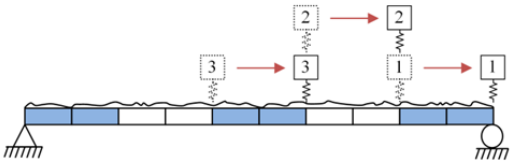	$\ddot{y}_{43}$	$\ddot{y}_{44}$	$\ddot{y}_{45}$
Stage 5	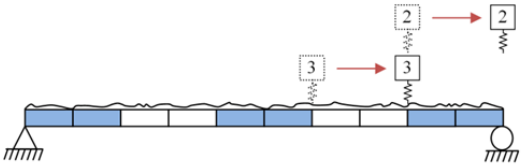	$\ddot{y}_{54}$	$\ddot{y}_{55}$	-

Figure 3-6 Subtraction of measured responses in the presence of a road profile.

3.4.1. Example of two following quarter-cars crossing a bridge with a Class A profile in the presence of other traffic

The same bridge as for Section 3.3 is now considered, except that a road profile is added. The irregularities of this profile are randomly generated according to the ISO standard (ISO8608:1995, 1995) for a road class 'A' (very good) profile, as would be expected in a well maintained highway.

To demonstrate the advantage of an external source of excitation (such as other traffic), a random force which is almost equal to the interaction force of an axle with weight of 4 tonnes is applied to all parts of the bridge. To further improve the quantity of the measured data, the speed of the vehicle is reduced to 1 m/s.

This time, the bridge is divided into six equal segments. The STFDD is applied to the short acceleration signals. As an example, the SVD diagram for Stage 3 is shown in Figure 3-7. Although the vehicle frequency is dominant in this SVD diagram, a peak around 5.65 Hz is also visible. However no detectable peak is observed for the second mode of the bridge (around 22.62 Hz) so the second mode shape is not detectable. The first mode shape is shown in Figure 3-8 and is less close to the exact shape than before (MAC = 0.9975).

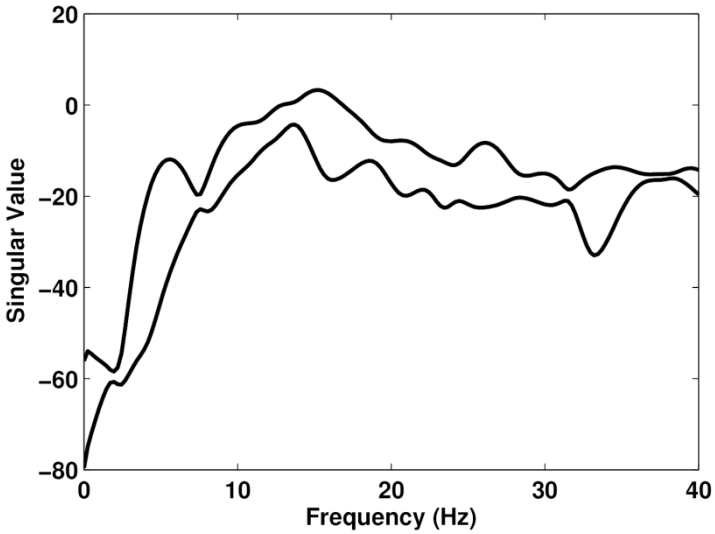

Figure 3-7 The SVD diagram obtained from Stage 3 when a Class A profile is present.

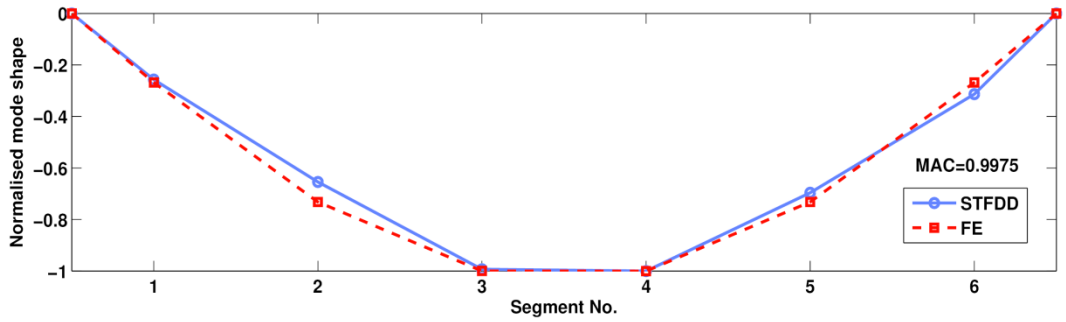

Figure 3-8 The first mode shape when a Class A profile is present.

While the proposed method is capable of obtaining the bridge fundamental mode shape in the presence of road roughness, it was found to be sensitive to some parameters: (a) the resolution of the measured accelerations which is related to the number of segments and the speed of the vehicle (it works better at lower speed and for longer segments) (b) the closeness

of the bridge frequency to a vehicle frequency (closer makes it harder to distinguish the bridge frequency).

As noise is a feature of all measurements, it is necessary to assess the proposed method in the presence of measurement noise. Previous studies (Zhang et al., 2012) have shown that the estimation of bridge dynamic properties from a passing vehicle is not significantly sensitive to noise, since the responses are measured at the same location as the excitation. White noise is added to the calculated vehicle responses to simulate noise-polluted measurements using Eq. (3-13):

$$w = w_{calc} + E_P N_{noise} \sigma(w_{calc}) \tag{3-13}$$

where w is the polluted acceleration, E_P is the noise level, N_{noise} is a standard normal distribution vector with zero mean value and unit standard deviation, w_{calc} is the calculated displacement, and $\sigma(w_{calc})$ is its standard deviation. The STFDD method is repeated for different levels of noise and the global mode shape vector is obtained for each level. Figure 3-9 shows that the STFDD method, when external excitation is present, can extract the bridge mode shape with acceptable accuracy in the presence of noise up to about 10 %. For noise levels of 5%, 10% and 15%, the MAC values are 0.9982, 0.9974 and 0.9893 respectively.

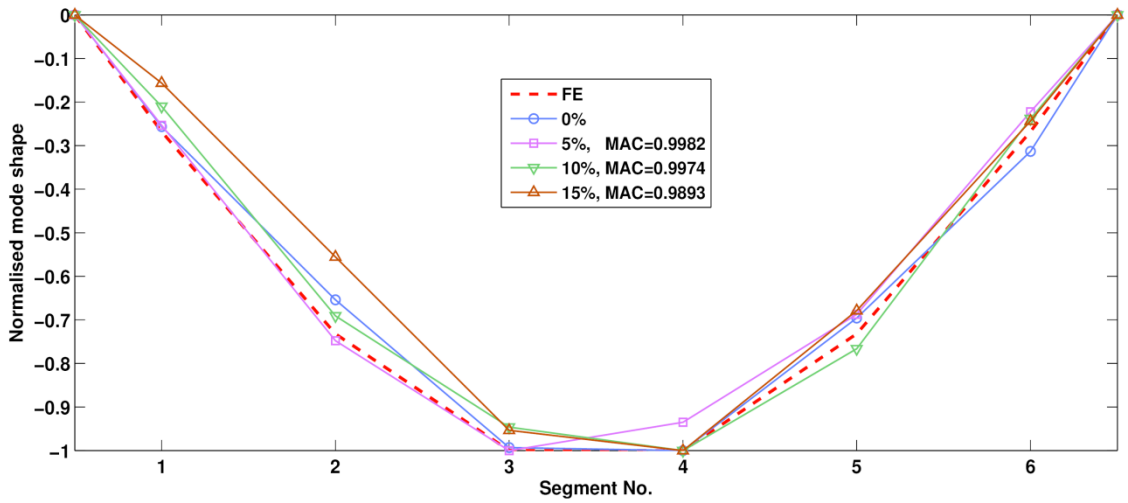

Figure 3-9 Comparison of the first mode shape vectors for different levels of noise when a Class A profile is present.

3.4.2. Three following quarter-cars on a bridge with Class A profile

In short span bridge, other traffic may not always be present to provide a source of external excitation. When other traffic is absent, subtracting acceleration responses in following axles is an alternative way to remove the effect of a road profile. To demonstrate the effectiveness of subtraction, three following quarter-cars are simulated travelling over the same bridge as before at a speed of 1 m/s. The bridge is divided into six segments on this occasion. As explained previously, the first signal is the difference in the responses of axles 1 and 2 while the second is the difference in responses of axles 2 and 3. As an example, the SVD diagram for the third stage is shown in Figure 3-10. The quality of the diagram is clearly improved in contrast to what was obtained in Section 3.4.1. This time, a dominant peak appears around the bridge natural frequency. The peak corresponding to the second mode of the bridge is also clearly detectable in this case. The first two global mode shapes are shown in Figure 3-11. The first mode shape is found with good accuracy while the second exhibits some deviation from the exact shape. As the negative effect of road roughness has been removed from the signal in this section, the results show better accuracy in comparison with those of Section 3.4.1

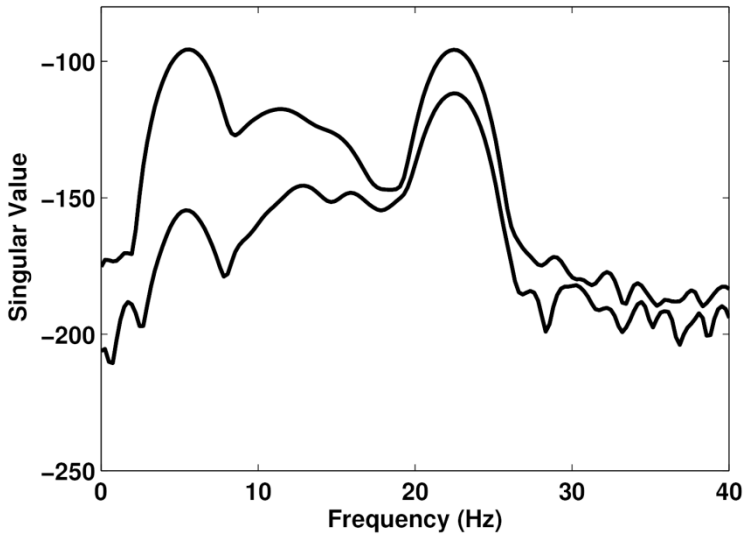

Figure 3-10 The SVD diagram obtained from Stage 3.

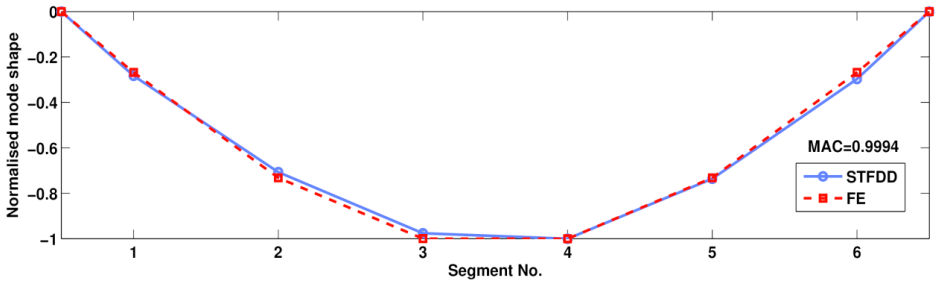

(a)

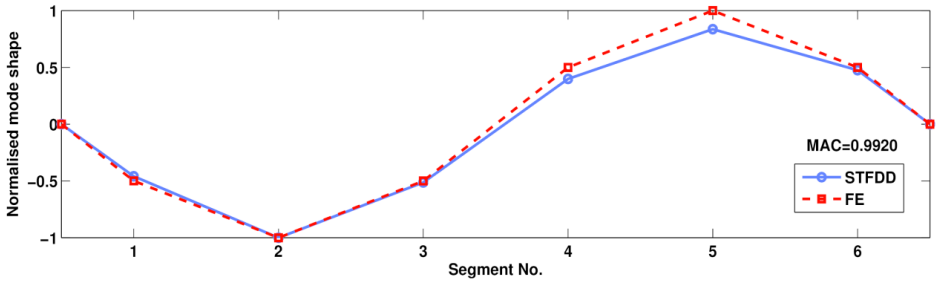

(b)

Figure 3-11 The first two mode shapes of the bridge (a) First mode shape, (b) Second mode shape.

3.5. Truck-trailers passing over a bridge with a Class A profile

A more general case of a truck with trailers is investigated in this section travelling over the same bridge as before with a Class A profile. The truck is heavy and used to excite the bridge. It is assumed to be towing two identical trailers, as illustrated in Figure 3-12, and travelling at 1 m/s.

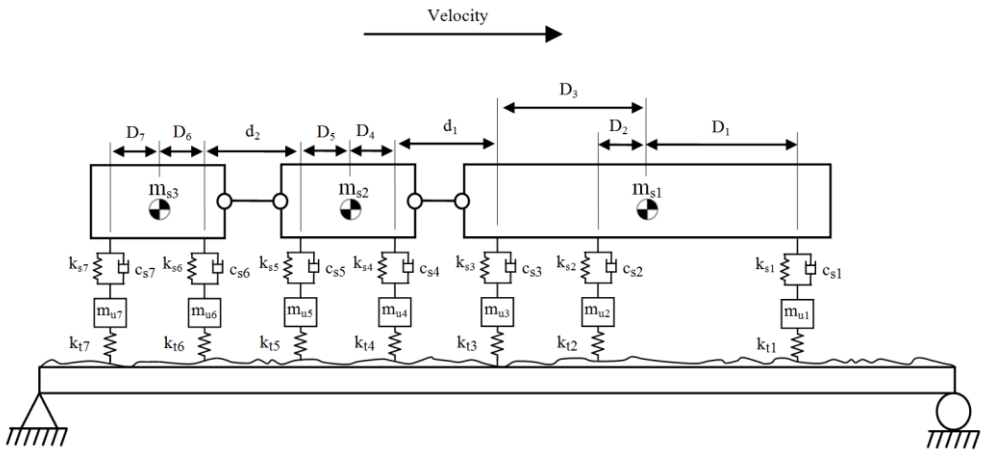

Figure 3-12 The truck-trailers model.

Table 3-4 Properties of the truck.

Property	Unit	Symbol	Value
Body mass	kg	m_{s1}	27100
Axle mass	kg	m_{u1}	700
		$m_{u2} = m_{u3}$	1100
Suspension stiffness	N/m	k_{s1}	4×10^5
		$k_{s2} = k_{s3}$	1×10^6
Suspension damping	Ns/m	c_{s1}	10×10^3
		$c_{s2} = c_{s3}$	20×10^3
Tyre stiffness	N/m	k_{t1}	1.75×10^6
		$k_{t2} = k_{t3}$	3.5×10^6
Moment of inertia	kg m^2	I_{s1}	1.56×10^5
Distance of axle to centre of gravity	m	D_1	4.57
		D_2	1.43
		D_3	3.23
Body mass frequency	Hz	$f_{body,1}$	1.32
Axle mass frequency	Hz	$f_{axle,1}$	8.82
		$f_{axle,2}$	10.17
		$f_{axle,3}$	10.20

Table 3-5 Properties of the trailers.

Property		Symbol	Value
Body mass	kg	m_{s2}	4000
Axle mass	kg	$m_{u4} = m_{u5} = m_{u6}$	50
Suspension stiffness	N/m	$k_{s4} = k_{s5} = k_{s6}$	4×10^5
Suspension damping	Ns/m	$c_{s4} = c_{s5} = c_{s6}$	10×10^3
Tyre stiffness	N/m	$k_{t4} = k_{t5} = k_{t6}$	1.75×10^6
Moment of inertia	kg m^2	I_{s2}	2401.67
Distance of axle to centre of gravity	m	$D_4 = D_5$	1.25
Body mass frequency	Hz	$f_{body,2}$	2.02
Axle mass frequency	Hz	$f_{axle,4}$	33.01
		$f_{axle,5}$	33.04
Distance of two trailers and truck to trailer	m	$d_1 = d_2$	1

OBrien et al. (2014) give details of truck-trailer modelling in MATLAB. The properties of the truck and trailers are given in Tables 3-4 and 3-5 respectively. The same procedure of vehicle bridge interaction modelling which was used in previous sections is used in this case. The acceleration responses of Axles 4 through 7 are assumed to be measured. To remove the effect of road profile from the measured signals, two difference signals are defined as $\ddot{x}_1 = \ddot{y}_6 - \ddot{y}_4$ and $\ddot{x}_2 = \ddot{y}_7 - \ddot{y}_5$. The STFDD method is applied to these difference

responses through five stages and five SVD diagrams are obtained. The SVD diagram from Stage 3 is shown in Figure 3-13 as an example. The first two natural frequencies of the bridge are clearly detectable from this diagram. The mode shapes shown in Figure 3-14 give a very good match to the exact shapes.

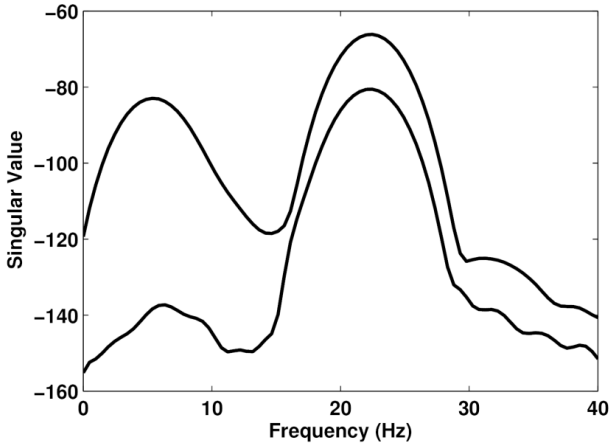

Figure 3-13 The SVD diagram obtained from Stage 3.

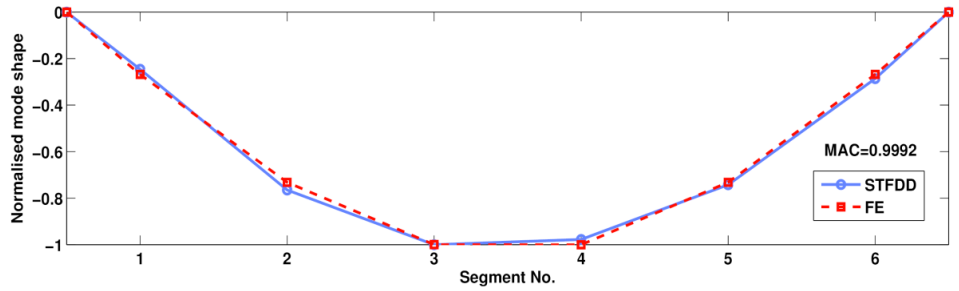

(a)

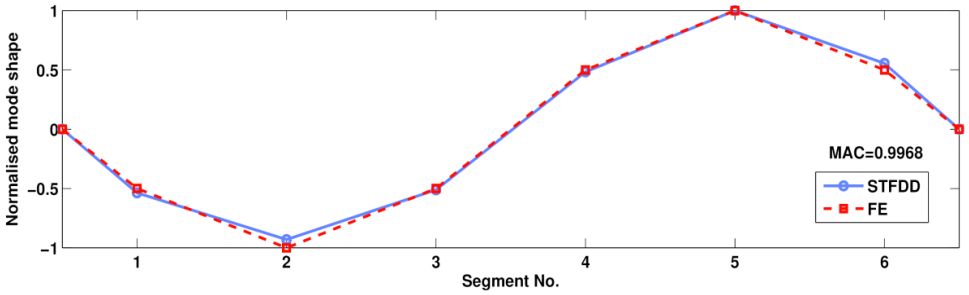

(b)

Figure 3-14 The first two mode shapes of the bridge. (a) First, (b) Second.

These calculated mode shapes are sensitive to noise, as can be seen in Figure 3-15. The first mode is more sensitive than the second. This may be because the trailer body mass frequency is closer to the bridge first natural frequency than the second. Clearly, high-accuracy accelerometers will be needed to minimise measurement noise in the response.

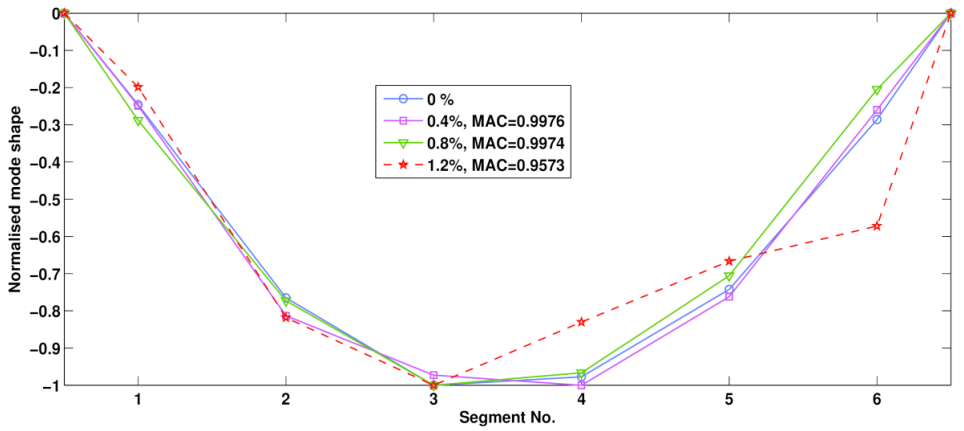

(a)

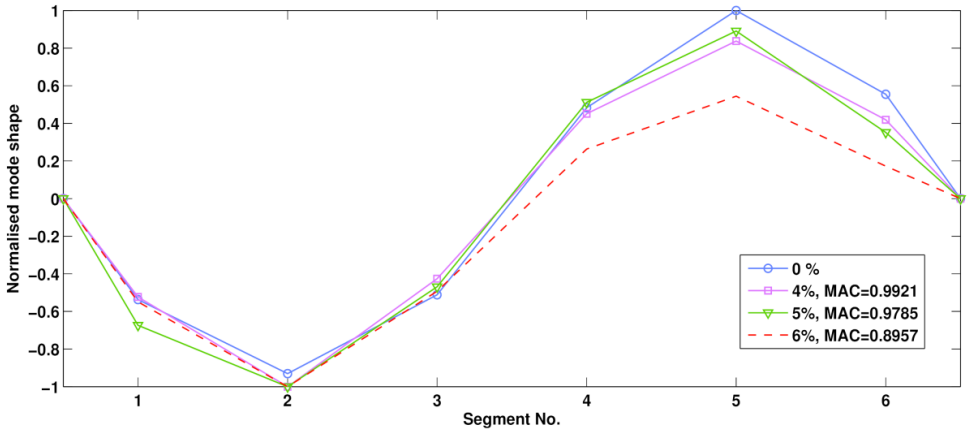

(b)

Figure 3-15 Sensitivity of calculated mode shape vectors to noise; (a) first mode shape, (b) second mode shape.

3.6. Conclusions

This chapter describes a novel method for indirect identification of bridge mode shapes. When two following axles are modelled passing over a bridge, the FDD method can be

applied to the short time measured signals obtained in several defined stages. By performing a rescaling procedure to the local mode shape vectors, the global mode shape is obtained. The performance of the proposed method is investigated using several numerical simulations. The effect of road profile in exciting the vehicle is a significant challenge for the method. Excitation of the bridge by other traffic improves the situation. In the absence of other traffic, subtraction of signals in identical axles is shown to be a feasible alternative. A truck towing two trailers is shown to be a possible arrangement for finding bridge mode shapes. Provided noise is sufficiently low, mode shapes can be found with good accuracy. With further improvement the method can be used for the identification of bridge mode shapes in many case studies for short, medium and long span bridges. The bridge mode shapes identified from this method can be used for damage detection, model updating and system identification.

Chapter 4: A mode shape-based damage detection approach using laser measurement from a vehicle crossing a simply-supported bridge

Authors:

Eugene J. OBrien

Abdollah Malekjafarian

Paper status:

Published in *Structural control and Health Monitoring, 2016,* DOI: 10.1002/stc.1841.

Not to the reader:

This work is entirely the work of the author under the supervision of Prof. Eugene OBrien.

Chapter 4: A mode shape-based damage detection approach using laser measurement from a vehicle crossing a simply-supported bridge

4.1. Introduction

Bridges are key components in the transportation infrastructure of all countries. Therefore, the structural health of bridges must be inspected regularly to ensure that they are in a safe and reliable condition. Traditionally, visual inspection is known as a simple and effective option for bridge health monitoring. However, damage can only be detected when it is visible that may result in cases where the inspector is unable to discover low levels of damage.

Structural Health Monitoring (SHM) is a fairly new concept to the field of Civil Engineering which relies on vibration data to infer information on structural health condition. Generally, SHM methods can be categorised into four main levels (Rytter, 1993): determining (i) the occurrence, (ii) the location, (iii) the severity of any damage to structures and (iv) predicting the remaining service life. The fundamental idea behind vibration-based damage identification is that the occurrence of damage involves changes in the physical properties (mass, damping, and stiffness) which, in turn, cause detectable changes in modal properties (natural frequencies, modal damping, and mode shapes). Traditionally, a number of sensors are installed directly on the structure to identify the dynamic parameters through vibration testing; these are referred to as *direct methods* (Fan and Qiao, 2011). Many studies have been carried out for direct damage detection based on changes in the natural frequency of the structure (Chinchalkar, 2001, Patil and Maiti, 2003). It is also shown that mode shapes (Shi et al., 2000, Qiao and Cao, 2008) and their curvature (Ratcliffe, 1997, Yoon et al., 2005) can be a reliable damage detection criterion. Recently, researchers have shown an increased interest in *indirect methods* in which data is collected from a vehicle passing over the bridge. Using indirect methods, all sensing equipment is installed on the vehicle while the traditional direct methods need considerable investment in each bridge in terms of installation, power supply and maintenance of the sensors.

In recent years, there has been an increasing interest in indirect methods (Malekjafarian et al., 2015). Some authors have focused on extracting the first natural frequency of a bridge

from the response measured on a passing vehicle (Yang et al., 2004, Yang and Lin, 2005). It was shown that the measured vehicle response is significantly influenced by the bridge dynamic properties which can reveal the bridge first natural frequency. Subsequently, the practical feasibility of the idea was confirmed in experimental case studies (Lin and Yang, 2005, Siringoringo and Fujin, 2012, Oshima et al., 2008, Toshinami et al., 2010). Several attempts have been made to improve the accuracy of the results and overcome the challenges in indirect frequency monitoring of bridges (McGetrick et al., 2009, Yang and Chang, 2009b, Yang and Chang, 2009a, Malekjafarian and OBrien, 2014a, Yang et al., 2013a, Yang et al., 2013b). In addition, a number of studies have investigated the potential of indirect methods for the identification of bridge damping (McGetrick et al., 2009, McGetrick et al., 2010, González et al., 2012b). Several studies (Zhang et al., 2013, Li and Au, 2014, Li and Au, 2015) consider bridge damage detection based on indirect measurements.

Most studies in the field of indirect methods have focussed on identifying bridge natural frequencies, while a few studies focus on identifying mode shapes (Malekjafarian and OBrien, 2014a). It is generally accepted that mode shapes are more sensitive to damage than natural frequencies (Fan and Qiao, 2011). In addition, mode shapes contain local information which can be used for damage localization. As one of the earliest attempts at indirect mode shape identification, Zhang et al. (2012) use a special "tapping" vehicle passing over a bridge in which a device installed on it applies a controlled force. The square of the mode shape (MOSS) obtained from the measurements on the vehicle is used for damage detection. A recent theoretical study by Yang et al. (2014b) involves the indirect identification of bridge mode shapes. They separate the component of the response measured on the vehicle which corresponds to the bridge frequency. It is shown that the instantaneous Hilbert amplitude of the distilled component response can be used to determine the bridge mode shape. Oshima et al. (2014) investigate a bridge damage detection method based on the estimation of bridge mode shapes from indirect measurements. They use Singular Value Decomposition (SVD) of the bridge response at the moving coordinate which is obtained from the responses measured by a laser distansometer and an accelerometer installed on the vehicle.

A method called Short Time Frequency Domain Decomposition (STFDD) is proposed in Chapter 3 for identification of bridge mode shapes from acceleration responses measured indirectly from two following axles travelling over a simply supported bridge. The

Frequency Domain Decomposition (FDD) method (Brincker et al., 2000) is applied to the response measured at several stages, corresponding to different locations on the bridge. A procedure of rescaling is performed on mode shape vectors obtained in the first step to construct the global mode shapes. A truck-trailer model is used in numerical simulations to demonstrate the performance of the method at low speeds. In another study, OBrien and Malekjafarian (2015) investigate the STFDD method with higher vehicle speed, showing that the method is applicable for a vehicle speed up to 8 m/s.

In this chapter, a novel algorithm is proposed for indirect damage detection of a bridge based on the mode shapes obtained using the STFDD method. A new measurement procedure inspired by Oshima et al. (2014) is proposed to overcome the effect of road profile. The STFDD method is also slightly modified to provide enough resolution in the mode shape estimate to provide more accurate local information about the damage. A numerical case study of a half-car vehicle passing over a bridge is used to investigate the efficiency of the algorithm. It is shown that it can detect the occurrence and location of damage with acceptable accuracy. Furthermore, the performance of the algorithm for higher vehicle speeds is discussed, showing good accuracy for speeds of up to 8 m/s. Finally, the influence of measurement noise on the results is investigated. More details about application of laser measurements are also provided in Appendix B.

4.2. Finite Element modelling of vehicle bridge interaction

A Finite Element (FE) Vehicle Bridge Interaction (VBI) model similar to that used by Malekjafarian and OBrien (2014b) is implemented in MATLAB for the investigation of the proposed method. In this model, VBI is represented as a coupled system in which the dynamic response is calculated at each time increment. The half-car model shown in Figure 4-1 is employed here as it is a good simplification of a real vehicle (Cebon, 1999). The half-car has four independent degrees of freedom corresponding to body mass translation and rotation and two axle mass translations. The vehicle body and axle component masses are represented by m_s, m_{u1} and m_{u2}. The axle masses and the road surface are connected to each other via a spring with linear stiffness k_t which simulates the tyre. The equations of motion of the vehicle model can be written by considering equilibrium of all applied forces and moments acting on the masses in terms of the all degrees of freedom:

$$M_v \ddot{y}_v + C_v \dot{y}_v + K_v y_v = f_{int} \tag{4-1}$$

where M_v, C_v and K_v are the mass, damping and stiffness matrices of the vehicle respectively and $\ddot{y}_v$, $\dot{y}_v$ and y_v are the vectors of acceleration, velocity and displacement of the all degrees of freedom respectively. f_{int} is the vector of interaction force that are applied to the vehicle degrees of freedom at each time step.

A simply supported beam is modelled using beam finite elements in this case study (Figure 4-1). Each beam element is represented by four degrees of freedom (two per node). *L* is the total length of the beam, *m* is constant mass per unit length, *E* is modulus of elasticity and *J* is second moment of area. The dynamic response of the beam when it is under a series of time-varying forces caused by the moving vehicle, is given by:

$$M_b\ddot{y}_b + C_b\dot{y}_b + K_b y_b = f_{int} \tag{4-2}$$

where M_b, C_b and K_b represent the mass, damping and stiffness matrices of the beam model, respectively and $\ddot{y}_b$, $\dot{y}_b$ and y_b are the vectors of beam accelerations, velocities and displacements, respectively. A low damping ratio, ξ, equals to 3% is considered for the beam model. Rayleigh damping is used here to represent viscous damping for the bridge:

$$C_b = \alpha M_b + \beta K_b \tag{4-3}$$

where α and β are constants. The same damping is considered for all the modes and α and β can be obtained from, $\alpha = 2\xi\omega_1\omega_2/(\omega_1 + \omega_2)$ and $\beta = 2\xi/(\omega_1 + \omega_2)$, where ω_1 and ω_2 are the first two natural frequencies of the bridge (Clough and Penzien, 1993).

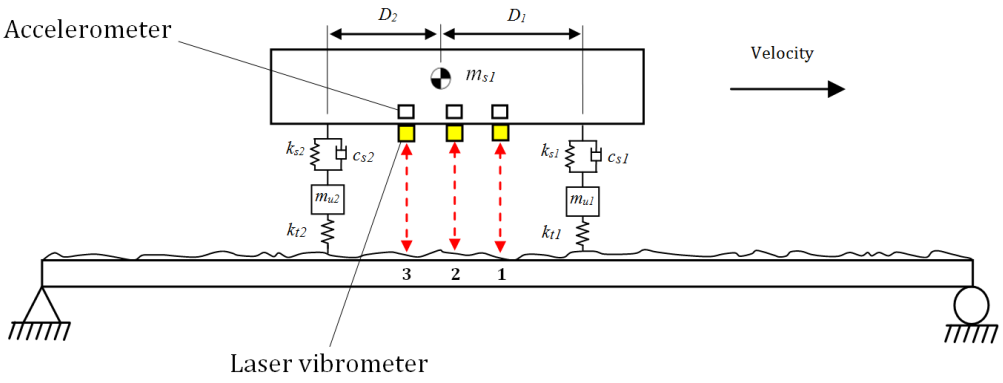

Figure 4-1 Laser and accelerometers measurements on the vehicle body.

An implementation in MATLAB is used for the dynamic interaction of the vehicle and the bridge. As the vehicle and the bridge are connected at the tyre contact points, they are coupled at those points by considering the interaction force vector. The equation of motion of the coupled system is formed by combining equations (4-1) and (4-2), as:

$$M_g\ddot{u} + C_g\dot{u} + K_g u = F \tag{4-4}$$

where M_g and C_g are the coupled system mass and damping matrices, respectively, K_g is the coupled system stiffness matrix which is time-varying and *F* is the system force vector. The vector, $u = \{y_v, y_b\}^T$, represents the displacement vector of the coupled system. The Wilson-Theta integration scheme (Tedesco et al., 1999) is employed here for solving Eq. 4-4. The optimal value of the parameter θ =1.420815 is selected as recommended in (González et al., 2012b) for unconditional stability of the integration scheme. The initial condition considered for the solution is zero displacement, velocity and acceleration for all the simulations.

4.3. Mode shape-based damage detection algorithm

The STFDD method (Malekjafarian and OBrien, 2014b) is one of the earliest methods for the identification of bridge mode shapes from indirect measurements. This method estimates bridge mode shapes from the response measured on a passing vehicle through a multi-stage process. Despite its success in the identification of bridge mode shapes in numerical studies, there are still some challenges in the application of the method for the purpose of bridge damage detection. The challenges can be given as (Malekjafarian et al., 2015):

1. The effect of road profile,
2. The limited resolution of the estimated mode shapes,
3. The effect of measurement noise.

Two alternatives are suggested in (Malekjafarian and OBrien, 2014b) to overcome the effect of road profile in the STFDD method; (a) applying other excitations to the bridge to strengthen the bridge response component in the measured response on the vehicle and (b) subtraction of the responses measured from following axles. The first idea is limited to longer-span bridges where there is enough ongoing traffic on the bridge to excite it. It is shown in Malekjafarian and OBrien (2014b) that the the second concept needs identical axles which is difficult to guarantee in practice and the results obtained are quite sensitive

to measurement noise. In Section 4.3.1, a new idea is presented to overcome the effect of road profile based on laser measurements on the passing vehicle. Oshima et al. (2014) first proposed the idea of measurement of bridge displacement response at the moving coordinate from the laser measurement. A similar procedure is used here to obtain the bridge velocity and acceleration at the moving coordinate.

It is shown in Malekjafarian and OBrien (2014b) that the resolution of the identified mode shape from the STFDD method is limited. This limitation may cause some restrictions in the use of these mode shapes for the purposes of damage detection and particularly damage localization. The resolution is related to the number of segments defined on the bridge. While defining more segments on the bridge would provide better mode shape resolution, it decreases the size of each segment that means providing shorter signals for the STFDD method. As processing of the shorter signals may give inaccurate results, decreasing the segment size is not recommended. Therefore, the current STFDD method can only provide a restricted mode shape resolution. In Section 4.3.2, the STFDD method is improved to provide better resolution. Finally in Section 4.3.3 a damage index is presented based on the mode shape estimated from the improved STFDD method.

The proposed damage detection algorithm includes the following steps:

- Measuring the relative velocity and vehicle acceleration on the vehicle.
- Obtaining the bridge acceleration at the moving coordinate.
- Identifying bridge mode shapes by applying the improved STFDD method.
- Damage detection based on the concept of mode shape squares (MOSS).

4.3.1. Measurement system

Oshima et al. (2014) use a laser distancemeter and an accelerometer on the vehicle axle to obtain the bridge deflection at the moving coordinate. In this chapter, laser vibrometers and accelerometers are assumed on the vehicle to measure the bridge accelerations at the moving coordinates (Figure 4-1).

The laser vibrometers measure relative velocities between the moving vehicle and the bridge $\dot{y}_b - \dot{y}_v$. The vehicle velocities are estimated by integrating the vehicle accelerations measured on the vehicle. By subtracting the estimated vehicle velocity from the measured

relative velocity, the bridge velocity at each moving coordinate can be obtained (Figure 4-2). The bridge acceleration at the moving coordinate can be obtained in the same way.

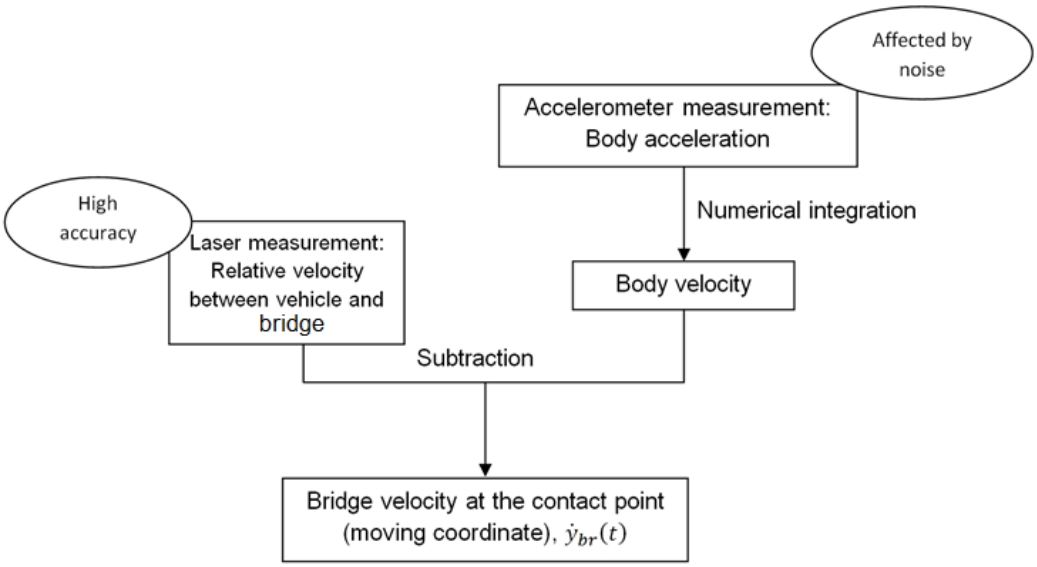

Figure 4-2 The subtraction concept.

In order to have enough responses for the STFDD method, a system including three laser vibrometers and three accelerometers on the vehicle, is used in this study (Figure 4-1). The measurement system can be installed on the vehicle axle (same as Oshima et al. (2014)) or it can be installed on the vehicle body. In addition, a geophone or servo velocity-meter can be used instead of an accelerometer to avoid the drifting problem caused by numerical integration. As the amplitude of the vehicle response is considerably greater than the bridge response, the estimated bridge response may be contaminated by noise or numerical errors. Therefore, a smaller vehicle/bridge response ratio will lead to more accurate results from the subtraction. In addition, the amplitude of vibration on the vehicle body is much less than the axles; therefore it is suggested to install the measurement system on the vehicle body (unlike Oshima et al. (2014)).

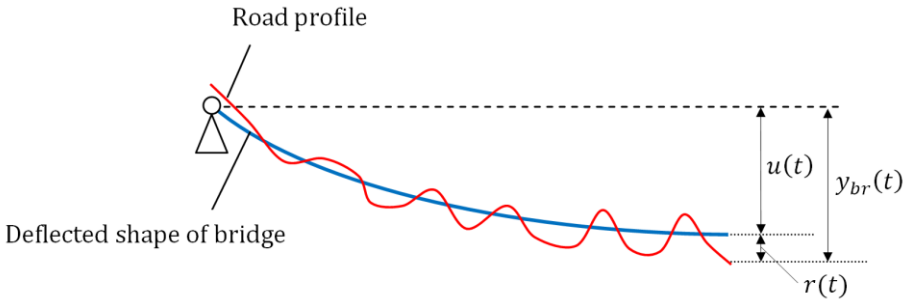

Figure 4-3 The bridge displacement under the laser.

When road roughness is present on the bridge (shown in Figure 4-3), the displacement measured under each laser vibrometer ($y(t)$) contains two parts; the bridge displacement ($u(t)$) and the road roughness ($r(t)$):

$$y_{br}(t) = u(t) + r(t) \tag{4-5}$$

Taking the derivative of both sides of Eq. 4-5:

$$\dot{y}_{br}(t) = \dot{u}(t) + \dot{r}(t) \tag{4-6}$$

where $\dot{y}_{br}(t)$ is the relative velocity measured by the laser (see Figure 4-2), $\dot{u}(t)$ is the bridge response under the laser and $\dot{r}(t)$ is the 'velocity' of the road roughness. As the laser is passing over the bridge, there is a spatial velocity related to changing of road profile through the length of the bridge. In order to remove the spatial velocity of the road profile from the response, the second response is subtracted from the first, with a time shift to allow for their relative positions:

$$\Delta\dot{y}_1 = \dot{y}_2(t + \Delta t) - \dot{y}_1(t) = \dot{u}_2(t + \Delta t) + \dot{r}_2(t + \Delta t) - \dot{u}_1(t) - \dot{r}_1(t) \tag{4-7}$$

where $\Delta\dot{y}_1$ is a time-shifted difference of bridge velocity and the time shift, Δt is the time difference between the 1st and 2nd lasers reaching a specific point and $\dot{y}_1$ and $\dot{y}_2$ are the velocities measured at the 1st and 2nd respectively. This means that the second response is shifted by Δt and becomes synchronised with the first response in terms of the location of scanning. As a result, each laser measures the same road profile velocity component, $\dot{r}_2(t + \Delta t) = \dot{r}_1(t)$. It follows that the road profile effect is largely removed from the response and a time shifted difference of the bridge response is obtained:

$$\Delta\dot{y}_1 = \dot{u}_2(t + \Delta t) - \dot{u}_1(t) \tag{4-8}$$

A second time shifted difference can be obtained from the second and the third laser measurements:

$$\Delta\dot{y}_2 = \dot{u}_3(t + 2\Delta t) - \dot{u}_2(t + \Delta t) \tag{4-9}$$

4.3.2. Improved STFDD method

The STFDD has been proposed by the authors (Malekjafarian and OBrien, 2014b) for the estimation of bridge mode shapes from indirect measurements. The method consists of two fundamental parts:

- Applying the FDD method to the response measured at two following axles in multiple stages and,
- Implementing a rescaling procedure to correct the local mode shapes estimated in each stage.

FDD is an output-only identification method in the frequency domain first proposed by Brincker et al. (2000). The method is based on decomposing the power spectral density matrix of the output data by Singular Value Decomposition (SVD). Natural frequencies of the structure can be estimated from the dominant peaks of an SVD diagram obtained by plotting the singular values of the outputs. The corresponding singular vectors are mode shapes of the structure.

The STFDD method is based on the fact that, if FDD is applied to the signals measured at the two following axles for short discrete time periods, the approximate bridge mode shapes can be obtained (see Figure 4-4). The bridge is divided into n equal segments with the length of each segment equal to the axle spacing. Allowing for the arrival and departure of the 2-axle vehicle, there will be $(n - 1)$ stages in which two short signals can be measured simultaneously. For example, a simple case with 5 segments is shown in Figure 4-4 which results in 4 stages; each stage involves two short signals. In the first stage, signals measured at the first axle from the second stage and at the second axle from the first segment are used.

By applying FDD to the measured data from each stage, the local mode shape vector, including two mode shape values, is estimated for each stage. In order to estimate the global mode shape vector, a rescaling procedure is applied by establishing a link between the local mode shape vectors obtained from the various stages. For example, the local mode shapes obtained for the first and the second segments from the first stage are considered as the global values of these two segments. Then, a scaling factor is defined using the ratio of the local mode shapes obtained for the second segment in the first and the second stages. By multiplying the scaling factor by the local mode shape value of the third segment from the second stage, the global scaled value of the third stage is estimated.

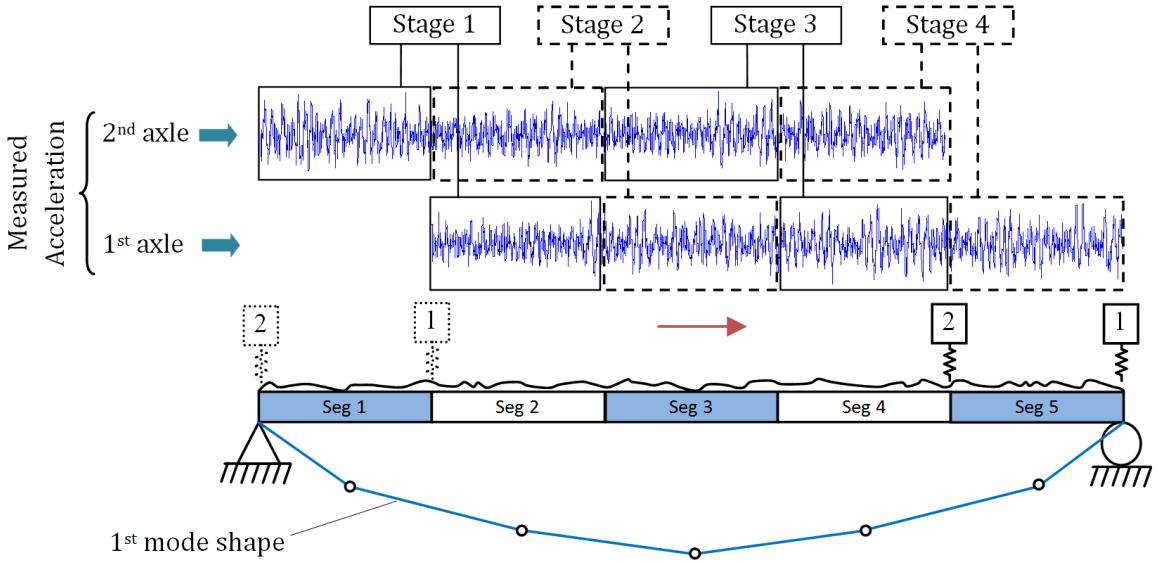

Figure 4-4 Summary of the STFDD method.

As a result, a global mode shape vector is obtained which incorporates contributions from each segment of the bridge to the mode shape. The method is based on the fact that the signal measured from each segment of the bridge demonstrates the dynamic nature of the bridge for that segment. More details of the STFDD method are provided in the literature and in Chapter 3 (Malekjafarian and OBrien, 2014b).

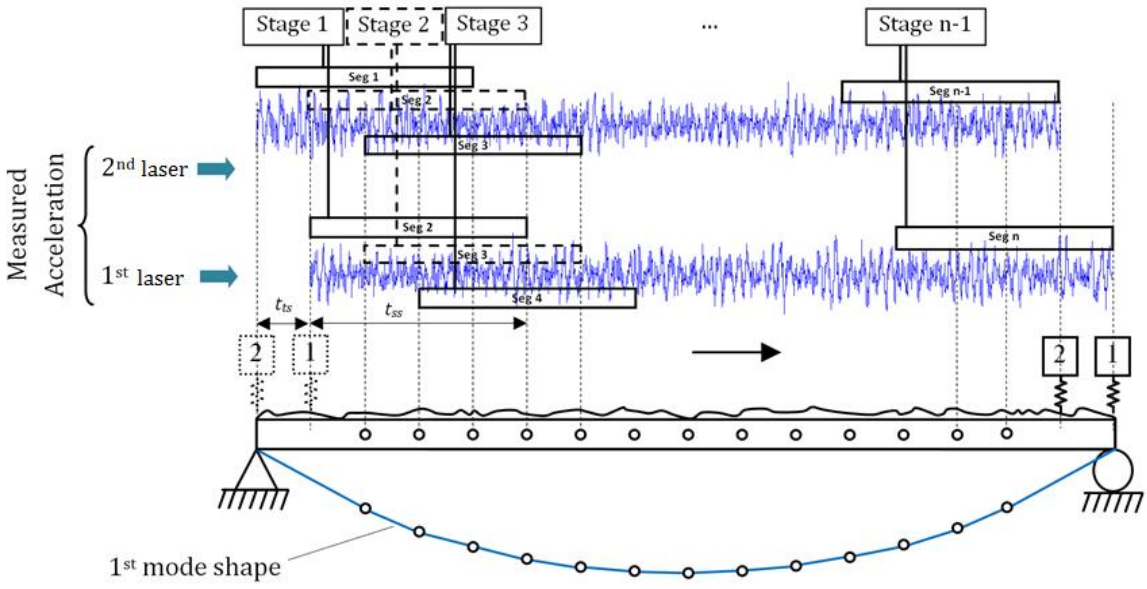

Figure 4-5 Summary of the Improved STFDD method.

In order to improve the resolution of the estimated mode shape, the STFDD method is modified in this chapter. Instead of defining the segments on the bridge, they are defined on the signal as shown in Figure 4-5. Firstly, the length of each signal segment t_{ss} is determined which must be long enough, to be processable by the FDD method. The time spacing between two short signals in each stage t_{ts} is determined based on the distance between two measurement points:

$$t_{ts} = {}^{d_{las}}/_{v} \tag{4-10}$$

where d_{las} is the distance between two laser vibrometers and v is the vehicle velocity. The number of points in the estimated mode shape is equal to:

$$n_{ss} = \frac{t_{tot} - t_{ss}}{t_{ts}} + 1 \tag{4-11}$$

where t_{tot} is the total time of the response measured from each laser.

By increasing the number of segments in this way, the length of the signal is constant, unlike the original STFDD method. As a result an approximate mode shape can be obtained with a better resolution which is required for damage detection. The number of points can be adjusted by changing the distance between the laser vibrometers.

4.3.3. Damage detection based on mode shape square

There is a long history of using mode shapes as a damage indicator (Fan and Qiao, 2011). Some of the methods (Shi et al., 2000, Hadjileontiadis et al., 2005, Fan and Qiao, 2009) use changes in the mode shapes for damage identification and some of them (Pandey et al., 1991, Li et al., 2005) use mode shape curvature which is more sensitive to damage. Although the methods based on modal curvature can detect the damage from an early stage, they need exact mode shapes. As the estimated mode shapes using the Improved STFDD method, are obtained from measurements at moving coordinates (not fixed coordinates), the results are approximate. Therefore, a damage index approach is developed here based on mode shape estimates.

The concept of mode shape square (MOSS) proposed by Zhang et al. (2012) is used here for damage detection. In this method, damage is indicated by a local change in the estimated

MOSS curve. As the mode shapes is normalized to unity, a scale factor α is introduced to provide a minimum distance between the damaged and healthy shapes (Zhang et al., 2012).

$$\alpha = \frac{MOSS_i^d . MOSS_i^u}{MOSS_i^d . MOSS_i^d} \tag{4-12}$$

where $MOSS_i^d$ and $MOSS_i^u$ are the i^{th} MOSS of the damaged and undamaged structure respectively. The damage index is defined based on the differences between the MOSS of the healthy and damaged bridges as (Zhang et al., 2012):

$$\Delta_i = MOSS_i^u - \alpha MOSS_i^d \tag{4-13}$$

By plotting Δ_i as a function of the length of the bridge, the damage location can be identified. When damage location is not required, a damage indicator based on summation of differences between the damaged and healthy MOSS can be defined as:

$$DI_i = \sum_{j=1}^{n_{ss}} \left| MOSS_i^u(j) - \alpha MOSS_i^d(j) \right| \tag{4-14}$$

4.4. Numerical simulations

The algorithm proposed in Section 4.3 is tested using numerical simulation. The VBI model described in Section 4.2 has been used to model a vehicle passing over a bridge. The FE method used to model the bridge utilizes 20 elements. The properties of the bridge are given in Table 4-1. The first three natural frequencies of the bridge are; 4.97, 19.88 and 44.73 Hz. The properties of the vehicle are given in Table 4-2.

Table 4-1 Properties of the bridge.

Properties	Unit	Symbol	value
Length	m	*L*	16
Mass per unit	kg/m	*m*	28125
Modulus of elasticity	MPa	*E*	35000
Second moment of area	m^4	*J*	0.5273

Table 4-2 Properties of the half-cars.

Properties	Unit	Symbol	Value
Body mass	kg	m_s	16200
Moment of inertia	kg m^2	I_s	93457
Axle mass	kg	m_{u1}	700
		m_{u2}	1100
Suspension stiffness	N/m	k_{s1}	4×10^5
		k_{s2}	1×10^6
Suspension damping	Ns/m	c_{s1}	10×10^3
		c_{s2}	20×10^3
Tyre stiffness	N/m	k_{t1}	1.75×10^6
		k_{t2}	3.5×10^6
Body bounce frequency	Hz	ω_b	1.58
Axle hop frequency	Hz	ω_{a1}	8.83
		$\omega a2$	10.21

4.4.1. Verification of the algorithm

The vehicle is first passed over the bridge at a speed of 1 m/s. The road profile irregularities are randomly generated based on the ISO standard (ISO8608:1995, 1995) for a road class 'A' (very good) profile which is a commonly adopted assumption for a well maintained highway. The distance between the laser vibrometers (d_{las}) is selected to be 0.5 m. The relative velocity responses and acceleration responses are taken to be measured on the vehicle.

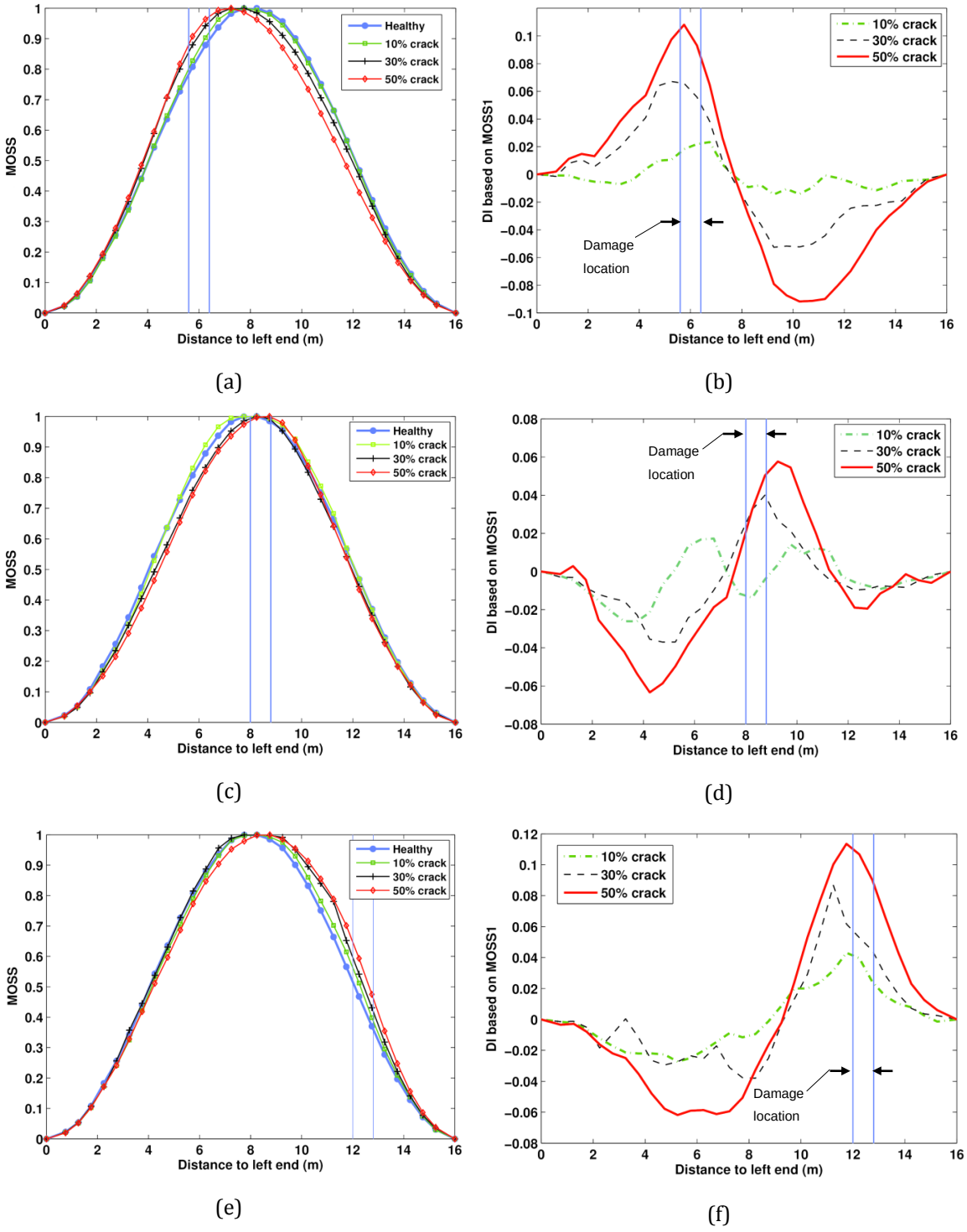

Figure 4-6 The first MOSS of the healthy and damaged bridges and the differences between the MOSSs, respectively for different damage location; (a and b) element 7, (c and d) element 11 and (e and f) element 15.

The bridge responses at the moving coordinate are estimated using the subtraction method described in Section 4.3.1. Once the bridge responses have been estimated, the Improved STFDD method is applied. The length of each signal segment t_{ssl} is selected to be 1.5 s

resulting in 30 points (n_{ss}) in the estimated mode shape. The first mode shape of the healthy bridge is then obtained and shown in Figure 4-6.

Damage is modelled based on a method proposed by Sinha et al. (2002). A crack is deemed to cause a stiffness loss over a region around itself, with the flexibility varying linearly on each side from the uncracked to the cracked beam section. The severity of the damage is represented by the crack depth, expressed as a percentage of the beam depth. Three different damage locations are considered, corresponding to elements 7, 11 and 15. For each location, three levels of damage, 10%, 30% and 50% are considered which results in a total of nine damage scenarios. Figure 4-6 (a), (c) and (e) show the estimated first MOSS for the three levels of damage at elements 7, 11 and 15, respectively. The damage index defined in Eq. 4-14, is calculated in each case. Figure 4-6 (b), 6(d) and 6(f) show the damage indices for the different levels of damage at elements 7, 11 and 15, respectively.

The results shown in Figure 4-6 demonstrate the ability of the algorithm to detect and, to some extent, to localize damage. The damage location can be detected better when it is located away from the mid-span. However, when the damage is located in the 11th element, the algorithm is able to detect it when the level of the damage is more than 10%. In addition, the damage indicator defined in Eq. 4-14 is calculated for all of the scenarios shown in Figure 4-7. It is clear that, at each location, the damage damage indicator is well correlated with the level of damage.

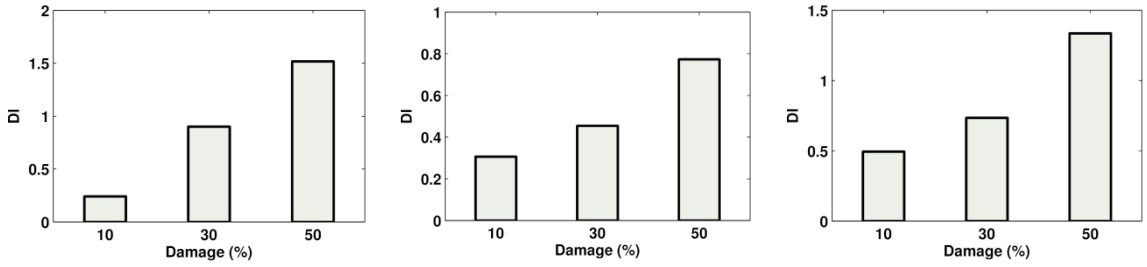

(a) (b) (c)

Figure 4-7 The damage indicator for different damage location; (a) element 7, (b) element 11 and (c) element 15.

4.4.2. Damage detection at higher speed

Low vehicle speed is one the challenges in most indirect bridge damage detection methods. In an earlier study, the authors (Malekjafarian and OBrien, 2014b) identify the bridge mode shapes from indirect measurement at a vehicle speed of 2 m/s but this is too slow for practical

implementation. In the previous section, the vehicle speed is considered to be 1 m/s. Once the speed is increased, the length of the signal measured on the vehicle is decreased. Therefore, there is not enough measured data for the STFDD method. To improve the quantity of measured data when the vehicle speed is higher, the concept of using more measurement points on the vehicle is used. Six laser vibrometers and six accelerometers are taken to be mounted on the vehicle body to obtain five difference signals (See Figure 4-8):

$$\begin{aligned} \Delta\dot{y}_1 &= \dot{u}_2(t+\Delta t) - \dot{u}_1(t) \\ \Delta\dot{y}_2 &= \dot{u}_3(t+2\Delta t) - \dot{u}_2(t+\Delta t) \\ \Delta\dot{y}_3 &= \dot{u}_4(t+3\Delta t) - \dot{u}_3(t+2\Delta t) \\ \Delta\dot{y}_4 &= \dot{u}_5(t+4\Delta t) - \dot{u}_4(t+3\Delta t) \\ \Delta\dot{y}_5 &= \dot{u}_6(t+2\Delta t) - \dot{u}_5(t+4\Delta t) \end{aligned} \tag{4-15}$$

The stages of the STFDD method can be defined based on the measured differences. For example for the i^{th} stage:

$$\begin{aligned} Y_i = \{&\Delta\dot{y}_1(\, x \in segment\ i); \Delta\dot{y}_2(x \in segment\ i); \Delta\dot{y}_3(x \\ &\in segment\ i); \Delta\dot{y}_4(x \in segment\ i)\} \\ Y_{i+1} = \Delta\dot{y}_{i+1}&(at\ x = segment\ 1) + \Delta\dot{y}_{i+1}(at\ x = segment\ 1) \\ &+ \Delta\dot{y}_{i+1}(at\ x = segment\ 1) + \Delta\dot{y}_{i+1}(at\ x = segment\ 1) \end{aligned} \tag{4-16}$$

In effect, the signal segments are stacked, one after another, as illustrated in Figure 4-9. Using a special truck like the Traffic Speed Deflectometer (TSD) (Flintsch et al., 2012) may be the practical implementation of such a case. TSD's are used in a number of countries to measure the deflection 'basin', i.e., the depression in the road pavement under a heavy axle as it passes. They operate at full highway speed and use laser vibrometers to measure the derivative of vertical displacement at very high accuracy. The inferred displacement has a resolution of tens of microns. It is anticipated that multiple laser vibrometers on a TSD could, in the future, be used to find the mode shapes in a bridge while the TSD is travelling at full highway speed.

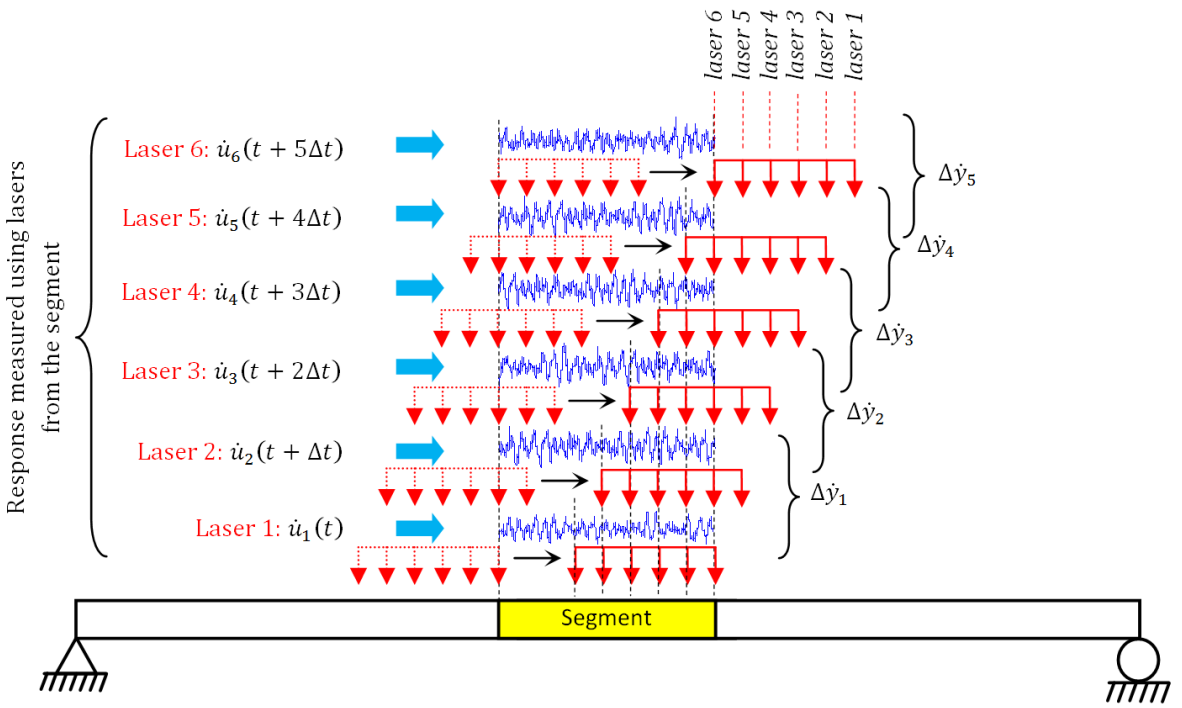

Figure 4-8 Summary of concept of consecutive measurement.

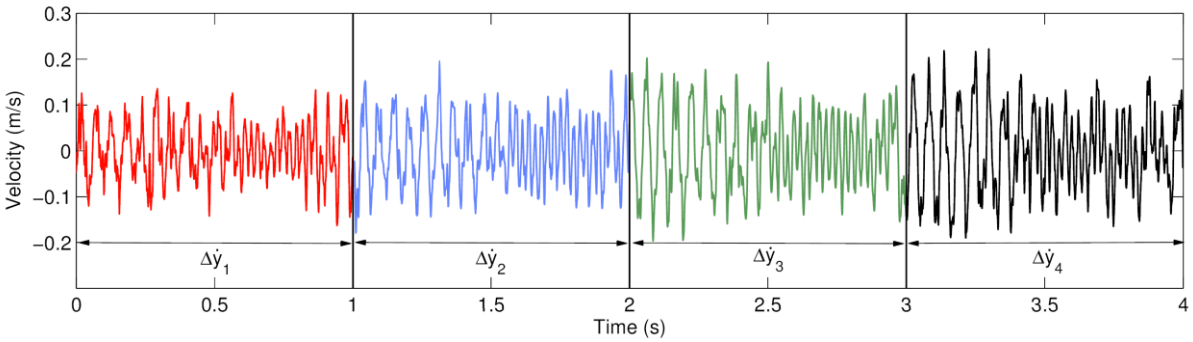

Figure 4-9 Velocity differences collected from six following laser vibrometers.

It is obvious that the length of the signal used here is four times of the length of the signal used in section 3.1. Therefore, it is possible to increase the velocity of the vehicle up to four times while retaining the quality of the inferred information. The approach is applied to the same case study as above with the same damage scenarios, using two different vehicle speeds; 4 and 8 m/s which results in 4 and 2 s signals respectively.

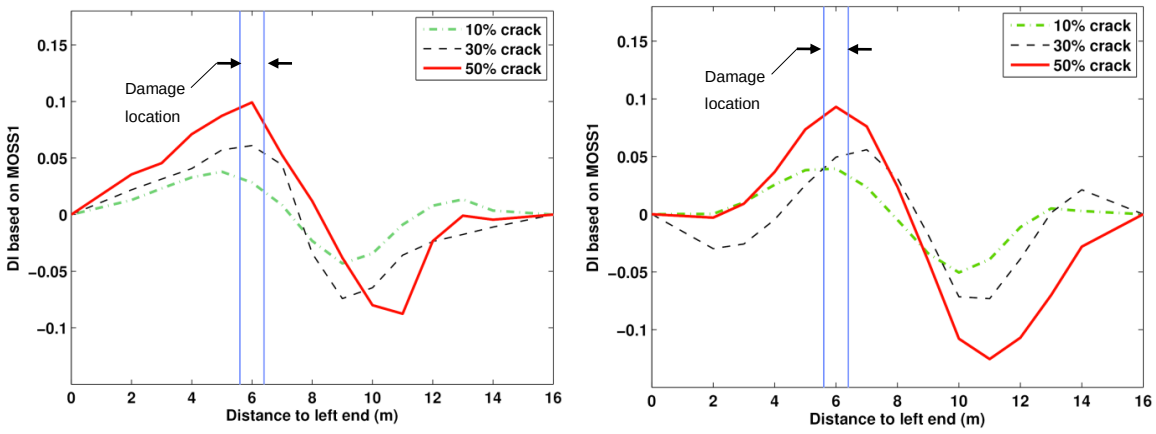

(a) (b)

Figure 4-10 Damage indicators based on the MOSS's for vehicle speeds of; (a) 4 m/s (b) and 8 m/s.

For the first case in which the vehicle speed is 4 m/s, (d_{las}) is selected to be 1 m which results in $t_{ts} = 0.25$ s and the length of each signal segment t_{ssl} is selected to be 1 s resulting in 13 points (n_{ss}) in the estimated mode shape. Using the process explained in Eq. 4-11, the length of the signal used in each stage is effectively increased to 4 sec (Figure 4-9). Figure 4-10 (a) shows differences of MOSS's between damaged and healthy bridges using this vehicle speed of 4 m/s. The same procedure is used, when the vehicle speed is 8 m/s (Figure 4-10 (b)). The algorithm can be seen to detect the damage with acceptable accuracy even for a vehicle speed of 8 m/s (28.8 km/h).

4.4.3. Influence of measurement noise

Noise is an inherent characteristic of any signal measurement, even for the most accurate sensors, and is investigated in this section. Additive white Gaussian noise (AWGN) is added in this section to the acceleration signals according to (Lyons, 2011), i.e., according to the equation:

$$A_{poll} = A + E_{nse} \times N \tag{4-17}$$

where A_{poll} is the signal containing noise, A is the original signal containing no noise, N is a standard normal distribution vector with zero mean and unit standard deviation and E_{nse} is the energy in the noise. The term, E_{nse}, is determined from the definition of SNR given by Eq. 4-18:

$$SNR = 10\log_{10}\frac{var(A)}{E_{nse}^2} \tag{4-18}$$

where SNR is the ratio of the power in the signal to the power in the noise and $var(A)$ is the variance of the signal.

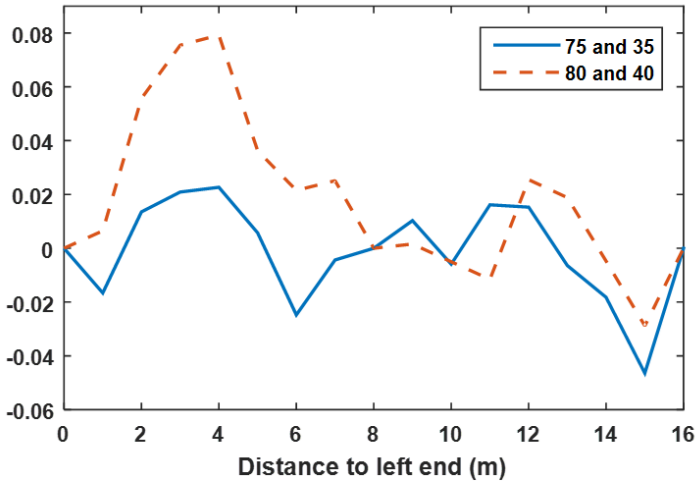

Figure 4-11 Differences between the healthy baseline MOSS's and for the laser and accelerometer SNR noise levels respectively of (a) 80 and 40 and (b) 75 and 35.

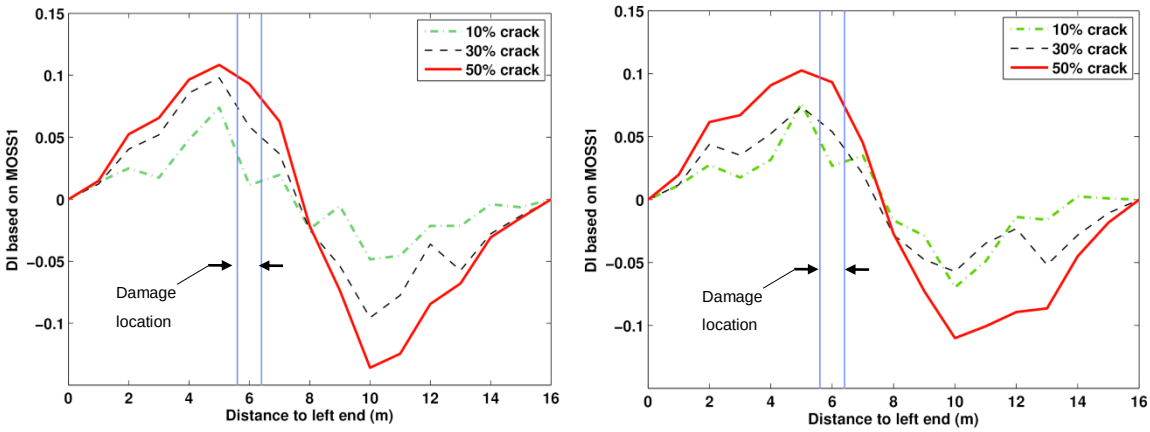

Figure 4-12 Differences between the MOSS's for laser and accelerometer SNR noise levels respectively of (a) 80 and 40 and (b) 75 and 35.

As mentioned before, two types of sensor are used in the measurement system defined in Section 4.3.1; laser vibrometers and accelerometers. Generally, a laser vibrometer is one of the most accurate sensors, so some low levels of noise with SNR levels of 60 and 50 are considered. On the other hand, noise at levels of 40 and 35 of are considered for the accelerometer measurement. Figure 4-12 shows the efficiency of the damage index when

noise is added to the baseline. Figure 4-12 shows that small levels of damage can still be detected in the presence of added noise.

4.5. Conclusions

This chapter presents a novel approach for indirect bridge damage detection. A measurement system based on laser vibrometers and accelerometers is employed to measure the bridge response at moving coordinates on a passing vehicle. An improved STFDD method is used to provide higher resolution for the mode shape estimated. The sensitivity of the proposed algorithm in the identification of presence and, to some extent, location of damage is confirmed through numerical investigations. The effectiveness of the approach using vehicle speeds up to 8 m/s is confirmed. The proposed method can be applied for damage detection of many bridge structures. The key guideline for application of this method is to use a high accuracy measurement system. As is observed, the accuracy of the measurement has a considerable influence on the accuracy of the method.

Chapter 5: Application of Empirical Mode Decomposition to the Drive-by Bridge Damage Detection

Authors:

Eugene J. OBrien

Abdollah Malekjafarian

Arturo González

Paper status:

Published in *European Journal of Mechanics / A Solids*,

DOI: 10.1016/j.euromechsol.2016.09.009.

Not to the reader:

This work is entirely the work of the author under the supervision of Prof. Eugene OBrien and Dr. Arturo González.

Chapter 5: Application of Empirical Mode Decomposition to the Drive-by Bridge Damage Detection

5.1. Introduction

Bridges play a key role in road and rail transportation. However, concrete and steel deteriorate over time and many bridges in the developed world are structurally deficient. Therefore bridge condition monitoring is becoming a key element in the planning of maintenance interventions in transport infrastructure. Today, visual inspections are widely used for bridge damage detection. While effective in many cases, visual inspection suffers variability in the judgments of inspectors and accessibility issues which may leave some types of damage undiscovered.

In recent years, there has been an increasing interest in vibration-based structural health monitoring methods for bridge damage detection. These approaches are mainly based on the variation of modal parameters of the structure (i.e. natural frequency, mode shape and damping ratio) with structural health condition. Natural frequency change is the most common damage indicator, but it is generally accepted that natural frequencies alone cannot provide local information about damage (Fan and Qiao, 2011). Recently more sensitive modal parameters such as mode shapes and modal curvatures have gained attention. These approaches have the potential to provide local information on the structural condition of the structure (Fan and Qiao, 2011).

Although these vibration-based methods can provide high quality information about bridge condition, they require the installation of many sensors and access to electrical power on the bridge. Considering the large number of short and medium span bridges, the instrumentation becomes expensive and smaller bridges are not routinely instrumented at this point in time. Recently, this drawback of direct methods has led to the concept of an indirect approach in which bridge condition is investigated using data measured on a passing vehicle (Malekjafarian et al., 2015). The idea is first proposed to extract the bridge natural frequency from indirect measurements (Yang et al., 2004). It is shown that the acceleration response measured on a vehicle passing over the bridge includes enough bridge response to reveal the bridge natural frequencies. Early research in this field is focused on the validation of the idea experimentally (Lin and Yang, 2005), improvement of the accuracy (Kim and Kawatani, 2009, Yang and Chang, 2009a, Yang and Chen, 2015) and accessing bridge

natural frequencies other than just the first one (Yang and Chang, 2009b). Recent research investigates other modal parameters such as damping ratio (González et al., 2012b, Keenahan et al., 2014) and mode shapes (Yang et al., 2014b, Oshima et al., 2014, Malekjafarian and OBrien, 2014b). Yang et al. (2014b) show that the bridge mode shape can be identified from the Hilbert amplitude of a filtered response measured on a passing axle. Oshima et al. (2014) propose a method in which the bridge mode shapes are found from the response measured on a truck-trailer system. The mode shapes are identified by applying Singular Value Decomposition (SVD) to the responses measured on several axles of the truck-trailer system. Malekjafarian and OBrien (2014b) propose Short Time Frequency Domain Decomposition (STFDD) for the identification of bridge mode shapes from the response measured on two following axles passing over the bridge. It is shown that the mode shapes can be constructed by applying Frequency Domain Decomposition (FDD) to the responses in a multi-step procedure.

Several attempts have been made to detect bridge damage using indirect measurements (McGetrick and Kim, 2014a, Li and Au, 2014, Lederman et al., 2014, Kim et al., 2014, Nguyen and Tran, 2010). Nguyen and Tran (2010) use a Symlet wavelet transform of the displacement response measured on a moving vehicle to identify the location of cracks in a bridge. McGetrick and Kim (2013), McGetrick and Kim (2014b) apply a Continuous Wavelet Transform (CWT) to the dynamic response of a passing vehicle. It is demonstrated that the CWT coefficients are affected when the axle passes over a damaged section. Li and Au (2014) suggest a multistage damage detection approach using modal strain energy and the genetic algorithm (GA). The approach successfully detects the location of damage in a two-span continuous bridge. OBrien and Keenahan (2014) introduce a new drive-by damage detection method using the concept of the apparent road profile. A mode-shape based damage detection method is proposed in OBrien and Malekjafarian (2016) using an improved version of the STFDD method. They obtain a better resolution of the bridge mode shapes which has good potential for damage detection.

In this chapter, the theoretical response of a vehicle passing over a bridge is presented first. It is shown in (Yang et al., 2004) that the response measured on a passing vehicle contains three main components; vehicle frequency, bridge natural frequency and the pseudo frequency associated with vehicle speed. The first of these relates to the vehicle dynamic response and the last two correspond to the bridge response. Generally, those components corresponding to the bridge dynamics reflect the bridge condition. He and Zhu (2015)

investigate the dynamic response of a bridge to a moving load (which is generally a moving vehicle). They show that the pseudo-frequency component of the response is more sensitive to damage and is preferred for damage localization. This finding is used in this chapter, by separating the pseudo-frequency component of the response and using it for damage detection. Empirical Mode Decomposition (EMD) is applied to the axle response to decompose it into different components using a sifting process. It is shown that the damage location can be detected using the intrinsic mode functions (IMFs) corresponding to the pseudo-frequency. A finite element (FE) model of Vehicle Bridge Interaction (VBI) is used to provide a numerical case study to validate the method. A simulation of a quarter car passing over a bridge with a smooth road surface is followed by a case with good road roughness. Finally, the sensitivity of the method to changes in the transverse position of the vehicle on the bridge is investigated.

5.2. Theoretical background

The basis of indirect bridge monitoring is to use the response measured on a passing vehicle. A comprehensive theoretical look at this response is necessary for a better understanding of the indirect approach. A closed-form VBI solution is presented in this section to identify the main components of the response measured on a passing vehicle.

5.2.1. The response measured on a passing vehicle

A greatly simplified model is first considered to identify the basic features of the system. The vehicle is modelled as a sprung mass and the bridge as a simply supported beam considering only the first mode. Then, the equation of motion for the sprung mass moving over the beam, shown in Figure 5-1 can be written as (Yang et al., 2004):

$$m_v \ddot{q}_v + k_v(q_v - u|_{x=vt}) = 0 \tag{5-1}$$

where q_v is the vertical displacement of the sprung mass, m_v and k_v are the mass and stiffness of the sprung mass and u is the beam deflection. By considering the contact force between the sprung mass and the beam and the beam displacement due to the moving load, Eq. (5-1) can be expressed as (Yang et al., 2004):

$$m_v \ddot{q}_v + ({\omega_v}^2 m_v) q_v - \left[{\omega_v}^2 m_v \sin\left(\frac{\pi v t}{L}\right)\right] q_b = 0 \tag{5-2}$$

where ω_v is the sprung mass natural frequency given by $\omega_v = \sqrt{\frac{k_v}{m_v}}$, v is the speed of the sprung mass, t is time, L is the total length of the beam and q_b is the deflection at mid-span of the beam.

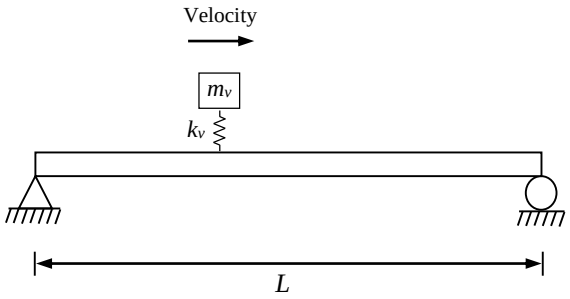

Figure 5-1 A sprung mass passing over a bridge

If the vehicle mass is much less than the total mass of the bridge, then the vehicle displacement can be approximated as (Yang et al., 2004):

$$q_v(t) = \frac{\Delta_{st}}{2(1-S^2)}\left[(1-cos\omega_v t) - \frac{cos2\pi vt/L - cos\omega_v t}{1-(2\mu S)^2} - S\frac{cos(\omega_b - \pi v/L)\,t - cos\omega_v t}{1-\mu^2(1-S)^2} + S\frac{cos(\omega_b + \pi v/L)\,t - cos\omega_v t}{1-\mu^2(1+S)^2}\right] \quad (5\text{-}3)$$

where μ is the the ratio of the bridge frequency to the vehicle frequency, $\mu = \omega_b/\omega_v$, Δ_{st} is the approximate static deflection at mid-span of the beam under the gravity action of the mass m_v at that point and S is defined as $S = {}^{\pi v}/_{L\omega_b}$. This can be calculated using:

$$\Delta_{st} = -\frac{2m_v g L^3}{\pi^4 EI} \quad (5\text{-}4)$$

where g is the acceleration due to gravity, E is the elastic modulus and I is the second moment of area.

The acceleration of the moving vehicle can be obtained by differentiating Eq. (5-3) twice (Yang et al., 2004):

$$\ddot{q}_v(t) = \frac{\Delta_{st}{\omega_v}^2}{2(1-S^2)}\left[cos\omega_v t - \frac{(2\mu S)^2 cos2\pi vt/L - cos\omega_v t}{1-(2\mu S)^2} - S\frac{\mu^2(1-S)^2\, cos(\omega_b - \pi v/L)\, t - cos\omega_v t}{1-\mu^2(1-S)^2} + S\frac{\mu^2(1+S)^2\, cos(\omega_b + \pi v/L)\, t - cos\omega_v t}{1-\mu^2(1+S)^2}\right] \quad (5\text{-}5)$$

For a better understanding of the different components of vehicle acceleration, Eq. (5-5) can be rewritten as:

$$\ddot{q}_v(t) = \frac{\Delta_{st}{\omega_v}^2}{2(1-S^2)}\left[A_1 cos\omega_v t + A_2 cos\frac{2\pi v}{L} + A_3 cos\left(\omega_b - \frac{\pi v}{L}\right) + A_4 cos\left(\omega_b + \frac{\pi v}{L}\right)\right] \quad (5\text{-}6)$$

where A_1, A_2, A_3 and A_4 determine the relative contributions of each component to the total acceleration response. These are given by:

$$A_1 = 1 - \frac{1}{1-(2\mu S)^2} - \frac{S}{1-\mu^2(1-S)^2} + \frac{S}{1-\mu^2(1+S)^2}$$

$$A_2 = \frac{(2\mu S)^2}{1-(2\mu S)^2} \quad (5\text{-}7)$$

$$A_3 = \frac{S\mu^2(1-S)^2}{1-\mu^2(1-S)^2}$$

$$A_4 = \frac{S\mu^2(1+S)^2}{1-\mu^2(1+S)^2}$$

From Eq. (5-6), three main components exists in the total response that can be written as:

$$\ddot{q}_{v_{veh}}(t) = \frac{\Delta_{st}{\omega_v}^2}{2(1-S^2)} A_1 cos\omega_v t$$

$$\ddot{q}_{v_{spe}}(t) = \frac{\Delta_{st}{\omega_v}^2}{2(1-S^2)} A_2 cos\frac{2\pi v}{L} \tag{5-8}$$

$$\ddot{q}_{v_{br}}(t) = \frac{\Delta_{st}{\omega_v}^2}{2(1-S^2)}\left[A_3 cos\left(\omega_b - \frac{\pi v}{L}\right) + A_4 cos\left(\omega_b + \frac{\pi v}{L}\right)\right]$$

where $\ddot{q}_{v_{veh}}$ is the component associated with the vehicle frequency, $\ddot{q}_{v_{spe}}$ is that part of the signal associated with vehicle speed and $\ddot{q}_{v_{br}}$ is the component associated with the bridge natural frequency.

A simple case study is considered here to demonstrate the different components of the vehicle response. A mass-spring system with properties of $m_v = 700$ kg and $k_v = 1.75 \times 10^6$ N/m is travelling over a simply supported beam with the properties given in Table 1. The vehicle speed is 10 m/s.

Table 5-1. Properties of the bridge

Properties	Unit	Symbol	value
Length	m	*L*	15
Mass per unit length	kg/m	*m*	28125
Modulus of elasticity	N/mm^2	*E*	35000
Second moment of area	m^4	*J*	0.5273
First natural frequency	Hz	ω_1	5.65

The acceleration of the moving axle is calculated using Eq. (5-5) and is shown in Figure 5-2(a). The Fast Fourier Transform (FFT) of the acceleration is plotted in Figure 5-2(b) and shows the dominant frequencies in the response. As was expected from Eq. (5-5), the response consists of three main components, the frequencies of which are numbered in the FFT spectrum: (1) the speed pseudo-frequency, (2) the bridge frequency and (3) the vehicle frequency (Yang et al., 2004).

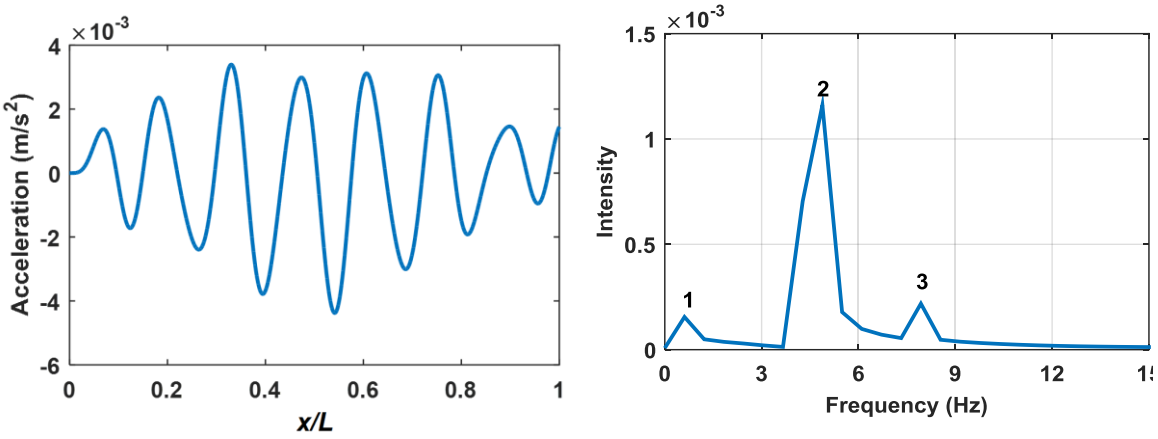

Figure 5-2 The response measured on a passing vehicle; (a) total acceleration, (b) FFT of the acceleration

For a better understanding of the response, each component is plotted separately in Figure 5-3 (a) shows the speed pseudo-frequency part of the response which is related to the vehicle speed and the total length of the bridge. Figure 5-3 (b) shows the bridge vibrations measured on the vehicle. As only the first mode of the bridge is considered in the closed-form solution, this part only presents the first mode shape, corresponding to the first natural frequency of the bridge. Finally Figure 5-3 (c) shows the vehicle's free vibrations.

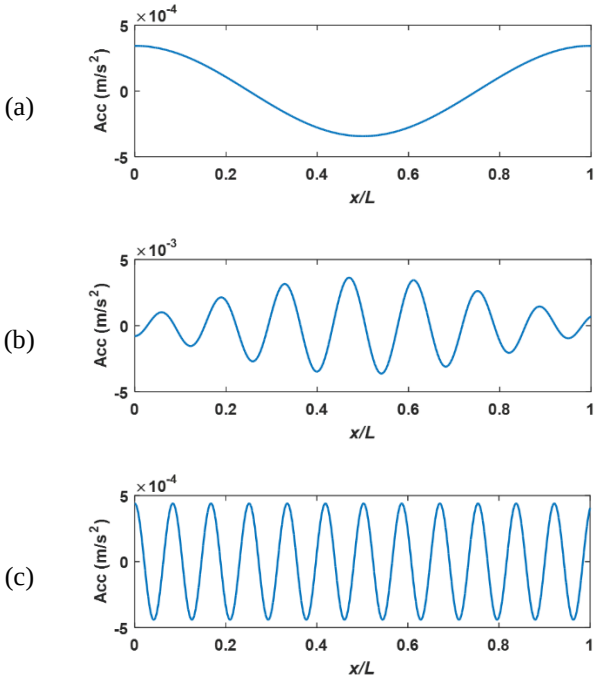

Figure 5-3 Components of the acceleration response; (a) speed pseudo-frequency part; (b) bridge frequency part and (c) vehicle frequency part

For monitoring purposes, the bridge components of the indirect response are of interest. Many researchers have carried out studies on indirect bridge monitoring that consider bridge

component in the measured response. These methods are usually based on the fact that damage to the bridge causes a change in its dynamic properties such as natural frequencies, damping ratios and mode shapes. By identifying these properties from the response measured on the vehicle, it is possible to investigate the bridge's health condition. The most common method is detecting changes in the bridge natural frequencies which could be observable in the FFT of the response measured on the vehicle, $\ddot{q}_v$ which originally comes from $\ddot{q}_{v_{br}}$. Some researchers believe that natural frequency is not a sufficiently sensitive parameter for damage detection and may be affected by environmental conditions such as temperature. For this reason, using other parameters such as bridge mode shape has been suggested. Recently, some new methods have been proposed for the identification of bridge mode shapes using indirect measurements (Malekjafarian and OBrien, 2014b, OBrien and Malekjafarian, 2015, Yang et al., 2014b). The concept behind these methods is that the bridge frequency component of the vehicle response includes the full mode shapes of the bridge as the vehicle is measuring this part of the response on a moving coordinate system. By applying a method such as STFDD (Malekjafarian and OBrien, 2014b), the bridge mode shape can be identified indirectly and used for damage detection purposes (OBrien and Malekjafarian, 2016). On the other hand, there are some publications that consider the measured signal directly, seeking a discontinuity at the damage location using methods such as the Wavelet transform. The basis behind these methods can be understood by looking at the bridge response. It is shown in He and Zhu (2015) that the speed pseudo-frequency part of the response is very sensitive to damage when the response is measured directly on the bridge. The same explanation can be given for indirect measurements. Therefore, it can be concluded that if the response measured on a passing vehicle can be decomposed into its original components, the speed pseudo-frequency part can show the damage location.

5.2.2. Empirical Mode Decomposition (EMD)

The EMD method (Huang et al., 1998, Huang et al., 1999) is a signal processing tool which decomposes any signal, non-stationary or even nonlinear, into several stationary so-called Intrinsic Mode Functions (IMFs). The procedure of extracting an IMF is called sifting and is as follows:

1. Identify all the local maxima and minima in the original time signal.
2. Connect all the local maxima and minima with cubic splines as the upper and lower envelopes.

3. Compute the mean value of the two envelopes and subtract it from the original signal.

The differences between the original time history and the mean value is the IMF, if it satisfies the following conditions: the number of extrema and the number of zero crossings must be equal or differ at most by one and at any point the mean value of the envelope defined by the local maxima and the envelope defined by the local minima must be zero. The sifting procedure continues until the residue becomes so small that it is less than a predetermined value of consequence, or the residue becomes a monotonic function. The original time signal can then be expressed as the sum of the IMFs and the final residue. The first IMF contains the highest frequency content of the original signal and the final residue contains the lowest frequency in the signal.

Cubic splines are suggested for use in the earliest version of the EMD, but they are known to give rise to over- and undershoot problems. The potential for IMFs to be corrupted by the cubic spline overshooting problem may be amplified by the iterative nature of the sifting process. The other types of spline (such as rational spline) can be used here to improve the accuracy of the results.

The bridge displacement and acceleration responses are obtained by theoretical calculation explained in Section 2.1. The EMD method is used in this section to decompose the theoretical responses. It is observed in the simulation that in some cases the EMD is not able to separate the vehicle frequency from the total signal when acceleration is considered. Therefore, before applying EMD, a moving average filtering (MAF) is set to the vehicle frequency and applied to the acceleration signal to remove the vehicle component from the total response measured on the vehicle. The IMFs obtained from the EMD and their FFT spectra are shown in Figure 5-4 and Figure 5-5 for displacement and acceleration respectively. It can be understood from the FFT spectrum of the first IMF that it is associated with the bridge first natural frequency (5.65 Hz) which is shifted by the vehicle speed. The second and third IMFs are related to the speed pseudo-frequency part of the signal. Therefore, by removing the first IMF from the original signal, the speed pseudo-frequency part which was previously shown to be sensitive to damage, can be extracted from the signal.

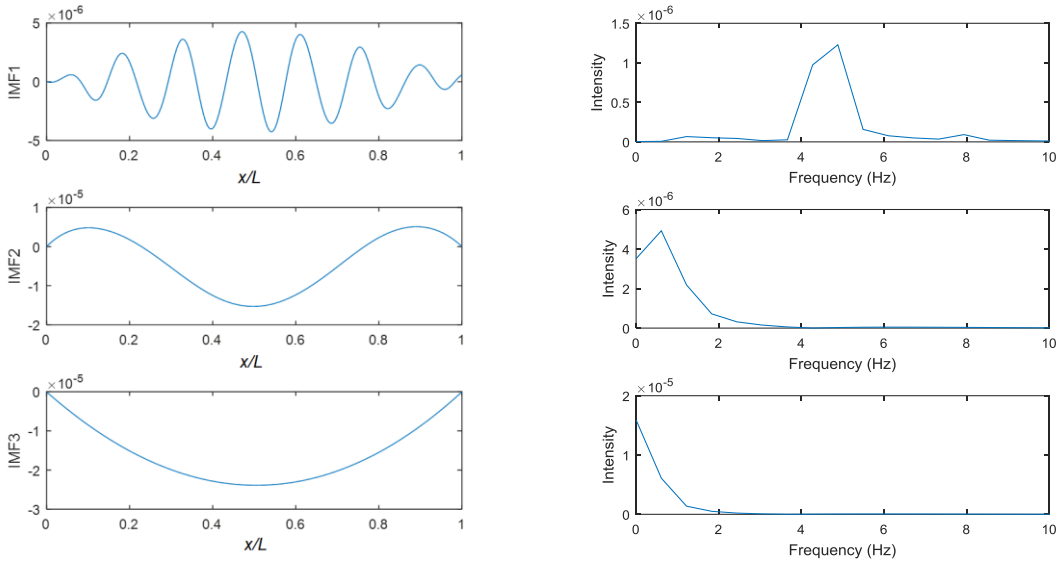

Figure 5-4 IMFs of the vehicle displacement response and their FFT spectra

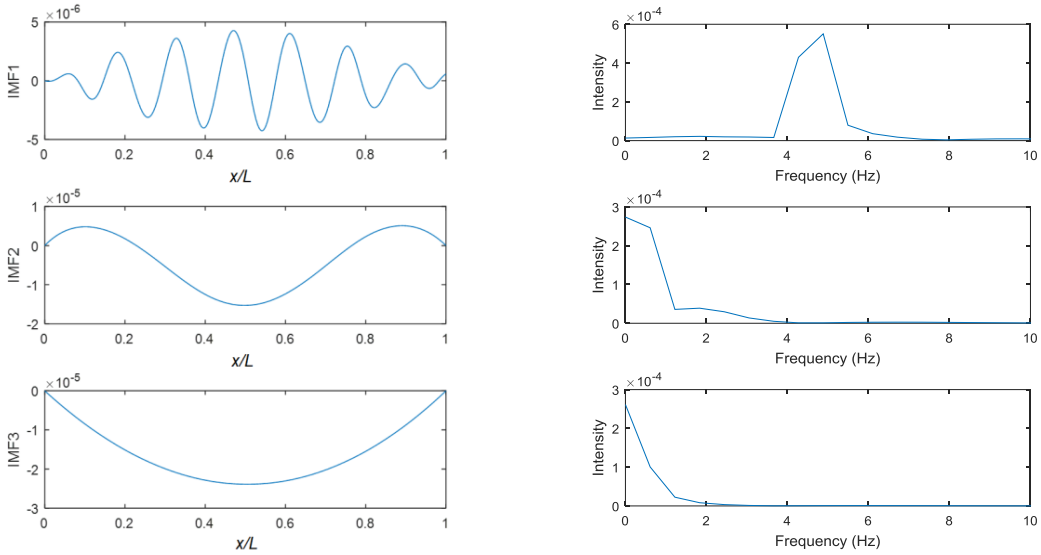

Figure 5-5 IMFs of the filtered vehicle acceleration response and their FFT spectra

Figure 5-6 (a) and (b) show sum of the second and third IMFs obtained from the displacement and acceleration responses respectively. It can be seen that they are similar to the speed pseudo-frequency part of the original signal shown in Figure 5-3.

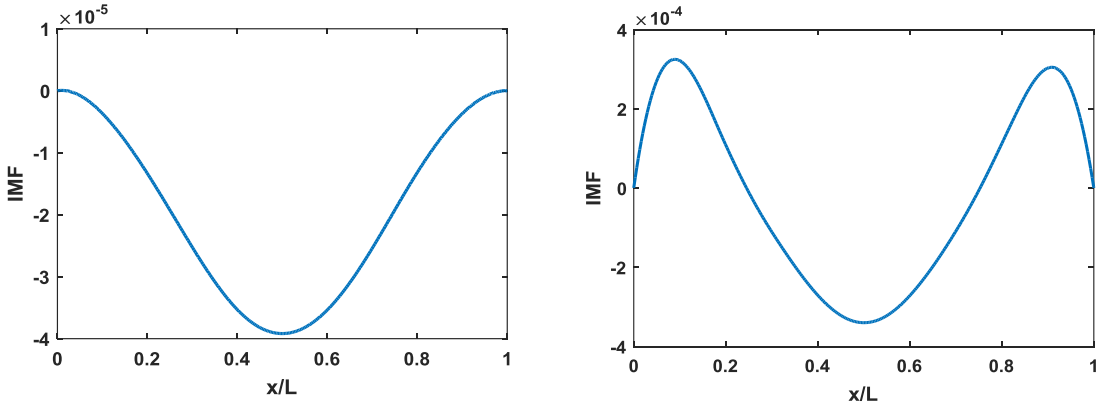

Figure 5-6 Sum of the second and third IMFs. (a) Displacement and (b) acceleration

5.3. Numerical modelling

5.3.1. Finite Element modelling of Vehicle Bridge Interaction

A Finite Element (FE) Vehicle Bridge Interaction (VBI) model is used here according to the procedure used by Malekjafarian and OBrien (2014b). In this model, a coupled VBI system is represented and the solution is calculated at each time step using an iterative procedure. The quarter-car model shown in Figure 5-7 is used in this chapter as it illustrates many of the important characteristics of VBI (Cebon, 1999). The vehicle has two independent degrees of freedom corresponding to body mass and axle mass translations. The vehicle body and axle component masses are represented by m_s and m_u and their displacements by y_s and y_u respectively. The axle mass is connected to the road surface via a spring with linear stiffness k_t which represents the tyre. By imposing equilibrium of all forces and moments acting on the vehicle masses, the equations of motion of the vehicle model can be obtained in terms of the degrees of freedom:

$$M_v\ddot{y}_v + C_v\dot{y}_v + K_v y_v = f_{int} \tag{5-9}$$

where M_v, C_v and K_v are the respective mass, damping and stiffness matrices of the vehicle and $\ddot{y}_v$, $\dot{y}_v$ and y_v are the respective vectors of nodal acceleration, velocity and displacement ($y_v = [y_s \quad y_u]^T$). The vector f_{int} contains the time-varying dynamic interaction forces applied to the vehicle degrees of freedom.

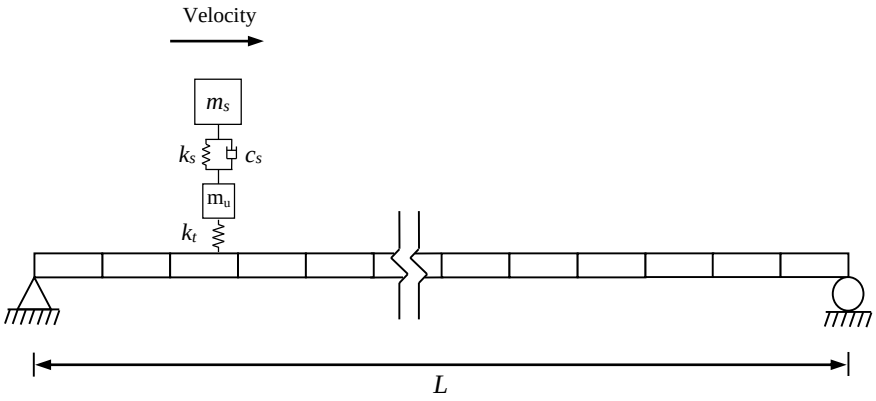

Figure 5-7 FE model of a quarter car passing over a bridge

The bridge is modelled as a simply supported beam with total span length L using beam finite elements (Tedesco et al., 1999) (Figure 5-7). Each beam element is represented by four degrees of freedom (one translational and one rotational for each of two nodes), constant mass per unit length, m, modulus of elasticity, E and second moment of area, J. The equations of motion of the beam under a series of moving time-varying forces can be written in terms of its degrees of freedom:

$$M_b\ddot{y}_b + C_b\dot{y}_b + K_b y_b = f_{int} \tag{5-10}$$

where M_b, C_b and K_b are the global mass, damping and stiffness matrices of the beam model, respectively and $\ddot{y}_b$, $\dot{y}_b$ and y_b are the vectors of nodal bridge accelerations, velocities and translation, respectively. For the case of low bridge damping, ξ, Rayleigh damping can be adopted to represent viscous damping and is given by Clough and Penzien (1993):

$$C_b = \alpha M_b + \beta K_b \tag{5-11}$$

where α and β are constants. The damping ξ is assumed to be 3% for all modes and α and β are obtained from, $\alpha = 2\xi\omega_1\omega_2/(\omega_1 + \omega_2)$ and $\beta = 2\xi/(\omega_1 + \omega_2)$ where ω_1 and ω_2 are the first two natural frequencies of the bridge (Clough and Penzien, 1993). The dynamic interaction between the vehicle and the bridge is implemented in MATLAB. The vehicle and the bridge are coupled at the tyre contact points via the interaction force vector. Combining equations (5-9) and (5-10), the coupled equation of motion of the vehicle and bridge is formed as:

$$M_g\ddot{u} + C_g\dot{u} + K_g u = F \tag{5-12}$$

where M_g and C_g are the combined system mass and damping matrices, respectively, K_g is the coupled time-varying system stiffness matrix and F is the system force vector. The vector, $u = \{y_v, y_b\}^T$, is the displacement vector of the system. The Wilson-Theta integration scheme (Tedesco et al., 1999) is used to solve the equations for the coupled system with the optimal value of the parameter θ =1.420815 for unconditional stability in the integration scheme. The initial condition of the solution is considered to be zero vertical translation, velocity and acceleration in all simulations.

A quarter-car with the properties given in Table 5-2 is modelled to pass over a bridge with the same properties given in Table 5-1. The bridge is modelled using 20 elements. The vehicle speed is 10 m/s and a smooth road profile is considered in this example.

Table 5-2 Properties of the quarter-car

Properties	Unit	Symbol	Value
Body mass	kg	m_s	9300
Axle mass	kg	m_u	700
Suspension stiffness	N/m	k_s	4×10^5
Suspension damping	Ns/m	c_s	10^4
Tyre stiffness	N/m	k_t	1.75×10^6
Body bounce frequency	Hz	ω_b	0.94
Axle hop frequency	Hz	ω_a	8.83

The first damage case is defined by imposing a crack in the 14th element of the bridge using the crack modelling method proposed by Sinha et al. (2002). Accordingly, the crack is deemed to cause a stiffness loss in a region on each side of it, with the flexibility varying linearly on each side from the uncracked to the cracked beam section. The severity of the damage is represented by the crack depth, expressed as a ratio of the beam depth. A crack ratio of 0.3 is considered in this example. The vehicle is simulated to pass over the healthy and damaged bridges and the acceleration responses in the axle for each simulation are presented in Figure 5-8.

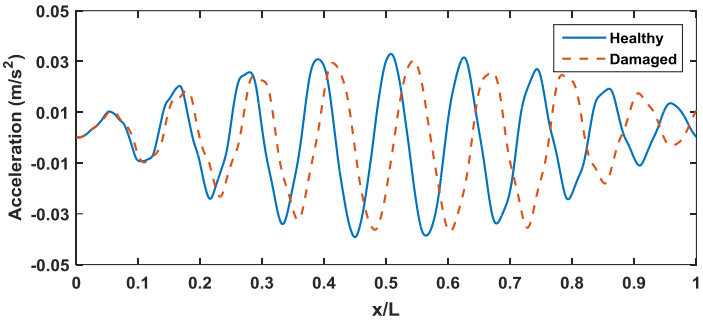

Figure 5-8 The acceleration measured on the vehicle passing over healthy and damaged bridges

5.3.2. Results for a quarter car on a smooth road profile

As introduced in Section 5.2, the speed pseudo-frequency components of the vehicle responses are extracted from the total response using EMD. The responses extracted in this way for both the healthy and damaged cases are compared in Figure 5-9 for displacement and acceleration. There is a clear difference between the healthy and damaged IMFs, confirming that it is damage-sensitive. Furthermore, the crack location aligns quite well with a peak in the differences between the healthy and damaged IMFs. This suggests that, not only can damage be detected, but the location of the damage might also be estimated.

To validate the effectiveness of the method for other damage locations, a second damage case is investigated using a new crack location. The new crack has the same depth as the first but is located in the 10th element of the 20 that make up the bridge. A comparison of the speed pseudo-frequency components of the vehicle displacements and accelerations for the healthy and the damage cases is presented in Figure 5-10. While there is a peak in the difference near the damage location, there are also peaks at other locations with no obvious association.

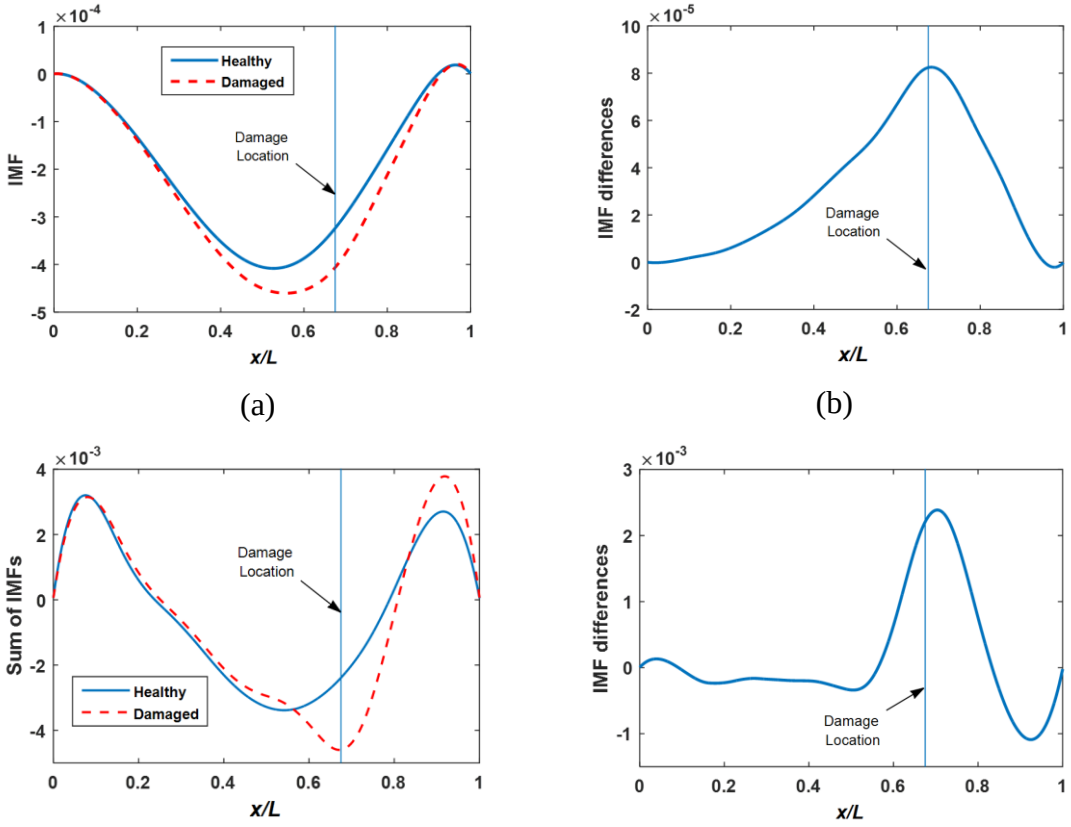

Figure 5-9 Speed pseudo-frequency component of vehicle response. (a) Comparison of healthy and damaged bridges for displacement and (b) their difference. (c) Comparison of healthy and damaged bridges for acceleration and (d) their difference

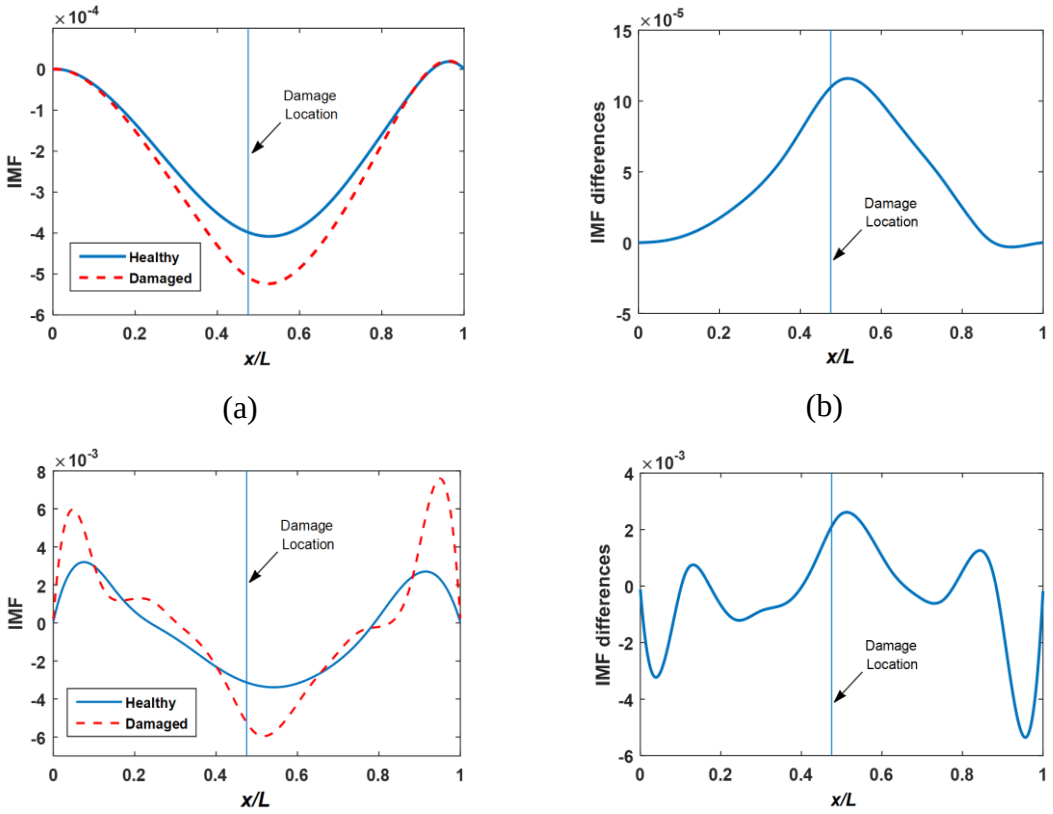

Figure 5-10 Speed pseudo-frequency components of the accelerations for damage in 10th element. (a) Displacement signal components for the healthy and damaged cases and (b) their difference. (c) Acceleration signal components for the healthy and damaged cases and (d) their difference

5.3.3. Damage indicator

As shown in section 3.2, the difference between the speed pseudo-frequency parts of the acceleration signals for the healthy and damaged structures is sensitive to damage. In this section a damage indicator is introduced that addresses the contamination introduced by the road surface profile. As shown schematically in Figure 5-11, the EMD is applied here to the *difference* between the acceleration signals for the healthy ($\ddot{y}_v^{he}(t)$) and damaged ($\ddot{y}_v^{da}(t)$) structures. The hypothesis is that this subtraction will remove the effects of road profile excitation which are assumed to be similar in the two cases.

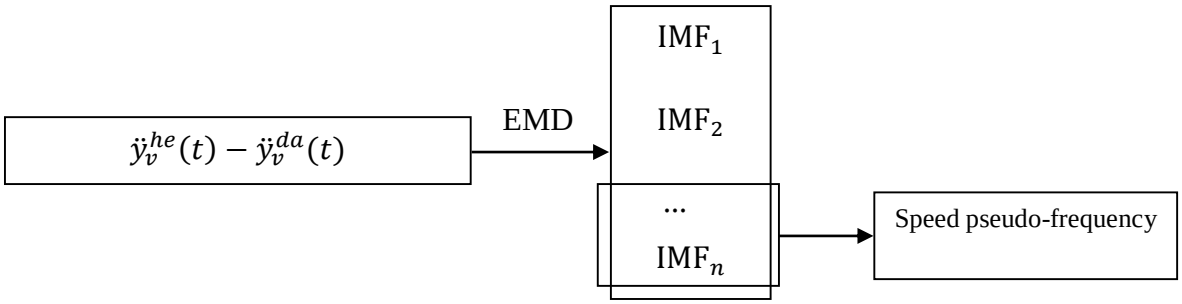

Figure 5-11 Schematic of damage detection procedure

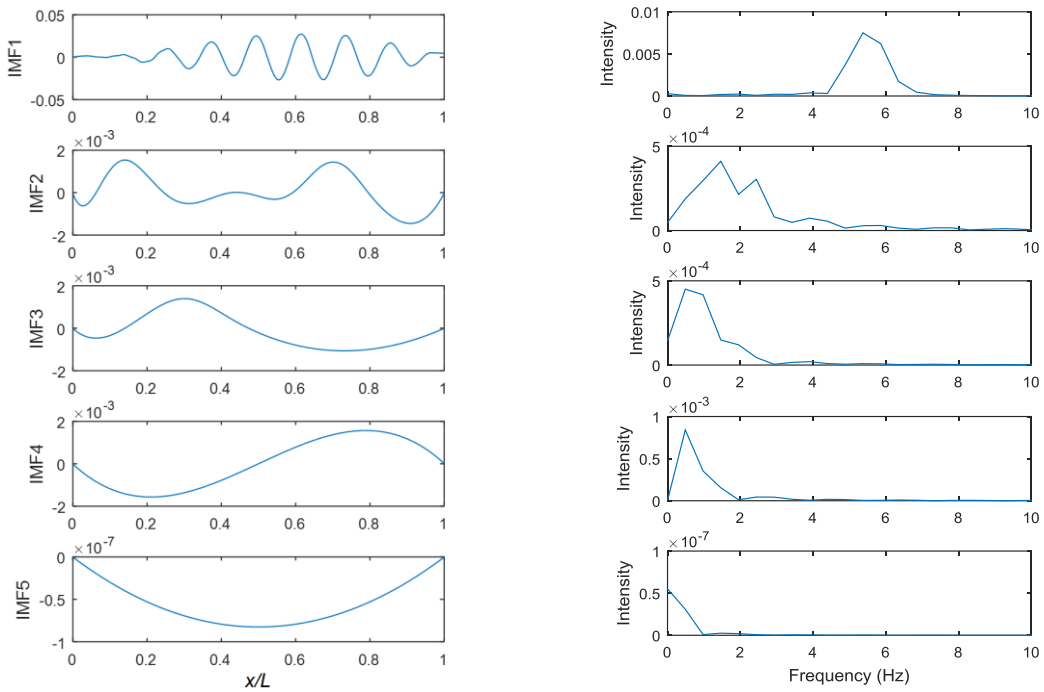

Figure 5-12 IMFs of the difference in the accelerations measured for the healthy and damaged cases and their FFT spectra

Figure 5-12 shows the IMFs obtained from applying EMD to such a difference for the first damage case. As is clear from the frequency content of the IMFs, IMF1 corresponds to the bridge natural frequency. Thus, the other IMFs correspond to the speed pseudo-frequency component of the signal. By adding all of the IMFs except the first, the damage indicator is obtained. The results for both damage cases are shown in Figure 5-13, using displacement and acceleration responses. There is a clear peak close to the damage location in each case.

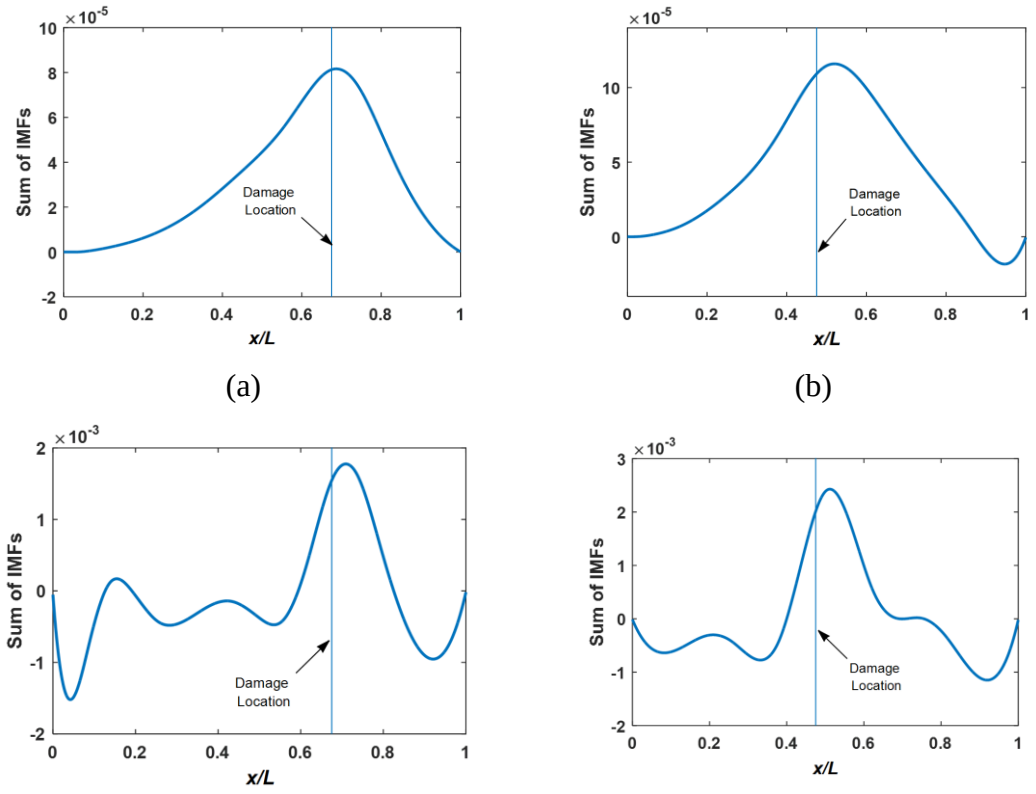

Figure 5-13 Speed pseudo-frequency part of the difference. (a) Damage case 1 and (b) damage case 2 using displacement. (c) Damage case 1 and (d) damage case 2 using acceleration

5.3.4. Two quarter cars on a Class A road profile

A number of researchers (Malekjafarian et al., 2015), (Keenahan et al. 2014) have reported that estimation of bridge frequency from the vehicle response is difficult when a road profile is present. In most cases, the vehicle and road profile frequencies are dominant in the vehicle response, while the bridge frequency may be barely detectable. Yang and Chang (2009a) illustrated that with high vehicle/bridge acceleration amplitude ratios, the probability of successfully identifying the bridge frequency is less. Recently, a subtraction idea has been proposed by Yang et al. (2012b) and. Keenahan et al. (2014) in which the effect of road profile is largely removed by subtracting the responses measured from identical following axles. Keenahan et al. (2014) propose the idea of subtracting the measured acceleration responses of two following axles travelling over a bridge. It is demonstrated that the effect of road profile is substantially removed from the residual acceleration response, provided the two axles have the same properties. However, the presence of road roughness is still

classified as one of the most important challenges in indirect bridge monitoring methods (Malekjafarian et al., 2015).

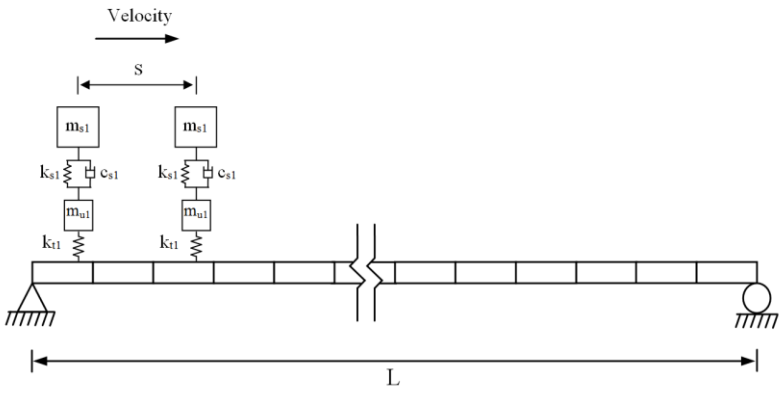

Figure 5-14 Two quarter cars passing over a bridge

It is suggested in this chapter, that if the same vehicle is employed for the healthy and damaged cases and the same road profile exists in each case, the effect of road profile can be removed by subtracting the responses. On the other hand, when a road profile is present in the simulation, it is recommended by Li (2014) to increase the amplitude of the bridge components at least to the same level as the road profile. The amplitude of the speed pseudo-frequency part corresponds to the static load applied to the bridge (the weight of the vehicle). Therefore, in this section two following axles are modelled passing over the bridge instead of one in order to increase the total moving load (Figure 5-14). The same bridge as for Section 2 is considered, except that a road profile is added. The vehicle speed is selected to be 5 m/s in this case. The irregularities of this profile are randomly generated according to the ISO8608:1995 (1995) standard for a road class ‘A’ (very good) profile, as expected in a well maintained highway. The speed pseudo-frequency component of the difference of the responses measured on the first axle passing over healthy and damaged bridges is obtained as before. The results are shown in Figure 5-15 for the two damage cases.

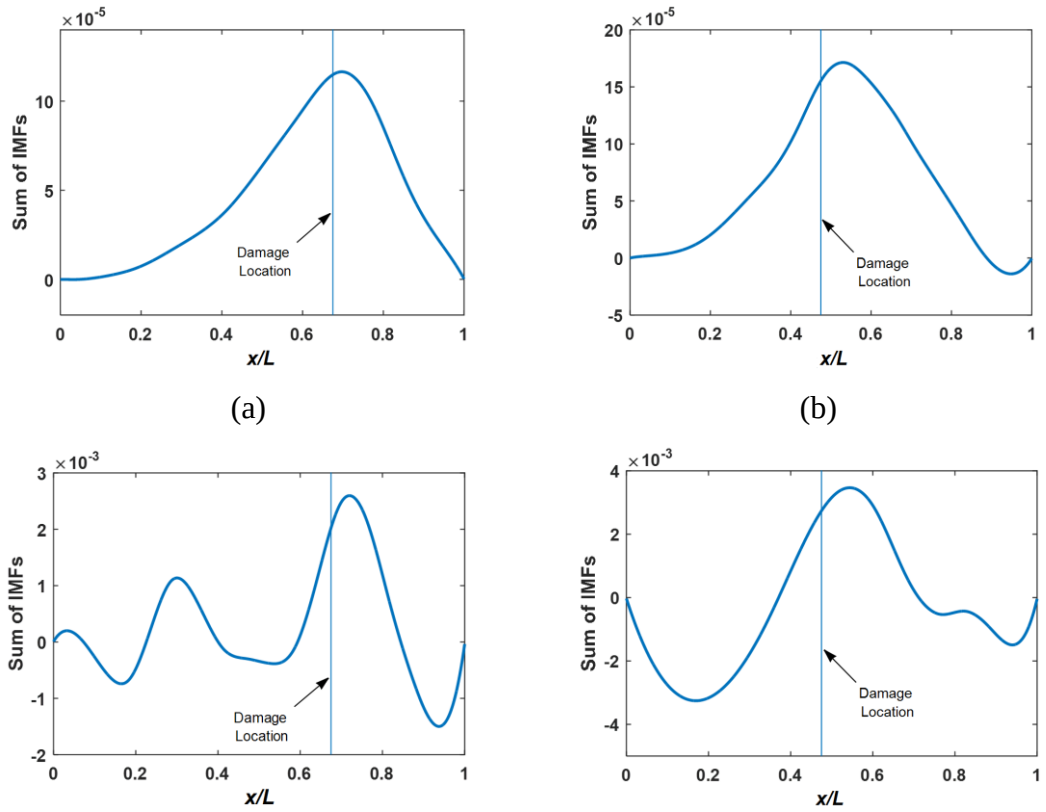

Figure 5-15 The speed pseudo-frequency part of the difference in the presence of a road profile. (a) Damage case 1 and (b) damage case 2 using displacement. (c) Damage case 1 and (d) damage case 2 using acceleration

Comparing Figure 5-13 and Figure 5-15 shows that the presence of road profile causes some more oscillation in the damage indicator. However, damage can still be detected, as evidenced by the non-zero results and there are still peaks adjacent to the damage locations.

5.3.5. Changes in the transverse position of the vehicle on the bridge

As explained in Section 5.3.3 the damage indicator is based on the difference between the responses for healthy and damaged bridges. The idea relies on the assumption that the vehicle excited by the same road surface before and after occurrence of damage. Achieving this in the filed may be difficult. The vehicle may pass along a parallel track, in a slightly different transverse position on the bridge. (The surface profile may also have changed due to pavement wear. The effect would be similar.) Therefore, the sensitivity of the algorithm is tested for changes in the transverse positon of the vehicle on the bridge. A carpet if correlated profiles (Figure 5-16) is generated (Cebon and Newland, 1983) from the initial

road profile. It is assumed that the vehicle passes the healthy and damaged structure in different relative lateral positions, Δr.

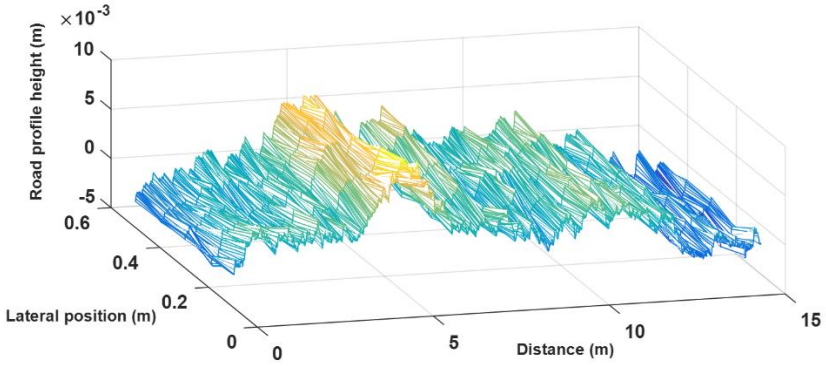

Figure 5-16 Carpet profile

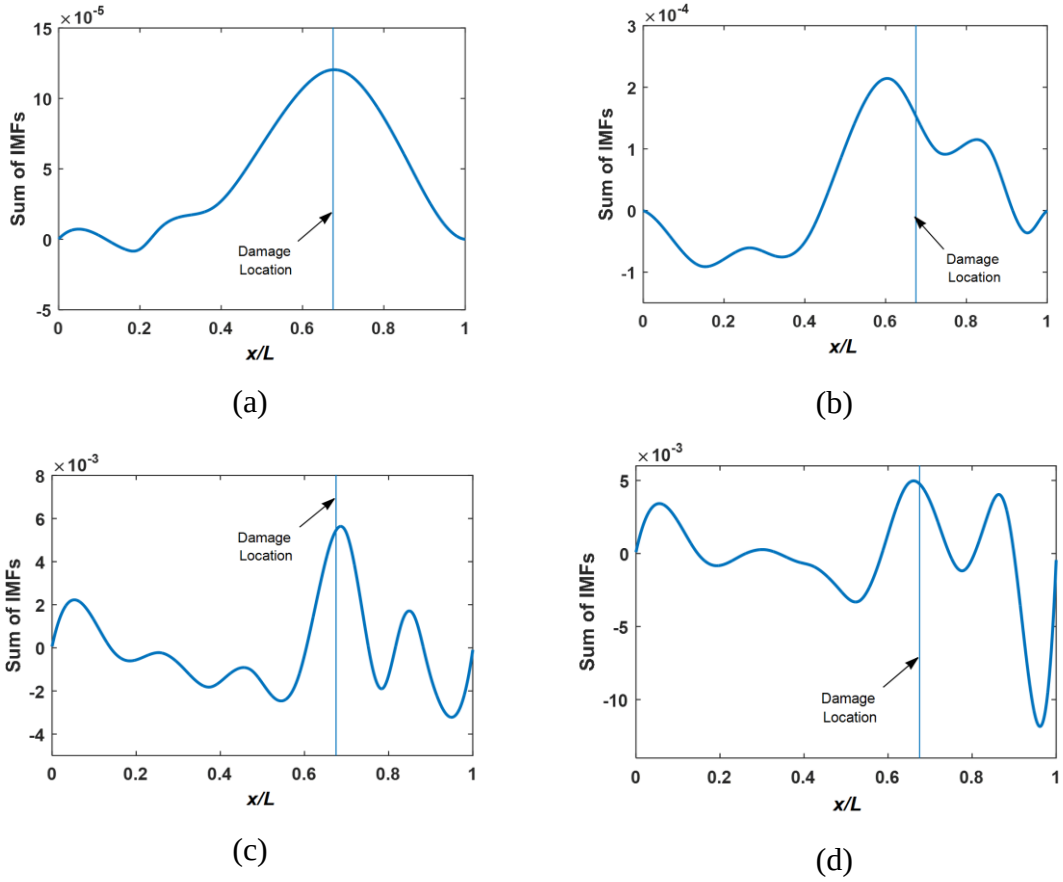

Figure 5-17 Speed pseudo-frequency part of the difference using a range of relative positions of the vehicle on the road carpet. (a) Δr = 0.001m and (b) Δr = 0.01m using displacement. (c) Δr = 0.0005m and (d) Δr = 0.001m using acceleration

Figure 5-17 (a) and (b) show the damage indicator using the vehicle displcement when Δr = 0.001m and Δr = 0.01m, respectively. The results for vehicle acceleration when Δr = 0.0005m and Δr = 0.001m are shown in Figure 5-17 (c) and (d), respectively. It can be seen that when displacement is used, the damage indicator is less sensitive to the changes in the lateral position of the vehicle.

5.4. Conclusions

A bridge damage detection procedure using Empirical Mode Decomposition is proposed in this chapter using the response measured on a passing vehicle. It is theoretically shown that the vehicle response contains three main parts and that the speed pseudo-frequency part is sensitive to damage. EMD is used to extract this part from the total response. A numerical case study of vehicle bridge interaction is modelled using the FE method to demonstrate the potential of the approach. It is shown that damage location may be identified with acceptable accuracy using the proposed method. However the method is sensitive to changes in the road profile as might be expected from changes in the the lateral position of the vehicle. It is concluded that the damage may be located by if the differences in the profile are small. The proposed approach can be considered as a guideline for bridge damage detection using drive-by measurements. A more rigorous damage detection strategy can be chosen based on the concepts presented in this chapter. It is recommended to apply the method using a high accuracy measurement system such as a TSD to achieve the best results.

Chapter 6: On the use of a passing vehicle for the identification of bridge mode shapes

Authors:

Abdollah Malekjafarian

Eugene J. OBrien

Paper status:

Submitted for publication in *Journal of Sound and Vibration*

Not to the reader:

This work is entirely the work of the author under the supervision of Prof. Eugene OBrien.

Chapter 6: On the use of a passing vehicle for the identification of bridge mode shapes

6.1. Introduction

Bridge health monitoring plays an important role in the maintenance and assessment of transportation infrastructure. Visual inspection is still the most common method used but vibration-based methods have attracted a lot of attentions in recent years. The idea is that any change in the bridge health condition causes a detectable change in its dynamic properties (Fan and Qiao, 2011). Many of these methods employ some means to identify the bridge modal parameters (natural frequencies, damping ratios and mode shapes) through vibration experiments. Many sensors need to be installed directly on the bridge to identify its modal parameters. The idea has been studied by many researchers through numerical (Grande and Imbimbo, 2016, Khiem and Toan, 2014) and experimental (Siriwardane, 2015, Magalhães et al., 2012, Dilena et al., 2015) approaches.

Recently a new idea of bridge monitoring using indirect measurement has been considered (Yang et al., 2004, Lin and Yang, 2005). The concept is to identify bridge dynamic properties using the response measured indirectly on a passing vehicle (Malekjafarian et al., 2015). Through vehicle bridge interaction, the vehicle suspension system is excited by the bridge displacement as well as the road or rail surface profile. Providing there is enough measurement time and good surface profile, it is possible to identify the bridge modal parameters from the indirect measurements. A considerable literature has been published on these methods and there is an increasing interest in them. Several investigations have been carried out targeting identification of the bridge natural frequencies (Oshima et al., 2008, Yang and Chang, 2009b, Siringoringo and Fujin, 2012). Damping is considered using the indirect methods by González et al. (2012). More recently the feasibility of identifying the bridge mode shapes using indirect measurements has been investigated (Yang et al., 2014b, Zhang et al., 2012, Oshima et al., 2014, Malekjafarian and OBrien, 2014b, OBrien and Malekjafarian, 2016).

Table 6-1 provides a summary of some of the attempts that have been proposed for the estimation of bridge mode shapes from indirect measurements. The earliest attempt is proposed by Zhang et al. (2012) for the purpose of damage detection. A moving vehicle called a ‘tapping vehicle’, equipped with an accelerometer and a shaker to control the

applied force artificially, is passed over the bridge. A point impedance is constructed using the applied force and the response, both measured at a moving coordinate. It is shown theoretically that the amplitude of the spectrum obtained from the point impedance is approximately proportional to the square of the mode shape. The mode shapes are constructed using the response and the applied force together, which needs the measurement of applied force.

Table 6-1 A summary of proposed methods for indirect identification of bridge mode shapes (STFFT= Short Time Fast Fourier Transform; SVD= Singular Value Decomposition; STFDD= Short Time Frequency Domain Decomposition).

	Method	VBI	Mode shape obtained from
1	(Zhang et al., 2012)	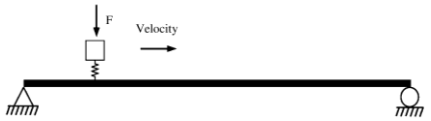	The amplitude of STFFT at different locations.
2	(Oshima et al., 2014)	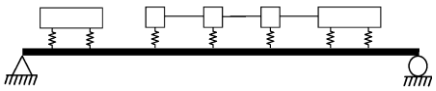	SVD of the response measured from three (or more) trailers.
3	(Yang et al., 2014b)		Hilbert amplitude of the filtered response.
4	(Malekjafarian and OBrien, 2014b)	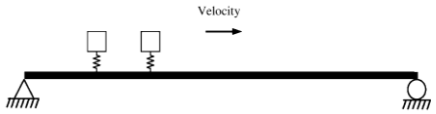	STFDD of the response measured from the following axles.
5	(OBrien and Malekjafarian, 2016)	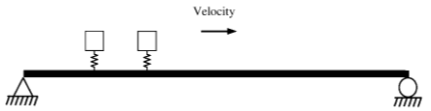	Improved STFDD of the response measured from the following axles.

Oshima et al. (2014) propose a damage detection procedure which uses the bridge mode shapes identified from the measurements on a passing vehicle. The authors propose a convoy truck-trailers system for two main reasons; firstly to excite the bridge and secondly, to measure the response at three or more moving points (depends on how many mode shape points are needed) at the same time. As shown in the second row of Table 1, the first and the last trucks excite the bridge and the middle trailers measure the response. For example, if three mode shape points are going to be identified, the spaces between trailers should be adjusted in a way that each trailer passes over one third of the bridge. As a result, three segments of bridge response are recorded at the same time at different locations on the bridge. By applying Singular Value Decomposition (SVD) to these signals, a mode shape

vector containing three members, corresponding to the defined areas, are identified for each mode. If greater mode shape resolution is needed, the number of trailers and their spacings should be adjusted accordingly.

In a theoretical study, Yang et al. (2014b) discuss the possibility of constructing the bridge mode shapes directly from the measured response on a passing vehicle. The authors consider a moving sprung mass on a bridge and theoretically show that the energy of the measured signal at a frequency equal to the bridge natural frequency, is the bridge mode shape corresponding to that frequency. The authors use bandpass filtering to get the distilled signal corresponding to a specific frequency and apply the Hilbert Transform to get the amplitude of the filtered signal. It is stated that the amplitude is the bridge mode shape for the corresponding mode. If the bridge is considered as a system, the idea is based on a single-input-single-output concept where the bridge is excited at only one point (which is a moving point) under the wheel and the response is measured at the same point. Although it is theoretically proven that the amplitude of the signal at the first natural frequency provides the first mode shape of the bridge, a more complicated case including more axles and many source of excitations, is not discussed.

Malekjafarian and OBrien (2014b) propose using a method called Short Time Frequency Domain Decomposition (STFDD) to identify bridge mode shapes from the response measured on a moving vehicle. Similar to the method proposed by Oshima et al., the bridge needs to be divided into a number of segments corresponding to the number of required mode shape points. However, instead of having one moving sensor for each segment, the authors propose using the response measured on two following vehicles. In a multi-step measurement process, short signals are measured from the following segments on the bridge. The local mode shape values corresponding to each step are identified using Frequency Domain Decomposition (FDD). A rescaling process is used to correlate the identified mode shapes at different locations, step by step. This method provides greater resolution and needs less equipment compared to the method proposed by Oshima et al. Nevertheless both methods provide an approximate mode shape which is the average of the mode shape values for the segment of the bridge where the response is measured. OBrien and Malekjafarian (2016) improve the STFDD method by modifying the segmentation to include some overlapping , thereby providing improved resolution. The most important advantage of the improved version is that it provides better resolution of the identified mode shapes which is

necessary for the purpose of damage detection. However it still gives only approximate mode shape values because of the averaging process.

Together these studies provide important insights into the indirect identification of bridge mode shapes. In this chapter a new algorithm is proposed, that builds on the previously proposed methods. A vehicle equipped with an exciter is suggested, combining the ideas of Zhang et al. (2012) and Oshima et al. (2014). The excitation device, which can apply a controlled force, is installed on an excitation vehicle which is not the same vehicle where the response is measured. The energy of the measured responses on two following axles are extracted using the Hilbert Huang Transform (HHT) in a process similar to that proposed by Yang et al. (2014b). However, while it is shown that the obtained Hilbert amplitude includes the mode shape information, for such a complicated excitation, it is not exactly the mode shape. Finally a rescaling process similar to that proposed by Malekjafarian and OBrien (2014b) is used to construct the mode shapes from the HHT amplitudes of two following axles.

6.2. The proposed algorithm using an exciter

A general view of the algorithm proposed in this chapter is shown in Figure 6-1. The first step is to define a specialized vehicle. It is proven that the axle response for good road conditions includes some information on the bridge dynamic properties including natural frequencies (McGetrick et al., 2009), mode shapes (Malekjafarian and OBrien, 2014b) and damping ratios (González et al., 2012b). One of the most important challenges is the ratio of the bridge response to the vehicle response (Yang and Chang, 2009a) which is mostly a small number. This causes the vehicle response to be dominant in most cases which overshadows the bridge dynamic properties (Malekjafarian et al., 2015). Some ideas have been used to improve this ratio such as using ongoing (ambient) traffic (Malekjafarian and OBrien, 2014b) or a vehicle equipped with an exciter (Zhang et al., 2012). The first one may be feasible as ongoing traffic would be expected in most highways, but there is little information available about the frequency content of the excitation coming from it. In some cases it could excite the vehicle frequency more than the bridge frequency in the response measured on the axle which is not helpful for the mentioned ratio. The second idea may be difficult and expensive to implement, but it provides many advantages. It is possible to excite the bridge at a desired frequency by controlling the applied force. A similar idea has been used in (Zhang et al., 2012, Li, 2014), where the excitation is applied at the point of

measurement. In this case, although the bridge vibration could be improved, but again the vehicle response to the external excitation is measured not to the excitation caused by the bridge vibration under the vehicle wheel. To overcome this drawback, it is suggested here to apply the external force in a different axle or even a different vehicle from that where the response is measured (Figure 6-2).

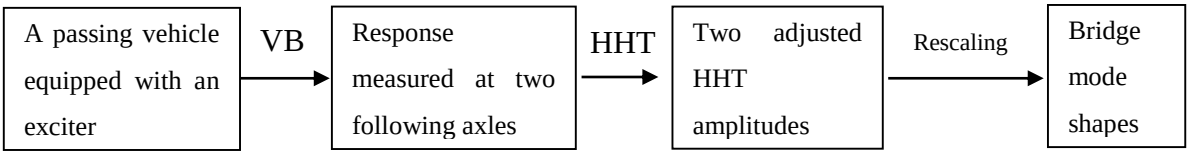

Figure 6-1 The algorithm (HHT= Hilbert Huang Transform).

Referring to Figure 6-2, the excitation is applied to the fourth axle and the measurement is done at the sixth and seventh axles. This approach provides the possibility of controlling the bridge vibration before the measurement. It means that, by applying a force with a frequency close to the first natural frequency of the bridge, it is possible to extract good information on the first mode shape.

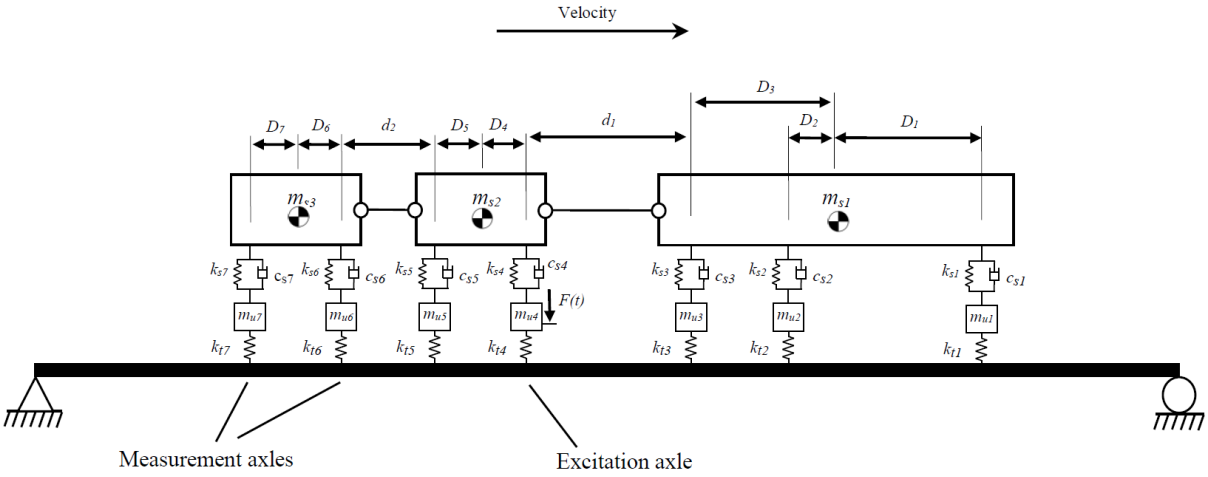

Figure 6-2 The truck-trailer model.

In the second step of

Figure 6-1, the response should be measured simultaneously at two following axles. It is necessary to have the bridge response corresponding to the first natural frequency at two

different locations at a same time. These responses will be used in the last step, called rescaling, to construct the global bridge mode shape from the HHT amplitudes.
The energy of each response at each natural frequency gives the bridge deflected shape at a particular location which is correlated with the corresponding bridge mode shape. Hence the responses are first decomposed to different modes using Empirical Mode Decomposition (EMD), and then the Hilbert amplitude of each Intrinsic Mode Function (IMF) represents the energy of the signal for the corresponding frequency. As a result, two HHT amplitudes from the two following axles are obtained.

The following axle amplitudes include the bridge mode shape information, but they are not mode shapes. They actually represent the energy of the bridge response at its natural frequency for different locations on the bridge at each time. To extract the bridge mode shapes from the amplitudes, a rescaling process is employed. The idea is based on the reference-based approach proposed in (Reynders and De Roeck, 2008) where some reference sensors are needed when different tests are carried out with different setups to cover all locations along a structure. The purpose of using the reference sensors is to establish a link between the setups. The two following moving sensors here are collecting data from different locations on the bridge at a constant distance from each other. Therefore through a multi-step procedure, one of them is always the reference sensor to construct the global mode shape (Malekjafarian and OBrien, 2014b, OBrien and Malekjafarian, 2016).

6.3. Theoretical background

6.3.1. Hilbert Huang Transform

The Hilbert-Huang transform (HHT) was first proposed by Huang et al. (1998) for analysing nonlinear and nonstationary signals. It is used for damage detection in structures under a moving load (Roveri and Carcaterra, 2012). The method introduces the concept of instantaneous frequency (IF) which provides the frequency of each mode in the signal as a function of time. It includes two main parts; EMD and the Hilbert Transform. Firstly a finite number of IMFs is obtained by applying the EMD. Once the signal has been decomposed, the IFs are determined by applying the Hilbert Transform to each of the IMFs. Each IF represents the frequency content of the corresponding IMF. The energy content of each IMF can also be found by calculating its Hilbert amplitude.

6.3.2. Empirical Mode Decomposition

EMD is an adaptive method which has been proposed for decomposing signals. It has been used for damage detection through vehicle bridge interaction (Meredith et al., 2012). It uses a sifting process to extract a series of IMFs. The decomposition process is based on two conditions; (i) the number of extrema and the number of zero crossings must be equal or differ by at most one and (ii) at any point the mean value of the envelopes defined by the local maxima and local minima must be zero. The sifting process can be performed using the following steps (Huang et al., 1998). First, connect the local maxima and minima of the original signal using a cubic spline to define the upper and lower envelopes. Then, subtract the envelope's mean from the original signal to generate the first IMF. The original signal is then decomposed into the first IMF and a residual. By repeating this procedure on the residual, the successive IMF's are constructed. The sifting process ceases when the last IMF has no more than one extremum.

6.3.3. Hilbert transform

The Hilbert transform of the i^{th} IMF, $x(t)$ is (Huang et al., 1998):

$$y(t) = \frac{1}{\pi} P \int \frac{x(\tau)}{t-\tau} d\tau \tag{6-1}$$

where P presents the Cauchy principle value of the singular integral. The analytic signal of $x(t)$ is defined by:

$$z(t) = x(t) + jy(t) \tag{6-2}$$

where j is $\sqrt{-1}$. The polar form of $z(t)$ is:

$$z(t) = a(t)e^{i\varphi(t)} \tag{6-3}$$

The instantaneous amplitude $a(t)$ and phase $\varphi(t)$ are calculated as:

$$a(t) = \sqrt{x^2(t) + y^2(t)} \tag{6-4}$$

$$\varphi(t) = \tan^{-1}\left(\frac{y(t)}{x(t)}\right) \tag{6-5}$$

The instantaneous frequency is determined as (Cohen, 1995):

$$\omega(t)\frac{d\varphi(t)}{dt} \tag{6-6}$$

By applying the Hilbert transform to the IMFs, a series of IF's, and their amplitudes, are calculated.

6.4. Numerical validation

Vehicle bridge interaction (VBI) is modelled using the Finite Element (FE) method. The bridge is defined here as a simply supported beam and a half car model is used for the vehicles. Discretized beam elements including 4 degrees of freedom (2 per node) with constant mass per unit length, *m*, modulus of elasticity *E* and second moment of area *J* are employed. A half car model with three axles is used to represent the truck and two half car models with two axles each are used for the trailers. The vehicle body has two independent degrees of freedom corresponding to body mass translation and rotation and each axle has a translational degree of freedom. m_s, m_{u1} and m_{u2} represent the vehicle body and axle component masses respectively. k_t is the stiffness of the tyre which connects the axle masses and the road surface. The mass and stiffness matrices of the bridge and the vehicle are constructed separately. Considering the fact that they are connected at the tyre contact points, a coupled VBI system of the equations of motion is constructed by imposing equilibrium of the interaction forces. The VBI is implemented in MATLAB.

6.4.1. Example of a truck-trailer equipped with an exciter on a smooth profile

A truck-trailer system is employed consisting of a three-axle truck towing two trailers (Figure 6-2). The bridge and vehicle properties are given in Table 6-2 to Table 6-4 respectively. The first three natural frequencies of the bridge are 5.65, 22.62 and 50.89 Hz respectively.

Table 6-2 Properties of the bridge.

	Unit	Symbol	Value
Length	m	L	15
Mass per unit length	kg/m	m	28125
Modulus of elasticity	MPa	E	35000
Second moment of area	m^4	J	0.5273

Table 6-3 Properties of the truck.

	Unit	Symbol	Value
Body mass	kg	m_{s1}	27100
Axle mass	kg	m_{u1}	700
		$m_{u2} = m_{u3}$	1100
Suspension stiffness	N/m	k_{s1}	4×10^5
		$k_{s2} = k_{s3}$	1×10^6
Suspension damping	Ns/m	c_{s1}	10×10^3
		$c_{s2} = c_{s3}$	20×10^3
Tyre stiffness	N/m	k_{t1}	1.75×10^6
		$k_{t2} = k_{t3}$	3.5×10^6
Moment of inertia	kg m^2	I_{s1}	1.56×10^5
Distance of axle to centre of gravity	m	D_1	4.57
		D_2	1.43
		D_3	3.23
Body mass frequency	Hz	$f_{body,1}$	1.32
Axle mass frequency	Hz	$f_{axle,1}$	8.82
		$f_{axle,2}$	10.17
		$f_{axle,3}$	10.20

In order to identify the first two mode shapes of the bridge, two simulations with different excitations are carried out. The vehicle is first simulated passing over the bridge with an excitation of amplitude 3 kN and frequencies of 5.5 Hz and 22.5 Hz at the speed of 2 m/s. The acceleration responses are assumed to be measured at the sixth and seventh axles for both cases. Figure 6-3 (a) shows the first case in which the first mode of the bridge is dominant in the response. The amplitudes of the signals, which represent their energies, look like the first mode shape, but they are not exactly the mode shape for two main reasons. Firstly, the first mode shape in this case must be symmetric and its peak should be at midspan, but it is clear in Figure 6-3 (a) that the peaks of both responses are located close to 6.5 m in the 15m bridge. Secondly, there are significant differences between the amplitudes of the two signals at different locations whereas, if they were the bridge first mode shape,

they should be the same, or at least very similar. A similar trend is observed in Figure 6-3 (b) where the second mode is dominant. Again the energy of the two signals are very similar and look like the bridge's second mode shape but are not.

Table 6-4 Properties of the trailers.

	Unit	Symbol	Value
Body mass	kg	m_{s2}	4000
Axle mass	kg	$m_{u4} = m_{u5}$	50
Suspension stiffness	N/m	$k_{s4} = k_{s5}$	4×10^5
Suspension damping	Ns/m	$c_{s4} = c_{s5}$	10×10^3
Tyre stiffness	N/m	$k_{t4} = k_{t5}$	1.75×10^6
Moment of inertia	kg m^2	I_{s2}	2401.67
Distance of axle to centre of gravity	m	$D_4 = D_5$	1.25
Body mass frequency	Hz	$f_{body,2}$	2.02
Axle mass frequency	Hz	$f_{axle,4}$	33.01
		$f_{axle,5}$	33.04
Gaps, truck-to-trailer and trailer-to-trailer	m	$d_1 = d_2$	1

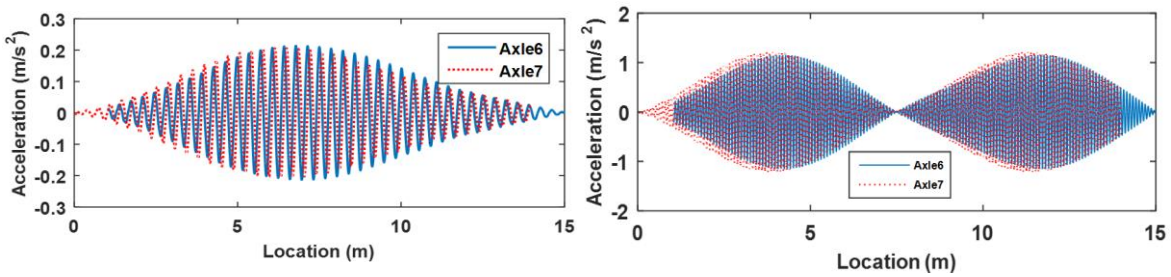

(a) (b)

Figure 6-3 Acceleration responses for different excitations; (a) excitation at frequency of 5.5 Hz and (b) excitation at frequency of 22.5 Hz.

The HHT is applied to the responses measured in each case. The IMFs and IFs obtained are shown in Figure 6-4 and Figure 6-5. The first IF of both cases shows that the corresponding IMF is dominant.

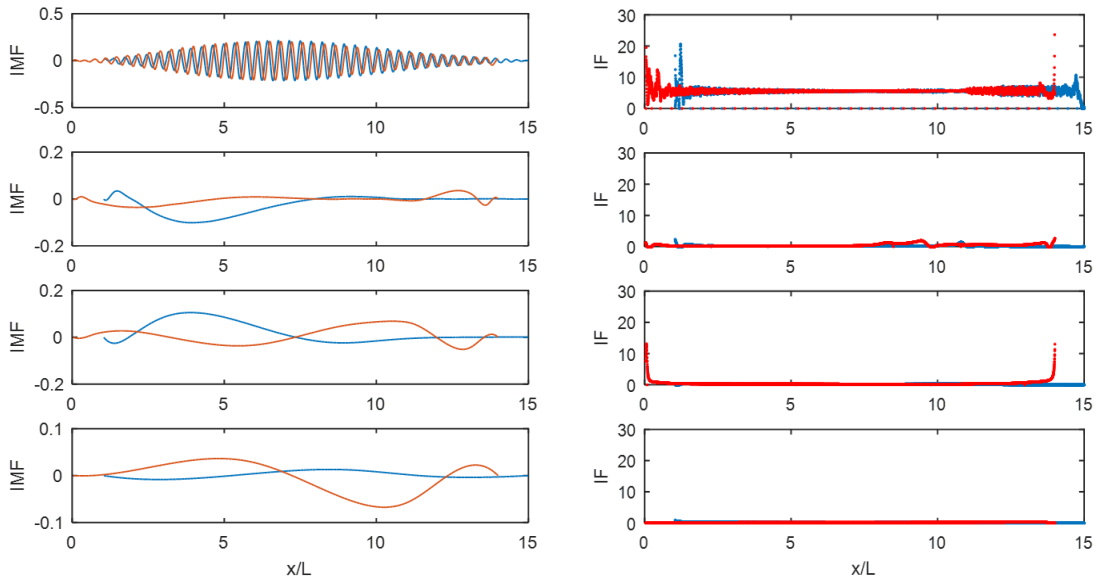

(a) (b)

Figure 6-4 HHT for first case (excitation at frequency of 5.5 Hz), (a) IMFs, (b) IFs.

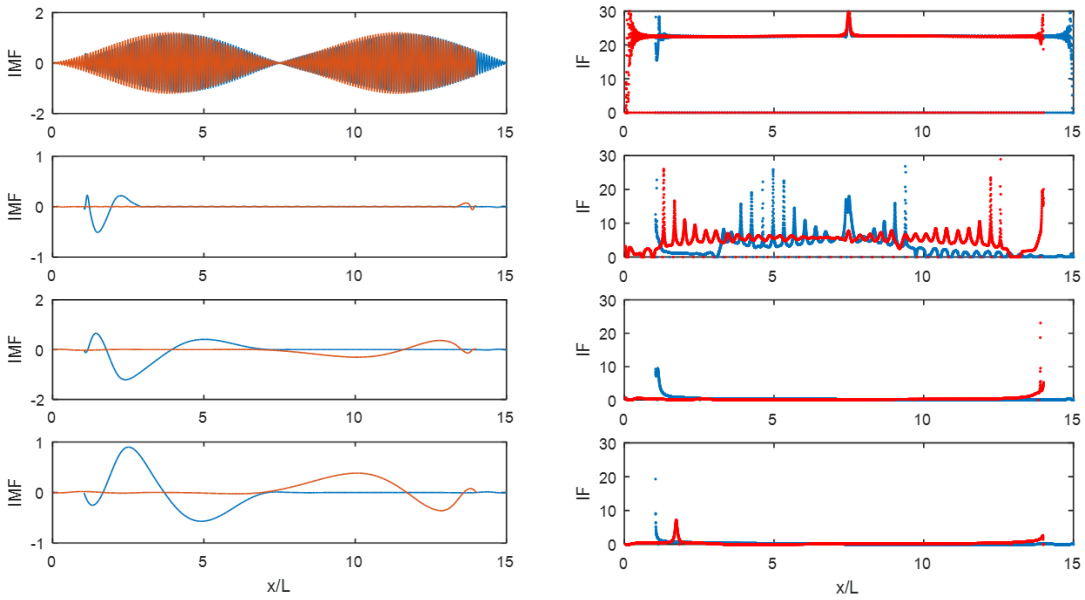

(a) (b)

Figure 6-5 HHT for second case (excitation at frequency of 22.5 Hz) (a) IMFs, (b) IFs.

The HHT amplitudes for the first case are shown in Figure 6-6 (a). A moving average of each amplitude is calculated to smooth the curve (Figure 6-6(b)). It can be seen that the amplitudes obtained from the two following axles are not the same (they would be the same if they were the bridge mode shape) and their peaks are not located at the bridge mid-span (where the peak of the first mode shape of the bridge is located). The first average amplitude is trimmed at 2 and 14 m and the second one at 1 and 13 m. This provides enough

information to obtain the bridge mode shape in an interval between 1 to 14 m. The amplitudes are a measure of the energy of the bridge response corresponding to the first mode at each location.

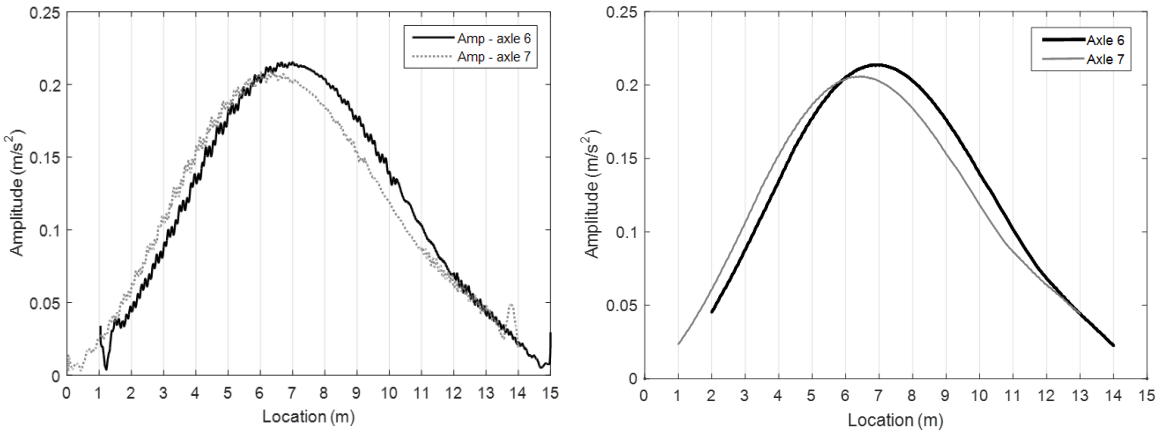

(a) (b)

Figure 6-6 Amplitudes obtained from two following axles, (a) Calculated raw amplitudes, (b) Smoothed and trimmed amplitudes.

As the spacing between the sixth and seventh axles is 1 m, the axle 7 amplitude for location *x* correlates to the axle 6 amplitude for location *x*+1. This concept is illustrated in Figure 6-7 which is a zoomed view of Figure 6-6 (b). To construct the global bridge mode shape, several points starting from x=2m for the sixth axle and x=1m for the seventh axle are selected with 1 metre spacing. Each of these points are marked as ψ_{ij} and are the local mode shapes that are obtained from the HHT amplitude at the i^{th} axle and the location of x=*j* m. For example $\psi_{23}$is the local mode shape at x=3 m and measured at the 7nd axle. The important point is that ψ_{21} and ψ_{12} are measured at a same time which is called t_1 here. It means that they give the ratio of the bridge response at the first natural frequency for two locations at the same time which is exactly the concept of mode shape. The same explanation can be presented for t_2, t_3 and t_4 in Figure 6-7. Therefore, the process starts by considering ψ_{21} and ψ_{12} as the global bridge mode shape values, $\phi_1$and ϕ_2 at x=1 and x=2, respectively. Then two local mode shapes, ψ_{13} and ψ_{22} at time t_2 are considered which include the ratio of the bridge global mode shapes at x=2 and x=3. As ψ_{12} is already considered as the global bridge mode shape at 2 m, consequently the bridge global mode shape at x=3m can be obtained as:

$$\phi_3 = \psi_{13}\frac{\phi_2}{\psi_{22}} \tag{6-7}$$

The first global mode shape of the bridge is obtained by continuing this process for the other points. The result is illustrated in Figure 6-8.

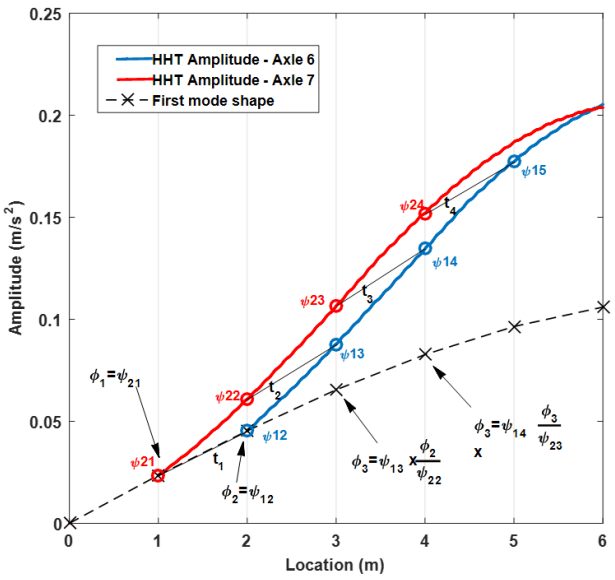

Figure 6-7 The rescaling process.

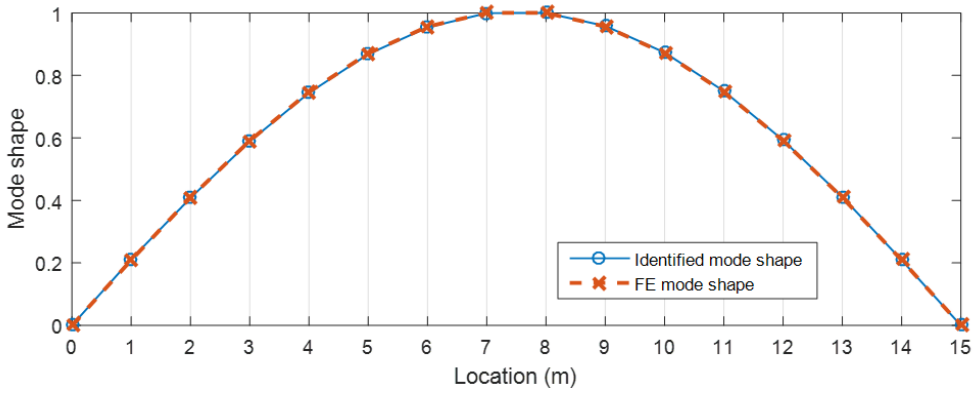

Figure 6-8 The first normalized mode shape of the bridge.

As can be seen in Figure 6-7, the process of rescaling started from *x*=1m and continued in intervals of 1m up to 14 m. Assuming there is a high quality amplitude over all the bridge, the process can start from any other point between 1 to 2 m and continue, again at 1m intervals, to a point between 13 and 14m. This results in the same mode shape at new locations. For example, instead of starting the process from x=1m, it can be started from x=1.2 or x=1.4. Consequently a high resolution mode shape of the bridge can be constructed.

The same procedure, as explained for the first mode, is applied to the results from the second mode. The HHT amplitude obtained from the second case is obtained and shown in Figure 6-9 (a). It is clear that the peaks of the two amplitudes are located at different locations which

proves that they are not the bridge mode shape. The bridge second mode shape is obtained using the same rescaling process that is used for the first mode and is shown in Figure 6-9 (b).

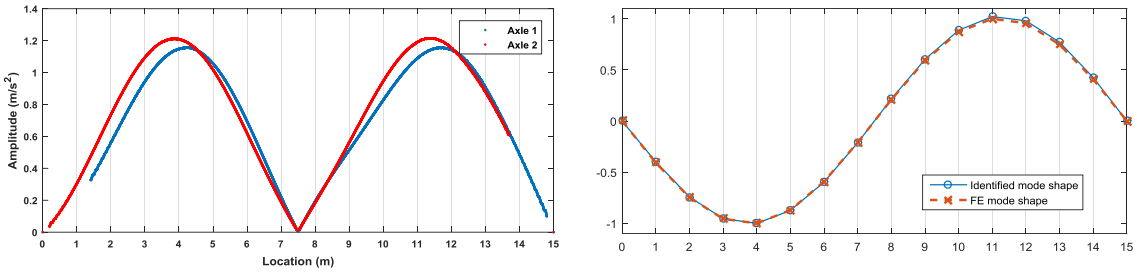

(a) (b)

Figure 6-9 Second mode shape: (a) The HHT amplitudes, (b) Inferred and true (FE) mode shapes.

6.4.2. Example of a truck-trailer equipped by an exciter on a class A road profile

A road roughness is generated using the ISO standard for a class 'A' profile, is added to the bridge (shown in Figure 6-10 (a)) as expected in a well maintained highway. A simulation similar to that used in Section 4.1, is employed here. The passes over the bridge were with an excitation of amplitude 30 kN and frequencies of 5.5 Hz and 22.5 Hz. The greater excitation was fond to be necessary in the presence of a profile.

The road roughness constitutes an extra source of excitation for the moving vehicle in addition to the sources discussed. The frequency content of the roughness is shown in Figure 6-10 (b) using its FFT around the bridge natural frequency. The road roughness includes many frequencies that may appear in the vehicle response. This causes a problem, particularly in a range close to the bridge natural frequency. Figure 6-10 (c) shows the bandpass-filtered road roughness in a range from 5.4 Hz to 5.8 Hz. It can be seen that road roughness adds a contribution to the bridge response in this frequency range which is not desirable.

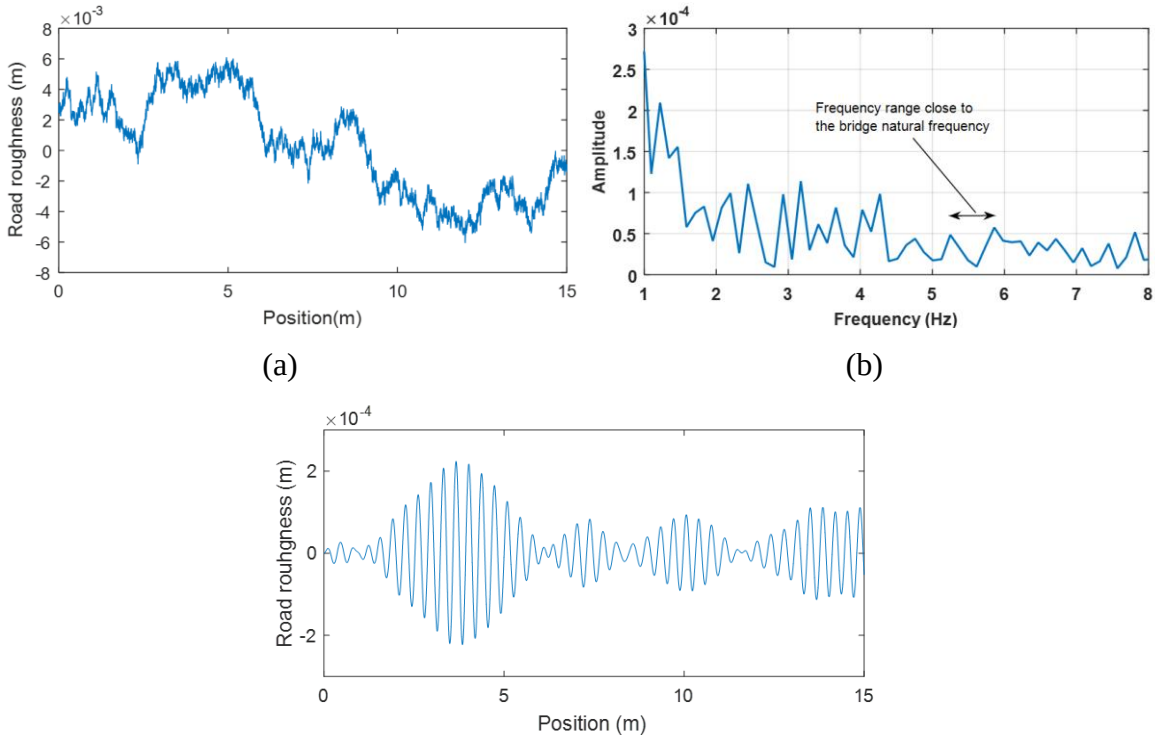

Figure 6-10 Class 'A' road profile, (a) road profile, (b) FFT of the profile, (c) the bandpass filtered profile.

In this case, the idea of subtraction which is proposed in (Yang et al., 2012b, Keenahan et al., 2014), is used to totally remove the effect of road profile. The acceleration responses of Axles 4, 5 and 7 are measured. Two difference signals are constructed as $\ddot{x}_1 = \ddot{y}_6 - \ddot{y}_4$ and $\ddot{x}_2 = \ddot{y}_7 - \ddot{y}_5$ to remove the effect of road profile. The HHT amplitudes for the first mode are shown in Figure 6-11. The first mode shape of the bridge is obtained using the rescaling process (Figure 6-12 (a)). The second mode shape of the bridge is obtained using the same procedure (Figure 6-12 (b)).

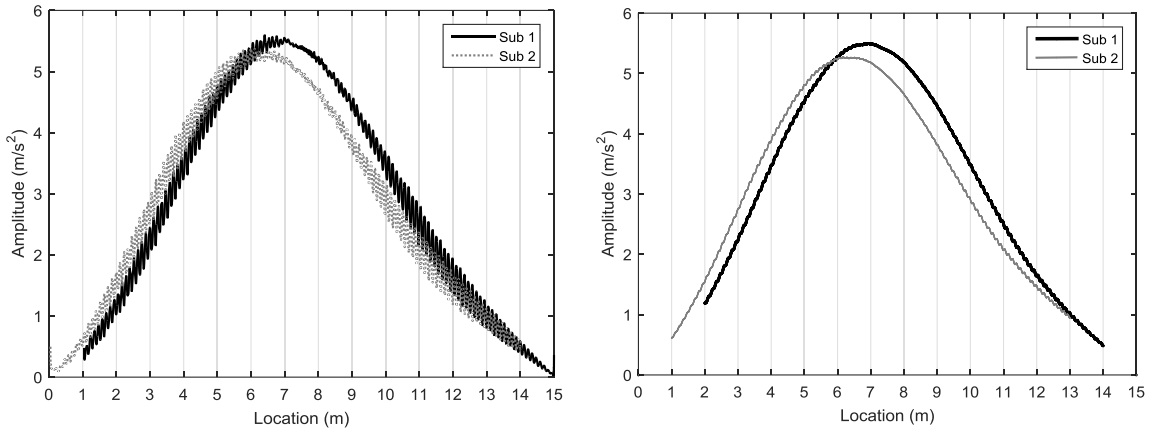

(a) (b)

Figure 6-11 Amplitudes obtained from two following differences, (a) Calculated raw amplitudes, (b) Smoothed and trimmed amplitudes.

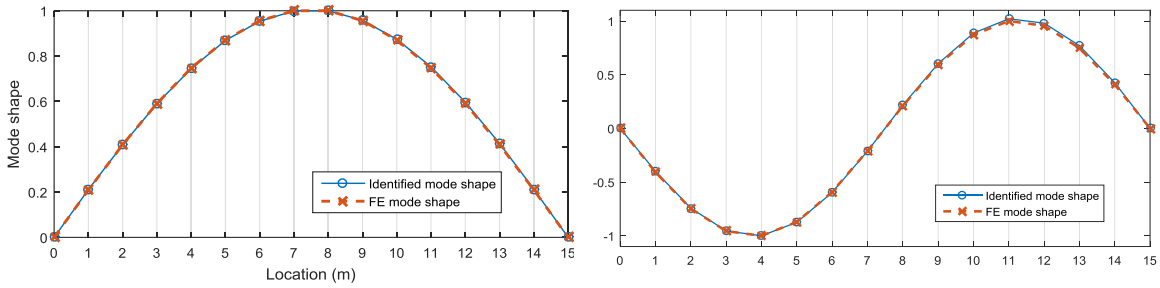

(a) (b)

Figure 6-12 The normalised bridge mode shapes, (a) the first mode, (b) the second mode.

6.5. Conclusions

This chapter describes an approach for indirect identification of bridge mode shapes from the response measured on a passing vehicle. A truck-trailer system equipped with an actuator is proposed. It is shown that the external excitation is beneficial for getting access to the energy of the bridge response at the key frequencies. It is shown that, unlike in the previous studies, this energy is not the bridge mode shape, but is correlated to the bridge mode shape at the time of measurement. A rescaling process is proposed to construct the bridge mode shapes using the amplitude of the responses measured on two following axles. The possibility of using the approach in presence of road profile is also studied. The concept of subtraction is employed to remove the effect of road profile in the measured responses.

Chapter 7: Conclusion

Chapter 7: Conclusion

7.1. Summary

This thesis is organised in five main chapters, each of which includes a journal paper that can be considered as an independent document. Therefore, each chapter presents its own conclusions section. The overall contribution of the work and the links between the chapters are summarized in this chapter. In addition, the main findings and results are incorporated here, in the context of the whole thesis.

This thesis has given an account of and the reasons for the use of an instrumented vehicle for the purpose of bridge monitoring. Chapter 2 has provided a comprehensive literature review of indirect bridge monitoring using passing vehicles. The current state of the art of the topic is well reviewed by summarizing the advantages and drawbacks of the relevant and important published works in this context. Subsequently, several gaps are identified and targeted to for study in the following chapters. The main challenges for this thesis are the development of new methods for identification of bridge mode shapes and improvement of modal and non-modal parameter-based damage detection methods.

Chapter 3 proposes a novel method called Short Time Frequency Domain Decomposition (STFDD) for the identification of bridge mode shapes. This study has shown that the bridge mode shapes can be constructed by applying an identification method to the short time segments of the measured signal. The second major finding is that the local mode shape vectors found for each segment should be corrected using a rescaling process.

Chapter 4 has presented a mode shape-based damage detection approach. The main purpose of this chapter is to show how the bridge mode shapes obtained in Chapter 3 can be used as a means of damage detection. This approach is again based on the STFDD method proposed in Chapter 3. It employs a simulated measurement system using laser vibrometers and accelerometers on a passing vehicle. The STFDD method is also slightly improved to provide higher resolution for the estimated mode shape. The results of this investigation support the idea that a mode shape-based damage detection method may be able to detect and localise the damage.

Chapter 5 provides a new understanding of the components that make up the response measured on a passing vehicle. The study theoretically shows that such a response can be

taken up into three main components; vehicle frequency, bridge natural frequency and a vehicle speed pseudo-frequency component. These findings suggest that in general the modal properties can be identified from the bridge natural frequency component and then be used in modal parameter-based damage detection methods. It also provides evidence that the vehicle speed pseudo-frequency component is also sensitive to damage which enhances our understanding about non-modal parameter-based damage detection methods using indirect measurement. A damage detection method is proposed in this chapter by separating this component from the total response using the EMD method. It is shown that the damage location can be detected with an acceptable accuracy if the road profile is constant.

Chapter 6 provides a numerical study on the identification of bridge mode shapes with high resolution. It suggests using a truck-trailer system equipped with an actuator to excite the bridge artificially. It is proposed that the external excitation is useful for getting access to the energy of the bridge response at the key frequencies. Some of the previous studies assumed that this energy is a normalised bridge mode shape. In contrast, the author shows that the energy is not the bridge mode shape, but is correlated to the bridge mode shape at the time of measurement. To obtain the bridge mode shapes, a rescaling process is proposed using the amplitude of the responses measured on two following axles. The study has gone some way towards enhancing understanding of contribution of the bridge mode shapes to the measured response in a vehicle.

This thesis has added several new ideas to the state of the art in indirect bridge monitoring. Two chapters (3 and 6) focus on the identification of bridge mode shapes and two chapters (4 and 5) study bridge damage detection. The first damage detection method is based on bridge mode shapes which are known as damage sensitive modal parameters. It reveals the existence of damage and localizes it. The second method (Chapter 5) does not use any modal parameter. It is based on the changes in the pseudo-static frequency part of the response which is sensitive to damage.

7.2. Recommendations for future research

The author believes that indirect bridge monitoring is a concept in its infancy in the literature. There are many challenges that need to be tackled to use the idea practically. The main challenges for future investigation of this topic are highlighted here.

This research has raised many questions in need of further investigation. The author believes that future work should be focused on full scale field testing of the idea on real bridges. A number of challenges should be considered for this purpose. Although good progress has been made in addressing the influence of road profile, more research is needed to to overcome this challenge in experimental work. Considering the speed of the vehicle, there is an inevitable shortage of vehicle bridge interaction measurement data. A further study could assess the optimum vehicle speed which does not create congestion in practical cases. In addition, most current field work is based on acceleration measurements on the vehicle axle which is usually contaminated by measurement noise. On the other hand, using laser measurements on the vehicle provides many advantages compared to accelerometers. Therefore, future research should examine using such a measurement system in a field test. A Traffic Speed Deflectometer (TSD) device seems to be a promising instrumented vehicle which could be used successfully for indirect bridge monitoring.

The author believes that performing laboratory scale experiments would provide an insight into the main difficulties of a real case study. Controlling the test situations such as; vehicle speed, road profile, damage location and bridge properties, would be very useful. Furthermore, the repeatability of the current methods could be assessed in a laboratory scale case study. However, to the author's knowledge, there is no laboratory, world-wide, where the vehicle crossing times are close to those on a real bridge (1 to 2 seconds).

Another possible area of future research would be to investigate employing an exciter installed on the vehicle. Controlling the force applied by the exciter would provide interesting findings. Therefore, it is recommended that further research be undertaken on this concept and the ideal properties of the applied load such as magnitude and frequency of the load.

References

AKGUL, F. 2012. A BMS development project with an integrated inspection program. *In:* BIONDINI, F. & FRANGOPOL, D. M. (eds.) *Proceedings of the Sixth International Conference on Bridge Maintenance, Safety and Management.* Italy.

ARORA, V., SINGH, S. P. & KUNDRA, T. K. 2009. Damped model updating using complex updating parameters. *Journal of Sound and Vibration,* 320**,** 438-451.

BRIGGS, R. C., JOHNSON, R. F., STUBSTAD, R. N. & PIERCE, L. 2000. A comparison of the rolling weight deflectometer with the falling weight deflectometer. *Nondestructive Testing of Pavements and Backcalculation of Moduli, 3rd Volume,* 1375**,** 444-456.

BRINCKER, R., ZHANG, L. M. & ANDERSEN, P. 2000. Modal identification from ambient responses using frequency domain decomposition. *Proceeding of IMAC-XVIII: A Conference on Structural Dynamics.* Texas, USA.

BRINCKER, R., ZHANG, L. M. & ANDERSEN, P. 2001. Modal identification of output-only systems using frequency domain decomposition. *Smart Materials & Structures,* 10**,** 441-445.

BU, J. Q., LAW, S. S. & ZHU, X. Q. 2006. Innovative bridge condition assessment from dynamic response of a passing vehicle. *Journal of Engineering Mechanics-ASCE,* 132**,** 1372-1379.

CANTERO, D., OBRIEN, E. & KAROUMI, R. 2014. Extending the Assessment Dynamic Ratio to Railway Bridges. *In:* POMBO, J. (ed.) *Proceedings of the Second International Conference on Railway Technology: Research, Development and Maintenance.* Ajaccio, Corsica, France: Civil-Comp Press.

CANTERO, D., OBRIEN, E. J. & GONZÁLEZ, A. 2010. Modelling the vehicle in vehicle-infrastructure dynamic interaction studies. *Proceedings of the Institution of Mechanical Engineers Part K-Journal of Multi-Body Dynamics,* 224**,** 243-248.

CAPRANI, C. C. 2012. Lifetime highway bridge traffic load effect from a combination of traffic states allowing for dynamic amplification. *Journal of Bridge Engineering,* 18**,** 901-909.

CAPRANI, C. C. 2013. Lifetime Highway Bridge Traffic Load Effect from a Combination of Traffic States Allowing for Dynamic Amplification. *Journal of Bridge Engineering,* 18**,** 901-909.

CAPRANI, C. C., GONZÁLEZ, A., RATTIGAN, P. H. & OBRIEN, E. J. 2012. Assessment dynamic ratio for traffic loading on highway bridges. *Structure and Infrastructure Engineering,* 8**,** 295-304.

CAPRANI, C. C. & OBRIEN, E. J. 2010. Recent Advances in the Governing Form of Traffic for Bridge Loading. *International workshop" Civil Structural Health Monitoring 2", WIM (Weigh In Motion), Load capacity and bridge performance In the Context of Risk Assessment, Maintenance and Life Cost Based Design.* Taormina-Sicily, Italy: ENEA.

CARDEN, E. P. & FANNING, P. 2004. Vibration based condition monitoring: A review. *Structural Health Monitoring,* 3**,** 355-377.

CEBON, D. 1999. *Handbook of Vehicle-Road Interaction,* London and New York, Taylor & Francis.

CEBON, D. & NEWLAND, D. 1983. Artificial generation of road surface topography by the inverse FFT method. *Vehicle System Dynamics,* 12**,** 160-165.

CERDA, F., CHEN, S., BIELAK, J., GARRETT, J. H., RIZZO, P. & KOVAČEVIĆ, J. 2014. Indirect structural health monitoring of a simplified laboratory-scale bridge model. *Smart Structures and Systems,* 13.

CERDA, F., GARRETT, J., BIELAK, J., BARRERA, J., ZHUANG, Z., CHEN, S., MCCANN, M., KOVACEVIC, J. & RIZZO, P. 2012. Indirect structural health monitoring in bridges: scale experiments. *In:* BIONDINI, F. & FRANGOPOL, D. M. (eds.) *Procedding of the 6th International Conference on Bridge Maintenance, Safety, Management, Resilience and Sustainability.* Italy.

CHANG, K. C., KIM, C. W. & BORJIGIN, S. 2014. Variability in bridge frequency induced by a parked vehicle. *Smart Structures and Systems,* 13**,** 755-773.

CHANG, K. C., WU, F. B. & YANG, Y. B. 2010. Effect of road surface roughness on indirect approach for measuring bridge frequencies from a passing vehicle. *Interaction and multiscale mechanics,* 3**,** 299-308.

CHEN, S. H., CERDA, F., RIZZO, P., BIELAK, J., GARRETT, J. H. & KOVACEVIC, J. 2014. Semi-Supervised Multiresolution Classification Using Adaptive Graph Filtering With Application to Indirect Bridge Structural Health Monitoring. *IEEE Transactions on Signal Processing,* 62**,** 2879-2893.

CHINCHALKAR, S. 2001. Determination of crack location in beams using natural frequencies. *Journal of Sound and Vibration,* 247**,** 417-429.

CHUPANIT, P. & PHROMSORN, C. 2012. The Importance of Bridge Health Monitoring. *International Science Index,* 6**,** 135-138.

CLOUGH, R. W. & PENZIEN, J. 1993. *Dynamics of Structures,* New York, McGraw-Hill.

COHEN, L. 1995. *Time-frequency analysis,* NJ, Prentice hall.

CURADELLI, R. O., RIERA, J. D., AMBROSINI, D. & AMANI, M. G. 2008. Damage detection by means of structural damping identification. *Engineering Structures,* 30**,** 3497-3504.

DAVIS, S. L. & GOLDBERG, D. 2013. The Fix We're In For: The State of Our Nation's Bridges 2013. USA: TRANSPORTATION FOR AMERICA.

DAWE, P. 2003. *Research perspectives: Traffic loading on highway bridges,* Thomas Telford.

DENG, L., YU, Y., ZOU, Q. L. & CAI, C. S. 2015. State-of-the-Art Review of Dynamic Impact Factors of Highway Bridges. *Journal of Bridge Engineering,* 20.

DILENA, M., LIMONGELLI, M. & MORASSI, A. 2015. Damage localization in bridges via the FRF interpolation method. *Mechanical Systems and Signal Processing,* 52**,** 162-180.

ENRIGHT, B., CAPRANI, C. & OBRIEN, E. 2011. Modelling of highway bridge traffic loading: Some recent advances. *Applications of Statistics and Probability in Civil Engineering***,** 111.

EWINS, D. J. 2000. *Modal testing : theory, practice, and application,* Baldock, Hertfordshire, England, Research Studies Press Ltd.

FAN, W. & QIAO, P. Z. 2009. A 2-D continuous wavelet transform of mode shape data for damage detection of plate structures. *International Journal of Solids and Structures,* 46**,** 4379-4395.

FAN, W. & QIAO, P. Z. 2011. Vibration-based Damage Identification Methods: A Review and Comparative Study. *Structural Health Monitoring,* 10**,** 83-111.

FLINTSCH, G. W., FERNE, B., DIEFENDERFER, B., KATICHA, S., BRYCE, J. & NELL, S. 2012. Evaluation of Traffic Speed Continuous Deflection Devices. *91st Annual Meeting, Transport Research Board,*. USA.

FUJINO, Y., KITAGAWA, K., FURUKAWA, T. & ISHII, H. 2005. Development of vehicle intelligent monitoring system (VIMS). *Proceeding of SPIE 5765, Smart*

Structures and Materials 2005: Sensors and Smart Structures Technologies for Civil, Mechanical, and Aerospace Systems.

FUJINO, Y. & SIRINGORINGO, D. M. 2011. Bridge monitoring in Japan: the needs and strategies. *Structure and Infrastructure Engineering,* 7**,** 597-611.

GOMEZ, H. C., FANNING, P. J., FENG, M. Q. & LEE, S. 2011. Testing and long-term monitoring of a curved concrete box girder bridge. *Engineering Structures,* 33**,** 2861-2869.

GONZÁLEZ, A. 2010. Vehicle-bridge dynamic interaction using finite element modelling. *Finite element analysis.* Rijeka, Croatia: Sciyo.

GONZÁLEZ, A., DOWLING, J., O'BRIEN, E. J. & ZNIDARIC, A. Experimental determination of dynamic allowance for traffic loading in bridges. TRB 89th Annual Meeting Compendium of Papers, 2010a. Transportation Research Board.

GONZÁLEZ, A., DOWLING, J. & OBRIEN, E. J. 2012a. Testing of a bridge weigh-in-motion algorithm utilising multiple longitudinal sensor locations. *Journal of Testing and Evaluation,* 40.

GONZÁLEZ, A., OBRIEN, E. J., LI, Y. Y. & CASHELL, K. 2008a. The use of vehicle acceleration measurements to estimate road roughness. *Vehicle System Dynamics,* 46**,** 485-501.

GONZÁLEZ, A., OBRIEN, E. J. & MCGETRICK, P. J. 2010b. Detection of Bridge Dynamic Parameters Using an Instrumented Vehicle. *Proceedings of the Fifth World Conference on Structural Control and Monitoring.* Tokyo, Japan.

GONZÁLEZ, A., OBRIEN, E. J. & MCGETRICK, P. J. 2012b. Identification of damping in a bridge using a moving instrumented vehicle. *Journal of Sound and Vibration,* 331**,** 4115-4131.

GONZÁLEZ, A., RATTIGAN, P., OBRIEN, E. J. & CAPRANI, C. 2008b. Determination of bridge lifetime dynamic amplification factor using finite element analysis of critical loading scenarios. *Engineering Structures,* 30**,** 2330-2337.

GONZÁLEZ, A. & ZNIDARIC, A. 2009. Recommendations on dynamic amplification allowance. Assessment Rehabilitation Center. Europe Highway Structure ARCHES.

GRANDE, E. & IMBIMBO, M. 2016. A multi-stage approach for damage detection in structural systems based on flexibility. *Mechanical Systems and Signal Processing,* 76-77**,** 455-475.

HADJILEONTIADIS, L. J., DOUKA, E. & TROCHIDIS, A. 2005. Fractal dimension analysis for crack identification in beam structures. *Mechanical Systems and Signal Processing,* 19**,** 659-674.

HAN, W. S., WU, J., CAI, C. S. & CHEN, S. R. 2015. Characteristics and Dynamic Impact of Overloaded Extra Heavy Trucks on Typical Highway Bridges. *Journal of Bridge Engineering,* 20.

HARRIS, N. K., OBRIEN, E. J. & GONZÁLEZ, A. 2007. Reduction of bridge dynamic amplification through adjustment of vehicle suspension damping. *Journal of Sound and Vibration,* 302**,** 471-485.

HE, W. & ZHU, S. 2015. Moving load-induced response of damaged beam and its application in damage localization. *Journal of Vibration and Control*.

HUANG, N. E., SHEN, Z. & LONG, S. R. 1999. A new view of nonlinear water waves: The Hilbert spectrum. *Annual Review of Fluid Mechanics,* 31**,** 417-457.

HUANG, N. E., SHEN, Z., LONG, S. R., WU, M. L. C., SHIH, H. H., ZHENG, Q. N., YEN, N. C., TUNG, C. C. & LIU, H. H. 1998. The empirical mode decomposition and the Hilbert spectrum for nonlinear and non-stationary time series analysis. *Proceedings of the Royal Society a-Mathematical Physical and Engineering Sciences,* 454**,** 903-995.

ISO8608:1995 1995. Mechanical Vibration-road Surface Profiles-reporting of Measured Data', International Standards Organisation.

KEENAHAN, J., MCGETRICK, P., OBRIEN, E. J. & GONZÁLEZ, A. 2012. Using instrumented vehicles to detect damage in bridges. *15th International Conference on Experimental Mechanics.* Porto, Portugal.

KEENAHAN, J. & OBRIEN, E. J. 2014. Allowing for a Rocking Datum in the Analysis of Drive-By Bridge Inspections. *In:* NANUKUTTAN, S. & GOGGINS, J. (eds.) *Civil Engineering Research in Ireland.* Belfast, Northern Ireland.

KEENAHAN, J., OBRIEN, E. J., MCGETRICK, P. J. & GONZÁLEZ, A. 2014. The use of a dynamic truck-trailer drive-by system to monitor bridge damping. *Structural Health Monitoring,* 13**,** 143-157.

KHIEM, N. & TOAN, L. 2014. A novel method for crack detection in beam-like structures by measurements of natural frequencies. *Journal of Sound and Vibration,* 333**,** 4084-4103.

KHORRAM, A., BAKHTIARI-NEJAD, F. & REZAEIAN, M. 2012. Comparison studies between two wavelet based crack detection methods of a beam subjected to a moving load. *International Journal of Engineering Science,* 51**,** 204-215.

KIM, C. W., ISEMOTO, R., MCGETRICK, P. J., KAWATANI, M. & OBRIEN, E. J. 2014. Drive-by bridge inspection from three different approaches. *Smart Structures and Systems,* 13**,** 775-796.

KIM, C. W., ISEMOTO, R., TOSHINAMI, T., KAWATANI, M., MCGETRICK, P. & OBRIEN, E. J. Experimental Investigation of Drive-by Bridge Inspection. 5th International Conference on Structural Health Monitoring of Intelligent Infrastructure (SHMII-5), 2011 2011 Cancun, Mexico.

KIM, C. W. & KAWATANI, M. Challenge for a drive-by bridge inspection. 10th International Conference on Structural Safety and Reliability ICOSSAR2009, 2009 Osaka, Japan. 758-765.

KIM, C. W., KAWATANI, M. & KIM, K. B. 2005. Three-dimensional dynamic analysis for bridge-vehicle interaction with roadway roughness. *Computers & Structures,* 83**,** 1627-1645.

KIM, J. T., RYU, Y. S., CHO, H. M. & STUBBS, N. 2003. Damage identification in beam-type structures: frequency-based method vs mode-shape-based method. *Engineering Structures,* 25**,** 57-67.

KIM, J. T. & STUBBS, N. 2003. Crack detection in beam-type structures using frequency data. *Journal of Sound and Vibration,* 259**,** 145-160.

KONG, X., CAI, C. S. & KONG, B. 2015. Damage Detection Based on Transmissibility of a Vehicle and Bridge Coupled System. *Journal of Engineering Mechanics,* 141**,** 04014102.

LAW, S. S. & ZHU, X. Q. 2005. Bridge dynamic responses due to road surface roughness and braking of vehicle. *Journal of Sound and Vibration,* 282**,** 805-830.

LEDERMAN, G., WANG, Z., BIELAK, J., NOH, H., GARRETT, J. H., CHEN, S., KOVACEVIC, J., CERDA, F. & RIZZO, P. 2014. Damage quantification and localization algorithms for indirect SHM of bridges. *In:* AIRONG CHEN, D. M. F., XIN RUAN (ed.) *Bridge Maintenance, Safety, Management and Life Extension.* Shanghai, China.

LI, H. J., HE, C. J., JI, J. L., WANG, H. & HAO, C. Z. 2005. Crack damage detection in beam-like structures using RBF neural networks with experimental validation. *International Journal of Innovative Computing Information and Control,* 1**,** 625-634.

LI, W. M., JIANG, Z. H., WANG, T. L. & ZHU, H. P. 2014. Optimization method based on Generalized Pattern Search Algorithm to identify bridge parameters indirectly by a passing vehicle. *Journal of Sound and Vibration,* 333**,** 364-380.

LI, Z. 2014. *Damage identification of bridges from signals measured with a moving vehicle.* PhD thesis, The University of Hong Kong (Pokfulam, Hong Kong).

LI, Z. & AU, F. T. K. 2015. Damage Detection of Bridges Using Response of Vehicle Considering Road Surface Roughness. *International Journal of Structural Stability and Dynamics,* 15.

LI, Z. H. & AU, F. T. K. 2014. Damage Detection of a Continuous Bridge from Response of a Moving Vehicle. *Shock and Vibration,* Vol. 2014.

LIN, C. W. & YANG, Y. B. 2005. Use of a passing vehicle to scan the fundamental bridge frequencies: An experimental verification. *Engineering Structures,* 27**,** 1865-1878.

LYONS, R. G. 2011. *Understanding digital signal processing,* Upper Saddle River, NJ, Prentice Hall.

MAGALHÃES, F., CUNHA, A. & CAETANO, E. 2012. Vibration based structural health monitoring of an arch bridge: from automated OMA to damage detection. *Mechanical Systems and Signal Processing,* 28**,** 212-228.

MALEKJAFARIAN, A., MCGETRICK, P. J. & OBRIEN, E. J. 2015. A Review of Indirect Bridge Monitoring Using Passing Vehicles. *Shock and Vibration*.

MALEKJAFARIAN, A. & OBRIEN, E. J. Application of output-only modal method to the monitoring of bridges using an instrumented vehicle. *In:* NANUKUTTAN, S. & GOGGINS, J., eds. Civil Engineering Research in Ireland, 2014a Belfast, Northern Ireland.

MALEKJAFARIAN, A. & OBRIEN, E. J. 2014b. Identification of bridge mode shapes using Short Time Frequency Domain Decomposition of the responses measured in a passing vehicle. *Engineering Structures,* 81**,** 386-397.

MCGETRICK, P. & KIM, C. A. 2014a. A Wavelet Based Drive-by Bridge Inspection System. *In:* AIRONG CHEN, D. M. F., XIN RUAN (ed.) *Proceedings of the 7th International Conference on Bridge Maintenance Safety and Management, IABMAS 2014.* Shanghai, China.

MCGETRICK, P., KIM, C. W. & OBRIEN, E. J. 2010. Experimental Investigation of the Detection of Bridge Dynamic Parameters Using a Moiving Vehicle. *The Twenty-Third KKCNN Symposium on Civil Engineering.* Taipei, Taiwan.

MCGETRICK, P. J., GONZÁLEZ, A. & OBRIEN, E. J. 2009. Theoretical investigation of the use of a moving vehicle to identify bridge dynamic parameters. *Insight,* 51**,** 433-438.

MCGETRICK, P. J. & KIM, C. W. 2013. A Parametric Study of a Drive by Bridge Inspection System Based on the Morlet Wavelet. *Key Engineering Materials,* 569**,** 262-269.

MCGETRICK, P. J. & KIM, C. W. 2014b. An indirect bridge inspection method incorporating a wavelet-based damage indicator and pattern recognition. *In:* CUNHA, A., CAETANO, E., RIBEIRO, P. & MÜLLER, G. (eds.) *9th International Conference on Structural Dynamics, EURODYN 2014.* Porto, Portugal.

MEREDITH, J., GONZÁLEZ, A. & HESTER, D. 2012. Empirical Mode Decomposition of the acceleration response of a prismatic beam subject to a moving load to identify multiple damage locations. *Shock and Vibration,* 19**,** 845-856.

MIYAMOTO, A. & YABE, A. 2011. Bridge Condition Assessment based on Vibration Responses of Passenger Vehicle. *In:* OUYANG, H. (ed.) *9th International Conference on Damage Assessment of Structures (DAMAS 2011).*

MIYAMOTO, A. & YABE, A. 2012. Development of practical health monitoring system for short- and medium-span bridges based on vibration responses of city bus. *Journal of Civil Structural Health Monitoring,* 2**,** 47-63.

MODENA, C., SONDA, D. & ZONTA, D. 1999. Damage localization in reinforced concrete structures by using damping measurements. *Key Engineering Materials,* 167-168**,** 132-141.

MOSES, F. 1979. Weigh-in-motion system using instrumented bridges. *Transportation Engineering Journal,* 105**,** 233-249.

NGUYEN, K. V. & TRAN, H. T. 2010. Multi-cracks detection of a beam-like structure based on the on-vehicle vibration signal and wavelet analysis. *Journal of Sound and Vibration,* 329**,** 4455-4465.

NORMALISATION 2002. EN 1991-2: Eurocode 1: Actions on structures-Part 2: Traffic loads on bridges. *COMITÉ EUROPÉEN DE.* Brussels.

OBRIEN, E. J., CANTERO, D., ENRIGHT, B. & GONZÁLEZ, A. 2010. Characteristic dynamic increment for extreme traffic loading events on short and medium span highway bridges. *Engineering Structures,* 32**,** 3827-3835.

OBRIEN, E. J. & ENRIGHT, B. 2012. Using weigh-in-motion data to determine aggressiveness of traffic for bridge loading. *Journal of Bridge Engineering,* 18**,** 232-239.

OBRIEN, E. J., GONZÁLEZ, A., DOWLING, J. & ZNIDARIC, A. 2013. Direct measurement of dynamics in road bridges using a bridge weigh-in-motion system. *Baltic Journal of Road and Bridge Engineering,* 4**,** 263-270.

OBRIEN, E. J., GONZÁLEZ, A. & ZNIDARIC, A. Recommendations for dynamic allowance in bridge assessment. *In:* FRANOGPOL, D., SAUSE, R. AND KUSKO, C, ed. Proceedings of the fifth International Conference on Bridge Maintenance, Safety, Management and Life-Cycle Optimization (IABMAS10), 2012 Philadelphia, USA. CRC Press.

OBRIEN, E. J. & KEENAHAN, J. 2014. Drive-by damage detection in bridges using the apparent profile. *Structural Control and Health Monitoring,* DOI: 10.1002/stc.1721.

OBRIEN, E. J. & MALEKJAFARIAN, A. 2015. Identification of bridge mode shapes using a passing vehicle. *7th International Conference on Structural Health Monitoring of Intelligent Infrastructure (SHMII).* Italy, Turin.

OBRIEN, E. J. & MALEKJAFARIAN, A. 2016. A mode shape-based damage detection approach using laser measurement from a vehicle crossing a simply supported bridge. *Structural Control and Health Monitoring,* DOI: 10.1002/stc.1841.

OBRIEN, E. J., MCGETRICK, P. J. & GONZÁLEZ, A. 2014. A drive-by inspection system via vehicle moving force identification. *Smart Structures and Systems,* 13**,** 821-848.

OBRIEN, E. J., QUILLIGAN, M. & KAROUMI, R. 2006. Calculating an influence line from direct measurements. *Bridge Engineering, Proceedings of the Institution of Civil Engineers,* 159**,** 31-34.

OBRIEN, E. J., RATTIGAN, P., GONZÁLEZ, A., DOWLING, J. & ŽNIDARIČ, A. 2009. Characteristic dynamic traffic load effects in bridges. *Engineering structures,* 31**,** 1607-1612.

OSHIMA, Y., YAMAGUCHI, T., KOBAYASHI, Y. & SUGIURA, K. Eigenfrequency estimation for bridges using the response of a passing vehicle with excitation system. *In:* KOH, H.-M. & FRANGOPOL, D., eds. Fourth International Conference on Bridge Maintenance, Safety and Management, IABMAS2008, 2008 Seoul, Korea. 3030-3037.

OSHIMA, Y., YAMAMOTO, K. & SUGIURA, K. 2014. Damage assessment of a bridge based on mode shapes estimated by responses of passing vehicles. *Smart Structures and Systems,* 13**,** 731-753.

OSHIMA, Y., YAMAMOTO, K., SUGIURA, K. & YAMAGUCHI, T. 2009. Estimation of bridge eigenfrequencies based on vehicle responses using ICA. *In:* FURUTA, H., FRANGOPOL, D. & SHINOZUKA, M. (eds.) *Proceedings of the 10th International Conference on Structural Safety and Reliability, ICOSSAR2009.* 13-17 September, Osaka, Japan.

PAEGLITE, I. & PAEGLITIS, A. 2013. The dynamic amplification factor of the bridges in Latvia. *Procedia Engineering,* 57**,** 851-858.

PAEGLITE, I., PAEGLITIS, A. & SMIRNOVS, J. 2015. Dynamic amplification factor for bridges with span length from 10 to 35 meters. *Engineering Structures and Technologies***,** 1-8.

PANDEY, A. K., BISWAS, M. & SAMMAN, M. M. 1991. Damage Detection from Changes in Curvature Mode Shapes. *Journal of Sound and Vibration,* 145**,** 321-332.

PARK, Y. S., SHIN, D. K. & CHUNG, T. J. 2005. Influence of road surface roughness on dynamic impact factor of bridge by full-scale dynamic testing. *Canadian Journal of Civil Engineering,* 32**,** 825-829.

PATIL, D. P. & MAITI, S. K. 2003. Detection of multiple cracks using frequency measurements. *Engineering Fracture Mechanics,* 70**,** 1553-1572.

QIAO, P. Z. & CAO, M. S. 2008. Waveform fractal dimension for mode shape-based damage identification of beam-type structures. *International Journal of Solids and Structures,* 45**,** 5946-5961.

RATCLIFFE, C. P. 1997. Damage detection using a modified laplacian operator on mode shape data. *Journal of Sound and Vibration,* 204**,** 505-517.

REN, W. X., PENG, X. L. & LIN, Y. Q. 2005. Experimental and analytical studies on dynamic characteristics of a large span cable-stayed bridge. *Engineering Structures,* 27**,** 535-548.

REYNDERS, E. & DE ROECK, G. 2008. Reference-based combined deterministic-stochastic subspace identification for experimental and operational modal analysis. *Mechanical Systems and Signal Processing,* 22**,** 617-637.

RICH, F. H. 2014. *Dynamic amplification factor for the design of reinforcement in the transverse direction of deck slab of box girder bridges.* MSc, Bangladesh University of Engineering and Technology.

ROVERI, N. & CARCATERRA, A. 2012. Damage detection in structures under traveling loads by Hilbert-Huang transform. *Mechanical Systems and Signal Processing,* 28**,** 128-144.

RYTTER, A. 1993. *Vibration based inspection of civil engineering structures.* PhD, Aalborg University.

SALAWU, O. S. 1997. Detection of structural damage through changes in frequency: A review. *Engineering Structures,* 19**,** 718-723.

SHI, Z., LAW, S. & ZHANG, L. 2000. Damage localization by directly using incomplete mode shapes. *Journal of Engineering Mechanics,* 126**,** 656-660.

SINHA, J. K., FRISWELL, M. I. & EDWARDS, S. 2002. Simplified models for the location of cracks in beam structures using measured vibration data. *Journal of Sound and Vibration,* 251**,** 13-38.

SIRINGORINGO, D. M. & FUJIN, Y. 2012. Estimating Bridge Fundamental Frequency from Vibration Response of Instrumented Passing Vehicle: Analytical and Experimental Study. *Advances in Structural Engineering,* 15**,** 417-433.

SIRIWARDANE, S. C. 2015. Vibration measurement-based simple technique for damage detection of truss bridges: A case study. *Case Studies in Engineering Failure Analysis,* 4**,** 50-58.

SUKHEN, C. 1992. The Design of Modern Steel Bridges. *Boston: London Edinburgh*.

TAN, G. H., BRAMELD, G. H. & THAMBIRATNAM, D. P. 1998. Development of an analytical model for treating bridge-vehicle interaction. *Engineering Structures,* 20**,** 54-61.

TEDESCO, J. W., MCDOUGAL, W. G. & ROSS, C. A. 1999. *Structural dynamics: theory and applications*, Addison Wesley Longman.

TOSHINAMI, T., KAWATANI, M. & KIM, C. W. 2010. Feasibility investigation for identifying bridge's fundamental frequencies from vehicle vibrations. *In:* DAN FRANGOPOL, R. S., CHAD KUSKO (ed.) *Fifth International Conference on Bridge Maintenance, Safety and Management, IABMAS2010.* Philadelphia, USA.

TSAI, H.-C., WANG, C.-Y., HUANG, N. E., KUO, T.-W. & CHIENG, W.-H. 2014. Railway track inspection based on the vibration response to a scheduled train and the Hilbert–Huang transform. *Proceedings of the Institution of Mechanical Engineers, Part F: Journal of Rail and Rapid Transit,* 229**,** 815-829.

WILLIAMS, C. & SALAWU, O. 1997. Damping as a damage indication parameter. *Proceedings of the 15th international modal analysis conference.* Orlando, FL, USA: The Society for Experimental Mechanics.

YABE, A., MIYAMOTO, A., ISODA, S. & TANI, N. 2013. Development of Bridge Monitoring System for Short- and Medium-Span Bridges Based on Bus Vibration. *Journal of Japan Society of Civil Engineers, Ser. F4 (Construction and Management),* 69**,** 102-120.

YANG, Y. & CHEN, W.-F. 2015. Extraction of Bridge Frequencies from a Moving Test Vehicle by Stochastic Subspace Identification. *Journal of Bridge Engineering***,** 04015053.

YANG, Y. B. & CHANG, K. C. 2009a. Extracting the bridge frequencies indirectly from a passing vehicle: Parametric study. *Engineering Structures,* 31**,** 2448-2459.

YANG, Y. B. & CHANG, K. C. 2009b. Extraction of bridge frequencies from the dynamic response of a passing vehicle enhanced by the EMD technique. *Journal of Sound and Vibration,* 322**,** 718-739.

YANG, Y. B., CHANG, K. C. & LI, Y. C. 2013a. Filtering techniques for extracting bridge frequencies from a test vehicle moving over the bridge. *Engineering Structures,* 48**,** 353-362.

YANG, Y. B., CHEN, W. F., YU, H. W. & CHAN, C. S. 2013b. Experimental study of a hand-drawn cart for measuring the bridge frequencies. *Engineering Structures,* 57**,** 222-231.

YANG, Y. B., CHENG, M. C. & CHANG, K. C. 2013c. Frequency Variation in Vehicle-Bridge Interaction Systems. *International Journal of Structural Stability and Dynamics,* 13.

YANG, Y. B., LEE, Y. C. & CHANG, K. C. 2014a. Effect of Road Surface Roughness on Extraction of Bridge Frequencies by Moving Vehicle. *Mechanics and Model-Based Control of Advanced Engineering Systems.* Springer Vienna.

YANG, Y. B., LI, Y. C. & CHANG, K. 2014b. Constructing the mode shapes of a bridge from a passing vehicles: a theoretical study. *Smart Structures and Systems,* 13**,** 797-819.

YANG, Y. B., LI, Y. C. & CHANG, K. C. 2012a. Effect of road surface roughness on the response of a moving vehicle for identification of bridge frequencies. *Interaction and Multiscale Mechanics,* 5**,** 347-368.

YANG, Y. B., LI, Y. C. & CHANG, K. C. 2012b. Using two connected vehicles to measure the frequencies of bridges with rough surface: a theoretical study. *Acta Mechanica,* 223**,** 1851-1861.

YANG, Y. B. & LIN, C. W. 2005. Vehicle-bridge interaction dynamics and potential applications. *Journal of Sound and Vibration,* 284**,** 205-226.

YANG, Y. B., LIN, C. W. & YAU, J. D. 2004. Extracting bridge frequencies from the dynamic response of a passing vehicle. *Journal of Sound and Vibration,* 272**,** 471-493.

YIN, S. H. & TANG, C. Y. 2011. Identifying Cable Tension Loss and Deck Damage in a Cable-Stayed Bridge Using a Moving Vehicle. *Journal of Vibration and Acoustics,* 133.

YOON, M. K., HEIDER, D., GILLESPIE, J. W., RATCLIFFE, C. P. & CRANE, R. M. 2005. Local damage detection using the two-dimensional gapped smoothing method. *Journal of Sound and Vibration,* 279**,** 119-139.

ZHANG, L., BRINCKER, R. & ANDERSEN, P. 2005. An Overview of Operational Modal Analysis: Major Development and Issues. *Proceeding of 1st IOMAC Conference.* Copenhagen, Denmark.

ZHANG, Q. L., VROUWENVELDER, A. & WARDENIER, J. 2001. Dynamic amplification factors and EUDL of bridges under random traffic flows. *Engineering Structures,* 23**,** 663-672.

ZHANG, Y., LIE, S. T. & XIANG, Z. H. 2013. Damage detection method based on operating deflection shape curvature extracted from dynamic response of a passing vehicle. *Mechanical Systems and Signal Processing,* 35**,** 238-254.

ZHANG, Y., WANG, L. Q. & XIANG, Z. H. 2012. Damage detection by mode shape squares extracted from a passing vehicle. *Journal of Sound and Vibration,* 331**,** 291-307.

ZHU, X. Q. & LAW, S. S. 2006. Wavelet-based crack identification of bridge beam from operational deflection time history. *International Journal of Solids and Structures,* 43**,** 2299-2317.

ZNIDARIC, A., PAKRASHI, V., O'BRIEN, E. & O'CONNOR, A. 2011. A review of road structure data in six European countries. *Proceedings of the ICE-Urban Design and Planning,* 164**,** 225-232.

Appendix A: Direct Field Measurement of the Dynamic Amplification in a Bridge

Authors:

Ciarán Carey

Eugene J. OBrien

Abdollah Malekjafarian

Myra Lydon

Susan Taylor

Paper status:

Published in *Mechanical Systems and Signal Processing*, Volume 85, Pages 601-609, 2017.

Not to the reader:

The author assumes this work as a minor contribution, as the majority of the work towards this publication was done by other authors. The author's contribution was the numerical processing of the measured strain data (Section A.5).

A.1. Introduction

Accurate bridge safety assessment requires a knowledge of load effect as well as the capacity to resist these effects. Allowances for dynamic amplification of load effects are often conservative. Hence, better information on the magnitude of dynamic amplification has the potential to reduce the number of bridges that are prematurely repaired or replaced. This chapter describes a study where the dynamic allowance for a bridge is directly measured on site.

Many studies have considered the dynamic impact factor for bridges subject to passing trucks (Law and Zhu, 2005, Deng et al., 2015, Han et al., 2015). The magnitude of the amplification of stress due to vehicle-bridge-interaction (VBI) is often (González et al., 2008b, Park et al., 2005, Caprani, 2012) studied using the Dynamic Amplification Factor (DAF), defined as the ratio of the total load effect (including dynamics) to the static load effect for a particular loading scenario on the bridge. DAF has been used in many studies (Sukhen, 1992, Zhang et al., 2001, Dawe, 2003, Paeglite et al., 2015, Rich, 2014, Caprani, 2013) for quantification of the dynamic increment of load effect on the bridge.

Paeglite and Paeglitis (Paeglite and Paeglitis, 2013) present a study of the DAF obtained from the results of dynamic load tests of bridges carried out from 1990 to 2012 in Latvia. The DAF values are obtained from the dynamic response measured using an optical vibration sensor. The values of DAF obtained were analyzed and compared to the values used in the definition of the Eurocode 1 traffic load model. The actual DAF values for a good quality bridge deck surface were, in most cases, less than the values incorporated in the Eurocode (NORMALISATION, 2002).

OBrien et al. (2009), (OBrien et al., 2010) suggest that DAF does not recognize the reduced probability of both maxima occurring simultaneously, i.e., static load effect and dynamic amplification. They point out that the maximum values of DAF tend to result from lighter vehicles and are not relevant when seeking characteristic maximum values. They propose the concept of Assessment Dynamic Ratio (ADR), defined as the ratio of characteristic maximum total load effect, to characteristic static load effect, which, in general, correspond to different loading scenarios. For both total and static effects, the characteristic value is the expected maximum, over all possible cases, for the specified return period. This ADR is more appropriate for dynamic assessment since it provides the Engineer with the ratio of

what is needed, to what can be found by static probabilistic analysis (OBrien and Enright, 2012).

Using ADR (Caprani and OBrien, 2010) found the "expected level of lifetime dynamic interaction" for a certain site and bridge to be approximately 1.06, significantly lower than the DAF prescribed in the Eurocode. González et al. (2010a) report that ADRs below 1.1 are typical for bridges with very good road profiles while González and Znidaric (2009) found that ADR, like DAF, tends to decrease with an increase in load. Both Enright et al. (2011) and Caprani (2013) state that the implication of such values for dynamics being much lower than expected is that the governing loading scenario for a majority of bridges is altered.

Caprani et al. (2012) utilize multivariate extreme value theory in conjunction with static simulations and finite element vehicle-bridge dynamic interaction models to simulate static and total load effects for the Mura River Bridge in Slovenia. It is shown for this bridge and traffic, that the required allowance reduces with increasing load effect and consequently, the dynamic allowance is significantly less than recommended by bridge codes in this case.

Cantero et al. (2014) extend the concept of ADR to railway bridges. Guidelines are provided in (OBrien et al., 2012) and (OBrien et al., 2013) on how to obtain a site-specific value for dynamic allowance, both numerically and by field measurement. A Bridge WIM system is used to record the total response and to infer the static response of about 74 000 5-axle trucks over the course of a 58-day period. Using the measured total and inferred static bending moment for this population of vehicles, the site-specific ADR value is found for a 50-year return period. It is shown that measured and numerically simulated data produce similar ADR values. However, it should be noted that, as static effects are inferred from the same sensors used to measure the total effects, there is a risk of bias. This risk is considered in [21] and numerical simulations suggest that the bias is small.

Whereas other investigations into ADR extrapolated the characteristic load effects using extreme value theory (OBrien et al., 2010) simulated 10 000 years of traffic which allowed for an interpolation of load effects. It is reported in (OBrien et al., 2012) that variability of ADR decreases as the sample size increases.

In this chapter, the static axle weights of passing vehicles are found using a piezo-polymer weigh-in-motion (WIM) system and the corresponding load effects found using the bridge

influence line. The total load effects (including dynamics) are measured directly using fiber optic sensors on the bridge.

A.2. Weigh in Motion and Influence Line

A.2.1. Data Collection and Site

A bridge structure at Loughbrickland in Northern Ireland, United Kingdom (UK), was instrumented with fiber optic sensors. The bridge span is 18.8 m with a skew of 22.7° (Figure A- 1). The beam-and-slab structure (Figure A- 2) is typical of many short-span new-build bridges across the UK and Ireland. The superstructure consists of 27 no. prestressed concrete Y4 girders, each 1 m in depth, spaced at 1.22 m centers. There is a 200 mm overlaid cast in-situ concrete deck which is supported by permanent glass reinforced concrete formwork, spanning transversely between the main beams. The abutments are supported by a pile cap which is integral with the deck beams.

Figure A- 1 Side elevation of Loughbrickland site.

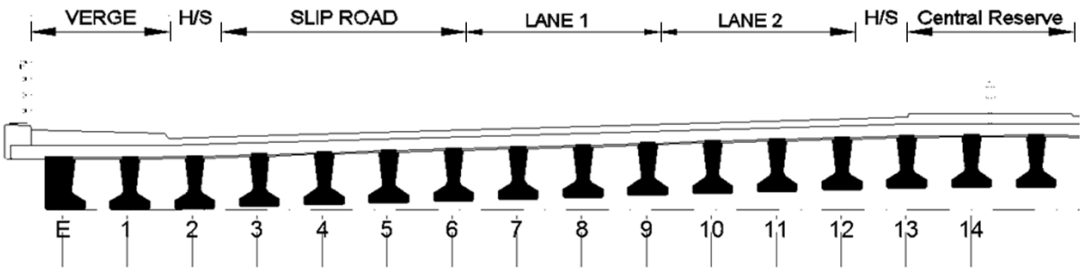

Figure A- 2 Section showing northbound carriageway.

The bridge structure forms part of the main Dublin to Belfast A1 road which was constructed in 2010. This route is ideal for an analysis of Heavy Goods Vehicles as it is an important link between the ports of Dublin, Warrenpoint and Belfast and forms a strategic cross-border economic link between Northern Ireland and the Republic of Ireland. The structure is on a central route through the island and has a high traffic volume. There are 10 000 to 12 000 vehicles travelling on the carriageway in each direction daily. The bridge also provides an underpass to give access to the southern end of the town of Loughbrickland. The traffic can pass under the main A1 carriageway and travel onto the B3 Dublin/Grovehill Road (Figure A- 3).

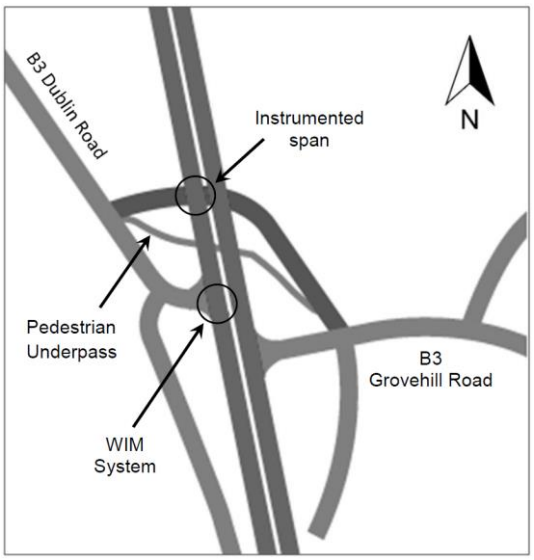

Figure A- 3 Site layout.

The bridge carries four traffic lanes, two in each direction, as well as two peripheral lanes for traffic joining/exiting the carriageway, as shown in Figure A- 2. A large central reserve separates the north- and south-bound carriageways; the northbound section was chosen for instrumentation.

Fiber optic sensors were installed on Beam No. 6 (Figure A- 2). Three sensors were installed in parallel, each on mechanical strain amplifiers as illustrated in Figure A- 4. The mechanical amplifiers – simple plates in a 'dog-bone' shape – served the function of concentrating most of the movement over their 150 mm length at the sensor location. The strains from three such amplifiers were averaged to further improve the resolution. The strain was output to the nearby control cabinet and saved for every six minutes of data. There is a 6 second delay between the end of one record and the beginning of the next.

(a)

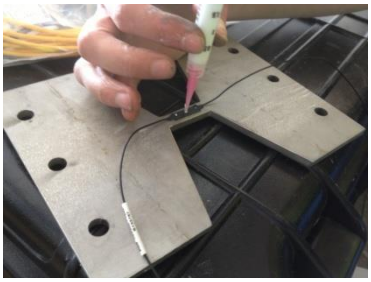

(b)

Figure A- 4 (a) Installation of the equipment, (b) mechanical strain amplifier.

A piezo-polymer pavement Weigh-in-Motion (WIM) system was embedded in the pavement on the approach to the structure (Figure A- 5). The system can provide much information about the passing trucks including; gross weight, axle weights, axle spacings, temperature, truck speed and number of axles. This information will be used later for the estimation of static load effects for each loading event.

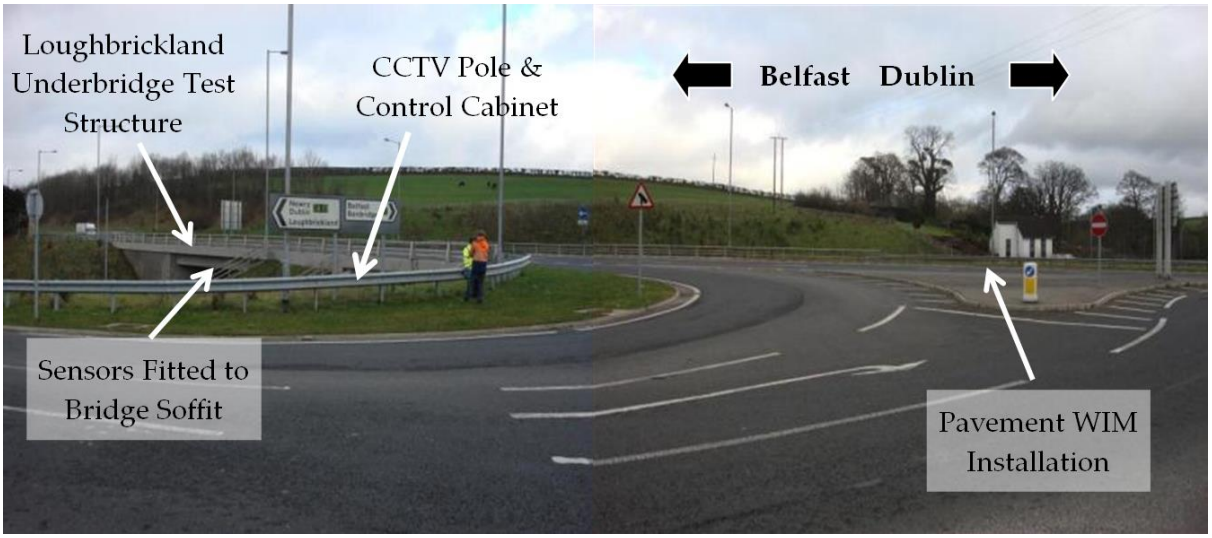

Figure A- 5 Overview of site and test structure.

A.3. Measured Influence Line

An influence line with high accuracy is required for the estimation of the static load effects for all events. Seven calibration trucks of known weight and the bridge response to them are used to infer the influence line from real measurements. One of the factors in choosing the site was the bridge's proximity to a static weigh station located just outside Loughbrickland Village at its northern end. This weigh station is used by the Driver and Vehicle Agency of Northern Ireland (DVANI) to check the weights of vehicles using the dual carriageway. The axle weights and spacings of the calibration trucks were measured statically at the weigh station and are given in Table 1.

Table A-1 Calibration truck properties.

Truck No.	No. of axles	Gross weight (kg)	Axle weights (kg)					
			1	2	3	4	5	6
1	4	14 100	4200	3700	2900	3300	-	-
2	5	13 300	4800	3300	1800	1800	1600	-
3	5	24 500	5300	6500	4100	4400	4200	-
4	3	10 000	3900	3800	2300	-	-	-
5	2	8 700	4600	4100	-	-	-	-
6	5	30 200	5800	8400	4000	5600	6400	-
7	6	35 100	5600	2400	7100	6500	7000	6500

The strain signal for Beam No. 6 due to the passage of the first calibration vehicle is shown in Figure A- 6.

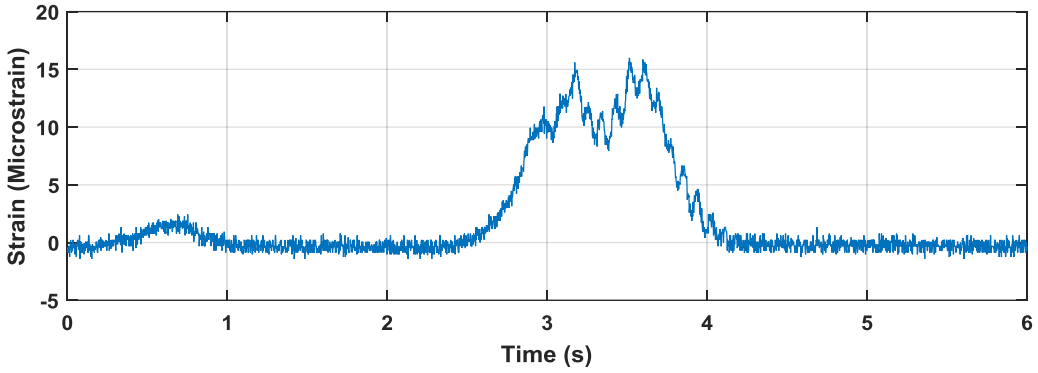

Figure A- 6 Strain in Beam 6 due to Truck No. 1.

To calculate the influence line corresponding to the passage of each calibration truck, the method developed by OBrien et al. (2006) is adopted. This uses the same principles developed by Moses (1979) to find unknown axle weight using a known influence line (Bridge WIM). An error function is defined as the sum of the squares of the differences between the measured and theoretical load effects:

$$E = \sum_{k=1}^{K} (\varepsilon_k^M - \varepsilon_k^T)^2 \tag{A-1}$$

where ε_k^M and ε_k^T are the k^{th} measured and theoretical strains respectively and K is the number of scans. The theoretical strain is a function of the axle loads and the corresponding influence line ordinates. In Bridge WIM the error function is differentiated with respect to the unknown axle weights and set to zero to minimize the error function. Here, the error function is differentiated with respect to each ordinate of the influence line. For the k^{th} ordinate,

$$\frac{\partial E}{\partial I_k} = 2[\varepsilon_k^M - (W_1 I_k + W_2 I_{k-t2} + W_3 I_{k-t3} + W_4 I_{k-t4})](-W_1) + 2[\varepsilon_{k+t2}^M - (W_1 I_{k+t2} + W_2 I_k + W_3 I_{k+t2-t3} + W_4 I_{k+t2-t4})](-W_2) + 2[\varepsilon_{k+t3}^M - (W_1 I_{k+t3} + W_2 I_{k+t3-t2} + W_3 I_k + W_4 I_{k+t3-t4})](-W_3) + 2[\varepsilon_{k+t4}^M - (W_1 I_{k+t4} + W_2 I_{k+t4-t2} + W_3 I_{k+t4-t3} + W_4 I_k)](-W_4) = 0, \quad k = 1,2,\dots,K \tag{A-2}$$

where *ti* is the number of scans between the passage of axles 1 and *i*. Solving these linear equations in the *K* unknowns, I_k, k =1, *K*, gives the influence line which best fits the measured response. While Eq. (2) applies to a 4-axle truck; similar equations exist for trucks with other numbers of axles.

Information on the vehicle speed and axle spacing was taken from other strain sensors located in the pavement WIM system. A unit influence line for each of the seven calibration vehicles listed in Table 1 was found. The average of these values was then calculated and is illustrated in Figure A- 7. The mean influence line was passed through a moving average filter as proposed by González et al. (2012a) and this was deemed to be the final 'measured' influence line. All of the calibration trucks traveled in the slow lane (lane 1 in Figure A- 2) so this influence line is only valid for trucks in that lane.

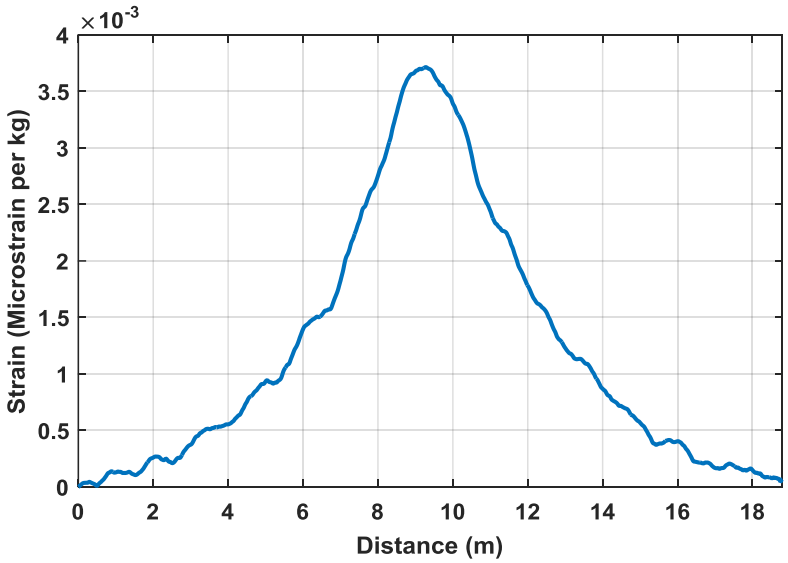

Figure A- 7 The unit influence line estimated from all seven calibration trucks.

A.4. Weigh-in-Motion data

Data from the piezo-polymer WIM system was found to be temperature sensitive and to drift over time. The mean steer axel weight in standard 5-axle trucks was found to be correlated with temperature, suggesting that temperature compensation was not enabled in the system or was not operating correctly. In addition, the distribution of steer axle weights for these trucks tended to decrease over time, even for trucks weighed at the same temperature – see Figure A- 8.

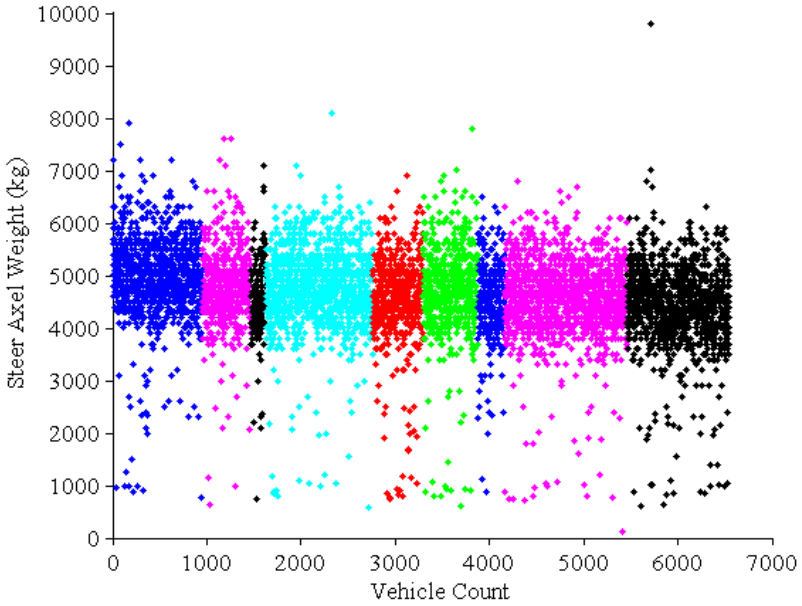

Figure A- 8 Time drift of steer axle weights measured at 10^0 C (vehicles are given in chronological order; colors indicate different months)

The static response of Beam 6 to the passage of each truck is calculated as a linear combination of axel weights and the corresponding influence line ordinates from Figure A-7. To correct for temperature and drift, the calculated static response is scaled to best fit the measured total response. This is illustrated in Figure A- 9. In effect, the WIM system is only being used to determine the *relative* weights of the axels of each truck while the fiber optic sensors are being used to determine the gross weight. The dynamic component is then defined as the ratio of the maximum measured total strain to the maximum scaled static strain.

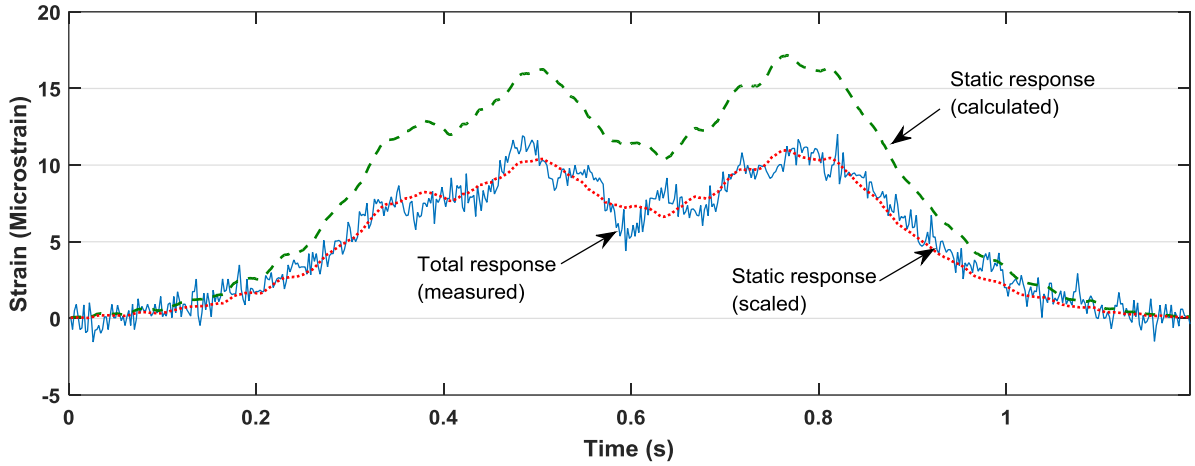

Figure A- 9 Fitting of the static response to the total response.

A.5. Results and Discussion

A.5.1. DAF and ADR

The measurements were carried out from March 15th to April 28th, 2015. The WIM data and the measured strain data were gathered and synchronized. Only events with trucks heavier than 10 tonnes were considered. For reference, the DAF values are calculated for all the events measured through the 45 days and are shown in Figure A- 10. The DAF values out of the range of 0.8 to 2.0 are removed as most of them are the result of error in the scaling process explained above. It can be seen that most values are in the range 0.9 to 1.6.

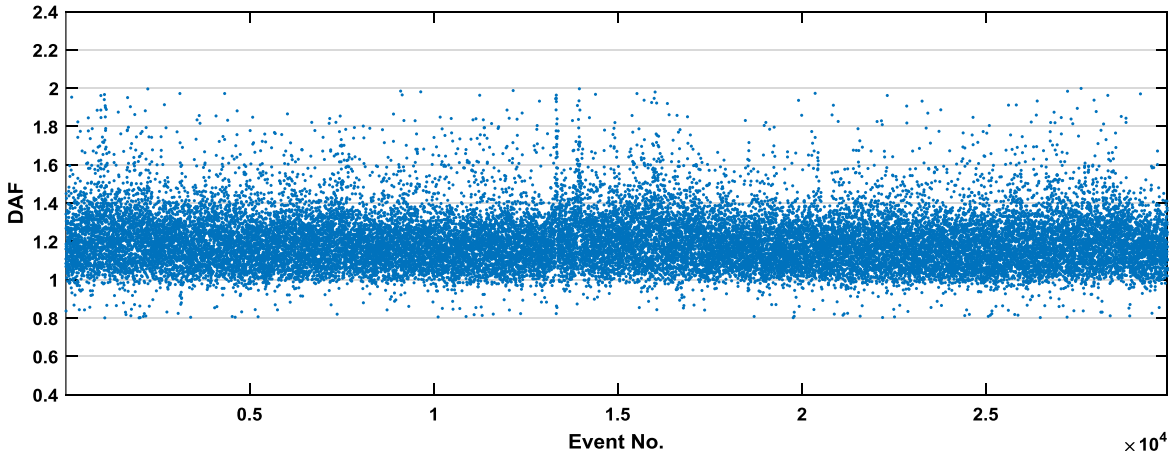

Figure A- 10 Dynamic Amplification Factor (DAF) calculated over 45 days.

Figure A- 11 shows the plot of total versus static load effect for all the events. It illustrates that many of DAF values in Fig. 10 correspond to events with lower magnitude load effect. DAF is the slope of a line joining the origin to the point representing the event in Figure A-11. A linear regression to these points shows that the points are getting closer to the diagonal as the strains get larger, i.e., the mean DAF tends towards unity as strain increases.

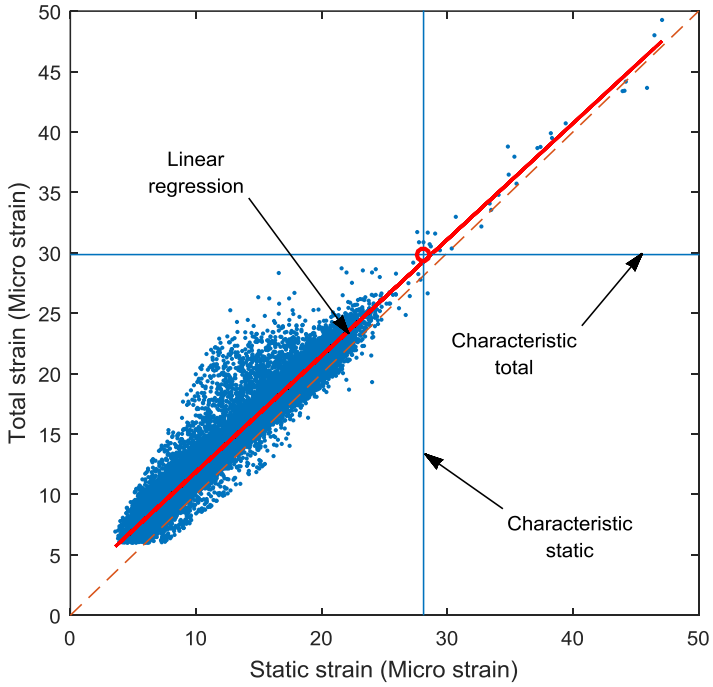

Figure A- 11 Total versus static load effect. ADR is a function of the return period considered – the 99.9% ADR is the slope of a line joining the origin to the small circle.

The characteristic total with 99.9% probability of non-exceedance is 29.85 while the 99.9 % characteristic static strain is 28.11. The ADR corresponds to the point where characteristic total meets characteristic static and is 1.062. This can be seen to be considerably less than the DAF values recorded (Figure A- 10), which generally correspond to smaller strains.

The Beam 6 strains are plotted on Gumbel probability paper in Figure A- 12. As expected, total strain exceeds static in general but there are a small number of exceptions. In particular, it can be seen that the 3rd, 4th and 5th largest static strains exceed the 3rd, 4th and 5th largest total strains. It should also be noted that there is a general trend of decreasing dynamics with increasing static load and this is expected (OBrien et al., 2009, OBrien et al., 2010).

The changing slopes in the curves suggests data consistent with statistical mixtures of event types, likely corresponding to different types of truck. Best fit trend lines are fitted to each segment of data, as shown in the figure. The 99.9% characteristic values correspond to the final group of trucks (the heaviest ones), as can be seen in Figure A- 12(b).

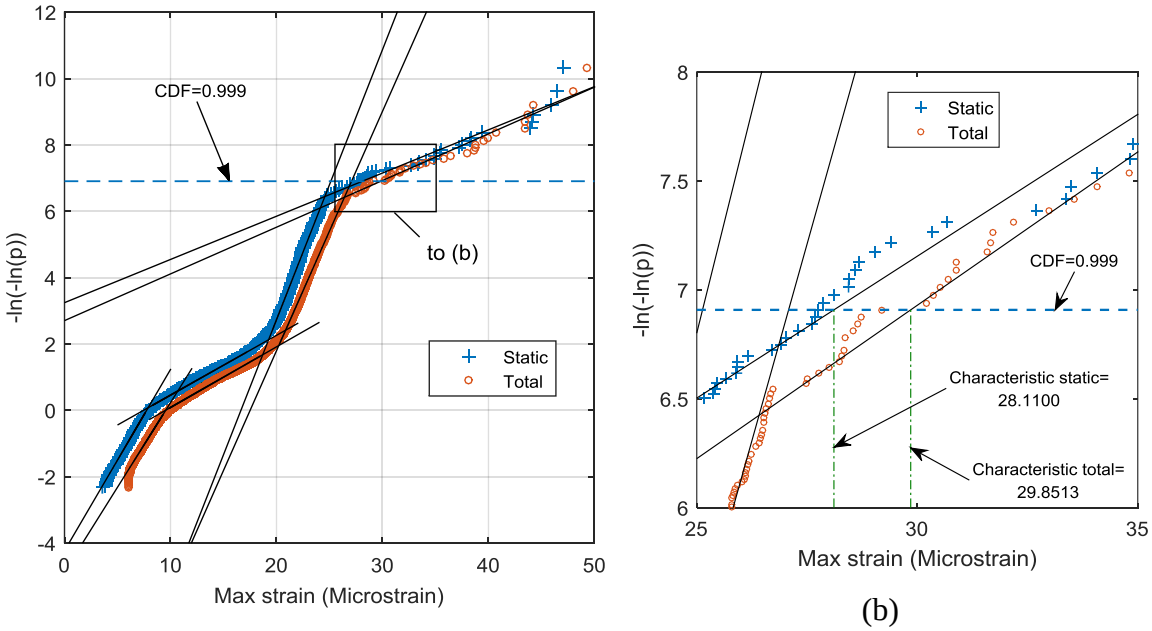

(a) (b)

Figure A- 12 Gumbel probability plot; (a) full plot, (b) a zoom view.

A.6. Conclusions

In this chapter, the dynamic amplification at a point in a bridge beam is determined from field measurements. Total strain is measured directly using fiber optic sensors. Static strain is measured from a piezo-polymer WIM system, scaled to remove the influence of temperature and drift. The WIM weights are converted to strains using an influence line inferred from the response to trucks weighed at a static weigh station. Dynamic Amplification Factor (DAF) is shown to be inappropriately high, driven by a large number of lighter trucks. Assessment Dynamic Ratio (ADR) is defined as the ratio of characteristic total to characteristic static strain and is found to be a great deal less.

Appendix B: Application of laser measurement to the drive-by inspection of bridges

Not to the reader:

This appendix evaluates the application of laser measurement to the drive-by inspection of bridges. It was presented in the 5th International Conference on Computational Methods in Structural Dynamics and Earthquake Engineering in Crete, Greece, 2015.

.

B.1. drive-by bridge inspection

B.1.1. Numerical case study

A same bridge as it is shown in Figure 4-1is investigated here as the half-car is travelling over it at a speed of 4 m/s.

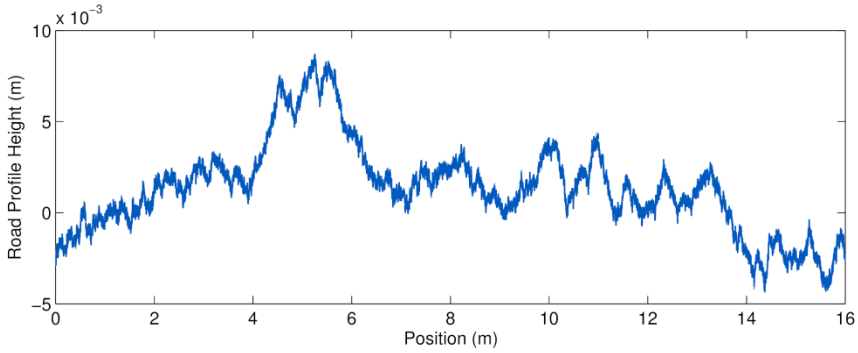

Figure B- 1 Class "A" road profile.

A road profile (shown in Figure B- 1) is included in the simulations. The irregularities of this profile are randomly generated according to the (ISO8608:1995, 1995) for a road class 'A' (very good profile, as expected in a well maintained highway). The simulation is carried out using the FE method programmed in the MATLAB software environment. The sampling time interval is selected to be 0.001 s. The total length of the acceleration response of the vehicle is 4 s.

B.1.2. Drive-by inspection using acceleration measured on the vehicle axle

Drive-by bridge monitoring is usually based on the acceleration response measured on the axle of the vehicle passing over the bridge. The acceleration response measured at the first axle of the vehicle is shown in Figure B- 2 (a). In order to analyse the axle response, a Fast Fourier Transform (FFT) is performed on the simulated vehicle response. The obtained FFT spectrum of the vehicle response is shown in Figure B- 2 (b). As expected, there is a small peak due to the fundamental frequency of the bridge and there is a dominant peak related to the axle frequency.

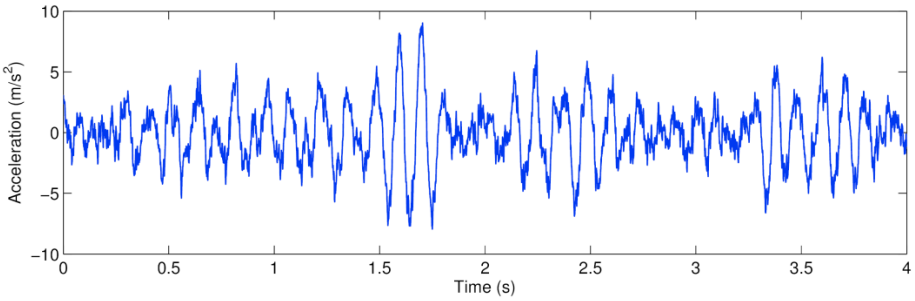

(a)

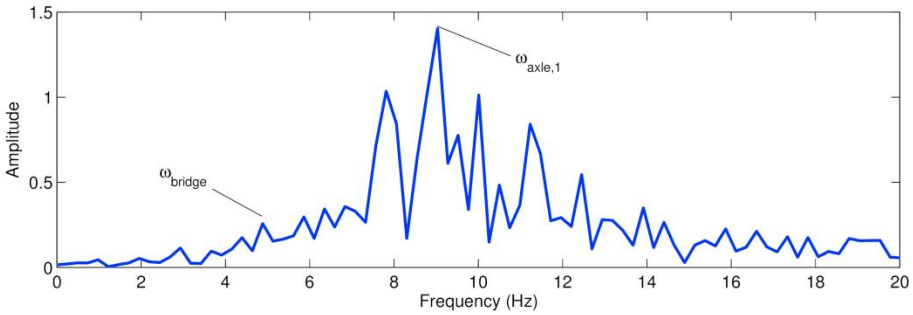

(b)

Figure B- 2 Response measured at the first axle; (a) acceleration, (b) FFT spectrum.

B.1.3. Drive-by inspection using laser measurement on the vehicle

In this section the concept of using laser vibrometer measurement on the vehicle to remove the vehicle frequency from the spectrum is introduced. A vehicle instrumented with two laser vibrometers and two accelerometers is used. Relative velocities among the bridge surface and the vehicle body are measured using two measurement points:

$$\dot{y}_{relative,i}(t) = \dot{y}_{body,i}(t) - \dot{y}_{bridge,i}(t),\ i = 1,2 \qquad \text{(B-1)}$$

The body acceleration is measured using the accelerometer installed at exactly the same location as the laser vibrometer. The velocity of the bridge is calculated by integration of the body acceleration (Figure B- 3). Therefore, the bridge spatial velocity $\dot{y}^{i}_{bridge}(t)$ can be obtained by subtracting the body velocity from the relative velocity.

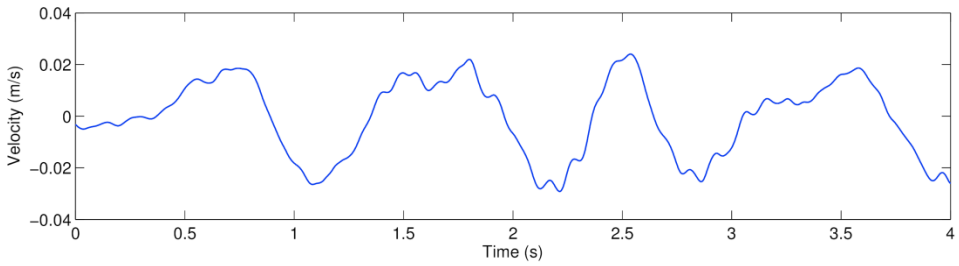

Figure B- 3 Body velocity measured at the first accelerometer ($\dot{y}_{body,1}(t)$).

The spatial velocity includes two parts. The first part is the bridge response relative to the moving reference and the second part is the spatial velocity of the road profile, i.e., the road profile converted to velocity relative to the moving reference:

$$\dot{y}_{bridge,i}(t) = \dot{u}_i^{'}(t) + \dot{r}_i(t), \quad i = 1,2 \tag{B-2}$$

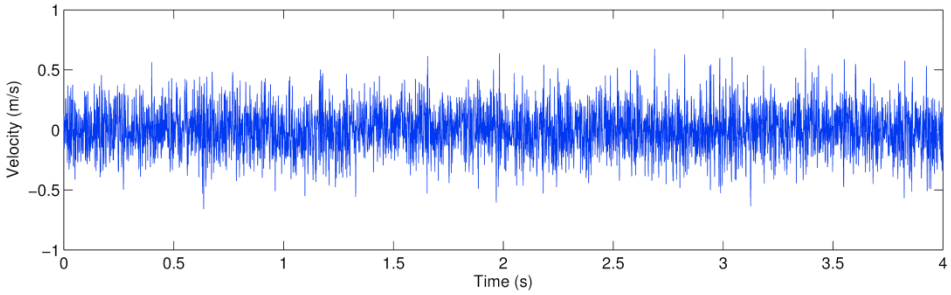

Figure B- 4 Relative velocity measured at the first laser ($\dot{y}_{relative,1}(t)$).

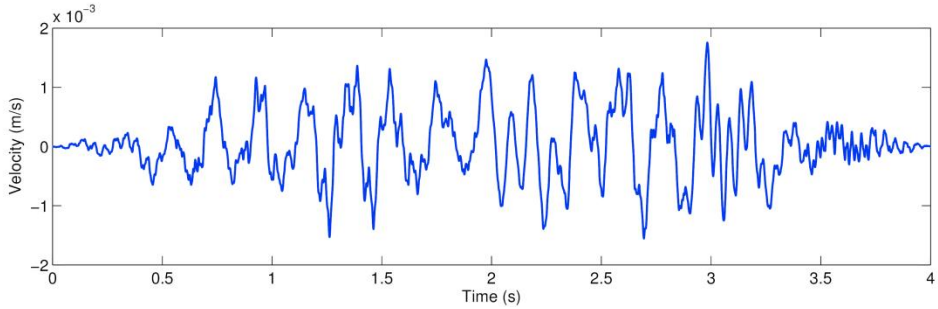

Figure B- 5 Velocity difference ($\Delta\dot{y}$).

The spatial velocities at two following points on the vehicle are measured (Figure B- 4). In order to remove the spatial velocity of the road profile from the response, the second response is subtracted from the first with a time shift to allow for their relative positions.

$$\begin{aligned} \Delta\dot{y} &= \dot{y}_{bridge,2}(t + \Delta t) - \dot{y}_{bridge,1}(t) \\ &= \dot{u}_2(t + \Delta t) + \dot{r}_2(t + \Delta t) - \dot{u}_1(t) - \dot{r}_1(t) \end{aligned} \tag{B-3}$$

where Δt is the time interval between two measurement points. If Δt is selected to that $r_2(t+\Delta t) = r_1(t)$, the road profile is removed from the response and a time shifted difference of the bridge response is obtained:

$$\Delta \dot{y} = \dot{u}_2(t+\Delta t) - \dot{u}_1(t) \tag{B-4}$$

The velocity differences obtained from Eq. B-4 are shown in Figure B- 6. As a result, a bridge response at the moving coordinate is obtained which can show the most important characteristics of the bridge dynamics. The frequency spectrum of the obtained bridge response is shown in Figure B- 7. A dominant peak is observable in the spectrum which is related to the bridge fundamental frequency. This can be expected to be damage sensitive.

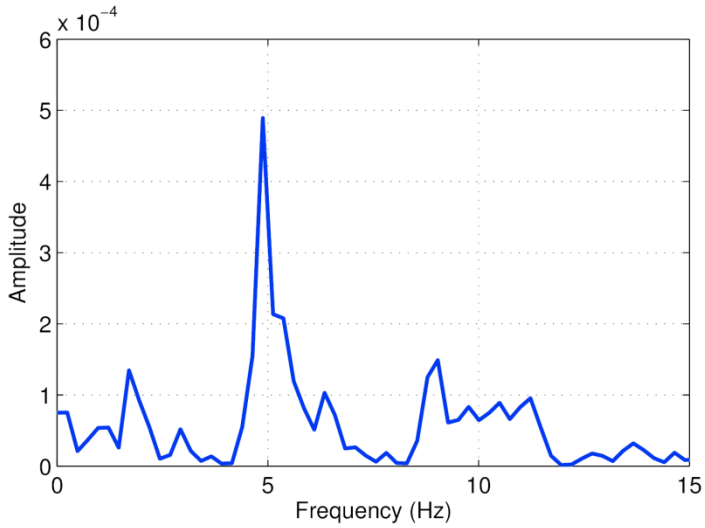

Figure B- 7 Frequency spectrum of the bridge response.

B.2. Conclusions

This chapter describes the application of laser measurement to the drive-by bridge inspection problem. Subtraction of responses measured using laser vibrometers and accelerometers is used to obtain the bridge spatial velocity. Finally, spatial velocity of road roughness is removed by subtraction of the bridge spatial velocities measured at two following laser vibrometers. It is shown that the FFT spectrum of the differences response shows a dominant frequency which is corresponds to the bridge fundamental frequency.

Appendix C: Identification of bridge mode shapes using a passing vehicle

Not to the reader:

This appendix presents further investigation on the STFDD method which is proposed in Chapter 3. The results were presented in 7th International Conference on Structural Health Monitoring of Intelligent Infrastructure, Torino, Italy, July 2015.

.

C.1. Numerical case study

A case of a truck towing two trailers same as Figure 3-12 is investigated travelling over a bridge. The bridge is divided into six equal segments (n = 6), so the mode shape vector obtained from the method has six elements. The truck-trailer travels over the bridge at a speed of 2 m/s to provide enough data for the method to work effectively. Four acceleration signals measured from the trailers' axles are defined as $\ddot{y}_5$, $\ddot{y}_6$, $\ddot{y}_7$ and $\ddot{y}_8$, using a time interval, dt = 0.001 s. To remove the effect of road profile from the measured signals, two difference signals are defined as $\ddot{x}_1=\ddot{y}_6-\ddot{y}_4$ and $\ddot{x}_2=\ddot{y}_7-\ddot{y}_5$. The first two mode shapes of the bridge obtained from the method are shown in Figure C- 1. The Modal Assurance Criteria (MAC) approach is used to compare the calculated mode shapes to the exact shapes obtained from the FEM method and shows a good match.

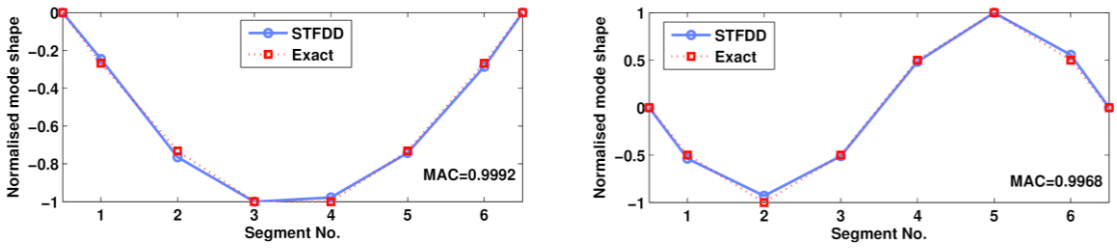

(a) (b)

Figure C- 1 The first two mode shapes of the bridge. (1) First (MAC = 0.9992) and (b) second (MAC = 0.9968).

C.2. Effect of sampling time interval

In frequency analysis of discrete time signals, the sampling time interval plays a significant role in the accuracy of results. This is more important when only a short signal is available as there may be an insufficient quantity of data. Therefore, the effect of time interval on the accuracy of the calculated mode shapes is investigated in this section. The same procedure as in the previous section is used here but employing several time intervals: 0.01, 0.005, 0.001 and 0.0005 s.

Figure C- 2 compares the first and second bridge mode shapes obtained from the STFDD method using the different time sampling intervals. It can be seen from Fig. 4(a) that the first mode shape is obtained with acceptable accuracy even with a large sampling interval (e.g. 0.01 s). The second mode shape, on the other hand, is more sensitive and can be calculated

best with a time interval of 0.001 s or less. Clearly a connection exists between the size of the time sampling interval and the quality of the results. Thus, it is generally recommended that the time interval be small enough based on the capability of the measurement equipment to provide enough vibration data for the signal processing.

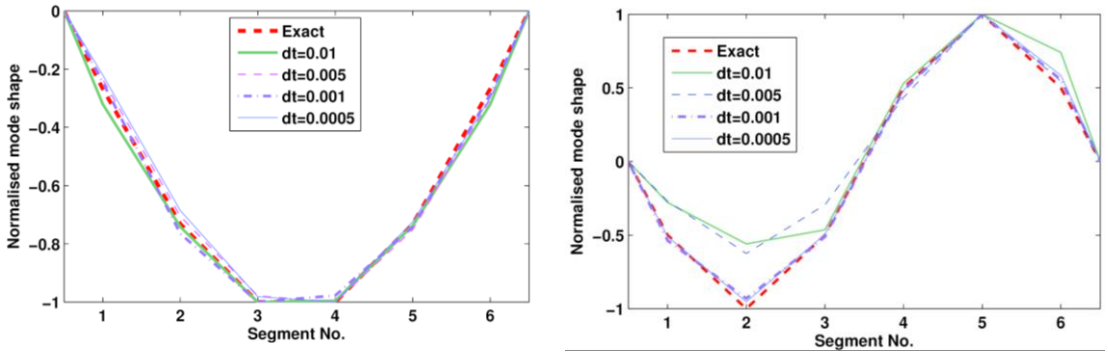

Figure C- 2 The first two mode shapes of the bridge using different time intervals. (1) First and (b) second.

C.3. Assessment of vehicle speed

Speed limitation is an important challenge in indirect bridge monitoring, particularly for the identification of bridge mode shapes (Malekjafarian et al., 2015). The very low vehicle speeds currently being considered are likely to require bridge lane closures in practice. In this section, the sensitivity of the STFDD method to vehicle speed is investigated. The same procedure used in previous sections is used here with vehicle speeds of 2, 4 and 8 m/s (7.2, 14.4 and 28.8 km/h).

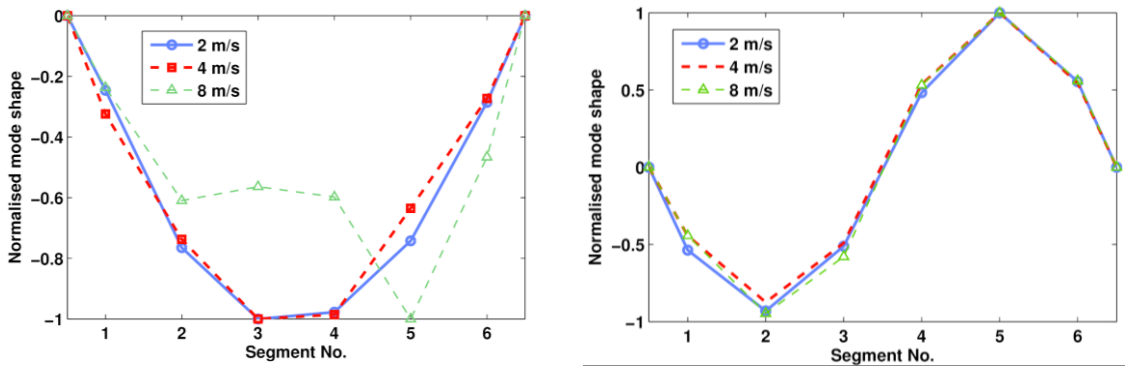

Figure C- 3 The first two mode shapes of the bridge using different vehicle speeds. (1) First and (b) second.

The results of the STFDD method using several vehicle speeds are illustrated in Figure C-3. It is clear from Figure C- 3 (a) that the first mode shape can be obtained only with a vehicle speed up to 4 m/s, while the second mode shape has been identified even when the speed is 8 m/s. In general in these simulations, travelling over the bridge with lower speeds gives better results for the STFDD method.

C.4. Conclusions

This chapter describes a novel method for the indirect identification of bridge mode shapes using a truck/trailer system. Subtraction of the responses measured on the following axles of the trailers are used in several defined stages. The importance of selecting a proper time sampling interval for the short signals used in the STFDD method is investigated. In addition, it is demonstrated that the first and second mode shapes can be estimated with acceptable accuracy for vehicle speed up to 4 m/s second.